THEORETICAL JUSTIFICATIONS FOR RATE DECLINE TRENDS IN SOLUTION-GAS DRIVE RESERVOIRS, AND RESERVOIR PROPERTY ESTIMATION USING PRODUCTION DATA

A THESIS SUBMITTED TO THE DEPARTMENT OF

PETROLEUM ENGINEERING

OF AFRICAN UNIVERSITY OF SCIENCE AND TECHNOLOGY, ABUJA

IN PARTIAL FULFILMENT OF THE REQUIREMENTS FOR THE DEGREE OF

MASTER OF SCIENCE IN PETROLEUM ENGINEERING

By

MOSOBALAJE Olatunde Olu

DECEMBER 2011

THEORETICAL JUSTIFICATIONS FOR RATE DECLINE TRENDS IN SOLUTION-GAS DRIVE RESERVOIRS, AND RESERVOIR PROPERTY ESTIMATION USING PRODUCTION DATA

By

MOSOBALAJE Olatunde Olu

RECOMMENDED:

_____

Chair, Professor Djebbar Tiab

_____

Professor Samuel Osisanya

_____

Dr. Alpheus Igbokoyi

APPROVED:

_____

Chief Academic Officer

to the ONLY WISE GOD …

TABLE OF CONTENTS

List of Figures vii

List of Tables viii

Acknowledgements ix

Abstract x

1. Introduction 1

1.1 Overview of Rate Decline Analysis 1

1.2 Statement of Problem 3

2 Literature Review 5

2.1 Fundamentals of Empirical Decline Curves Analysis 5

2.2 Modern Decline Curve Analysis 6

2.3 Effects of Reservoir/Fluid Properties and Drive Mechanism on Production Rate Decline 8

2.4 Performance Prediction of Two-Phase Flows in Saturated Reservoirs 11

2.4.1 Material Balance for Saturated Reservoirs 12

2.4.2 Inflow Performance Relationships for Solution-Gas Drive Reservoirs 13

2.4.3 Diffusivity Equation for Solution-Gas Drive Reservoirs 17

2.5 Decline Curves Analysis for Multi-Phase Flows 20

2.6 Theoretical Basis for Decline Curves Analysis in Solution-Gas Drive Reservoirs 22

2.6.1 Fetkovich Type Curves 22

2.6.2 Camacho and Raghavan Attempt 25

2.6.3 The Non-Darcy Considerations 27

3. Theoretical Developments 29

3.1 Overview and Background Information 29

3.2 Relationship between Empirical and Theoretical Decline Parameters 30
3.2.1 Derivation of Relationship 32
3.2.2 Significance of Relationship: Permeability Estimation ... 35
3.3 Considerations for the Effects of Non-Darcy Flow on the Decline Parameter 36
3.4 Inner Boundary Condition and the Existence of Hyperbolic Family in Solution-Gas Drive Reservoirs 46
4. Simulation and Computational Procedures **52**
4.1 Reservoir and Fluid Data Set 53
4.2 Simulation Data Deck and Run Specifications..... 58
4.2.1 Simulation Data Deck 58
4.2.2 Simulation Specifications and Controls 59
4.2.3 Output Requests 60
4.2.4 Simulation Initial Solution 62
4.3 Computational Procedures 62
5. Verification of Theories and Reservoir Property Estimation **66**
5.1 Theoretical Decline Parameter Trend through Time 67
5.2 Theoretical Justifications for the Decline Parameters Trend 68
5.3 Effects of Incorporating Non-Darcy Flow 71
5.4 Verification of Derived Relationships 73
5.5 Proposed Reservoir Property Estimation Techniques 76
5.5.1 Reservoir Permeability Estimation: Procedures and Application 76
5.5.2 Reservoir Radius Estimation 82
5.6 Sensitivity Analysis 83
5.6.1Case 1: Effects of Critical Gas Saturation 84
5.6.2 Case 2: Effects of Permeability Value 87
5.6.3 Case 3: Effects of Reservoir Drainage Radius 89
5.6.4 Case 4: Effects of Critical Bottomhole Pressure..... 92
5.6.5 Case 5: Effects of Peak/Initial Rate 95

5.6.6 Case 6: Effects of Reservoir Heterogeneity …….. 99

6. Conclusions and Recommendations **103**

Nomenclature **108**

References **109**

Appendix **113**

LIST OF FIGURES

1.1 Typical Oil Well Production Profile 1

4.1 Oil PVT Properties 55

4.2 Gas PVT Properties 56

4.3 Relative Permeability Characteristic Curves 58

5.1 Base Case: Production History: Rate-Time and Solution-Gas Drive Index 67

5.2 Base Case: Theoretical b_{th} Trend through Time 68

5.3: Base Case: Theoretical b_{th} and b_{th-nD} through Time 72

5.4: Base Case: Verification of Equations 3.8 and 3.9 75

5.5: Base Case: Permeability Estimates through Time 80

5.6: Comparing Permeability Estimates using different Techniques 81

5.7: Base Case: Reservoir Radius (r_e) Estimates through Time 83

5.8: Case 1: Production History: Rate-Time and Solution-gas Drive Index 84

5.9: Producing Gas-Oil Ratio, GOR Trend: Base Case and Case 1 85

5.10: Case 1: Theoretical b_{th} Trend through Time 86

5.11: Case 1: Permeability Estimates through Time 87

5.12: Case 2: Theoretical b_{th} Trend through Time..... 88

5.13: Case 2: Permeability Estimates through Time 89

5.14: Case 3: Theoretical b_{th} Trend through Time 90

5.15: Case 3: Reservoir Radius (r_e) Estimates through Time 92

5.16: Case 4: Theoretical b_{th} Trend through Time 93

5.17: Case 4: Permeability Estimates through Time 94

5.18: Case 4: Verification of Equations 3.8 and 3.9 95

5.19: Case 5: Production History: Rate-Time and Solution Gas Drive Index..... 96

5.20: Case 5: Theoretical b_{th} Trend through Time 97

5.21: Case 5: Permeability Estimates through Time 98

5.22: Case 5: Reservoir Radius (r_e) Estimates through Time 98

5.23: Case 6a: Verification of Equations 3.8 and 3.9 100

5.25: Case 6a: Permeability Estimates through Time 101

5.26: Case 6b: Permeability Estimates through Time 102

LIST OF TABLES

2.1: Summary of Empirical Decline Models 5
4.1: Reservoir Properties Data Set 53
4.2: Oil PVT Properties Data Set 54
4.3: Gas PVT Properties Data Set 55
4.4: Undersaturated Oil Compressibility Data Set 57
5.1: Grid Data for Heterogeneous Case 99

AKNOWLEDGEMENTS

I would like to thank my Supervisor, Professor Djebbar Tiab, first for his enthusiasm about the proposal for this work, and then for his patience and guidance through the course of this work. Dr. Alpheus Igbokoyi's timely reviews are equally appreciated.

Valuable discussions I had with my colleagues, Anthony Ike, Oscar Ogali and Salako Rashidi were crucial to the successful and timely completion of this work.

At different times I had to consult the following for expert's advice: Dr. Nnaemeka Ezekwe (BP), Professor Emeritus D.O Ogbe (Greatland Solutions) and Mr. Kingsley Akpara (Schlumberger); many thanks to you, sirs.

Computational facility was provided by Schlumberger through a donation to African University of Science and Technology, AUST, Abuja

I wish to thank Micah Maku for lending me his PC for this work.

Finally, to all those who wished and prayed for the success of this endeavor, I cannot say enough of you all – million thanks!

ABSTRACT

Rate decline analysis is an essential tool in predicting reservoir performance and formation property estimation. The use of historical production data to predict future performance is the focus of the empirical domain of decline analysis while the theoretical domain focuses on the use of such data to estimate formation properties.

A number of attempts have been made to establish the theories of rate decline in solution-gas drive reservoirs. Such attempts have established the theoretical decline exponent b as a function of formation properties. However, none of the attempts have established a direct link between the empirical and theoretical domains of decline analysis. The purpose of this work is to establish the missing link and deploy such link in reservoir property estimation.

In this work, a functional relationship (equation) between the empirical (b_{emp}) and the theoretical (b_{th}) was derived; based on the definition of a new parameter known as time-weighted average of the theoretical exponent, $\overline{b_{th}}$. This new parameter was found to be related to the empirical exponent, b_{emp} thus establishing the link. Theoretical justifications for the ranges of values of the theoretical exponent were also offered. Consequent upon the establishment of the relationship, this work developed a new improved technique for estimating reservoir permeability. The technique was applied to a number of cases and was found to yield excellent estimates of permeability even for an heterogeneous reservoir. Sensitivity analyses were performed on the results. The work also investigated non-Darcy flow effects on decline parameters. Lastly, this work provided mathematical justification for the existence of the hyperbolic family of curves in solution-gas drive reservoirs.

CHAPTER 1

INTRODUCTION

1.1 OVERVIEW OF RATE DECLINE ANALYSIS

Production rate decline analysis is an essential tool for predicting reservoir/well performance and for estimating reservoir properties. The production life of hydrocarbon reservoirs typically shows three phases: the build-up phase, the peak phase, and the rate decline phase[1]. The build-up phase corresponds to the increasing field production rate as new wells are drilled. Thereafter, the field peak rate is attained and maintained for some time after which the rate decline phase sets in. For a well, during the peak phase, the bottomhole flowing pressure P_{wf} declines until it reaches a critical value, P_{wfc} whereupon the production begins to decline as the critical bottomhole pressure P_{wfc} is maintained[3].

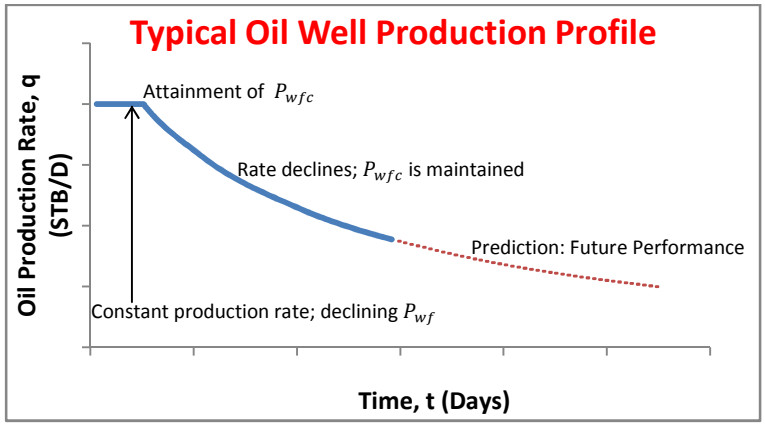

Figure 1.1: Typical Oil Well Production Profile

If there is no external influence on the factors affecting production, the decline period would follow a fairly regular trend; hence analysis of the historical data could be useful in predicting the future performance of the field[3,4]. However, decline curve analysis is to a large extent based on Arps[2] empirical models that have only little theoretical basis. The use of historical production data to predict future performance is the focus of the empirical domain of decline analysis while the theoretical domain focuses on the use of such data to estimate formation properties.

The empirical analysis typically involves plotting the historical data against time and extrapolating the curve to the future to predict the future performance. This extrapolation is strictly based on the assumption that the controlling factors of the past production trend will continue into the future and that the well must have been producing at full capacity[4]. In a rather more rigorous approach, decline curve analysis involves the mathematical estimation of the decline model parameters and then the substitutions of such estimated parameters into the model equations to estimate recoverable reserves and predict future production rates.[4] The estimation of recoverable reserves leads to the economic evaluation of oil properties (assets) while the prediction of future performance gives a measure of the revenue generation pattern of oil field development projects. Both oil property evaluation and revenue generation pattern prediction are essential in carrying out capital investment analysis before scarce resources are committed[5].

The theoretical approach of decline analysis is primarily concerned with investigating the various reservoir/fluid factors that governs the past production trend and the effects of these factors on the empirical decline model parameters. These factors include relative

permeability characteristics of the rock, fluid PVT properties, rock properties, wellbore conditions and the prevailing drive mechanism in the reservoir.[6-11] The essence of the theoretical approach is to derive functional relationships between the empirical decline model parameters and the physical reservoir/fluid properties. Such relationships are useful in formulating procedures for reservoir properties estimation using field production data in a kind of inverse problem. The compelling advantage of this approach to formation evaluation lies in the fact that the data required are easy (inexpensive, requires no shut-in) to acquire and to analyze.

1.2 STATEMENT OF PROBLEM

Many previous attempts[12-15] at establishing functional relationships between the empirical decline model parameters and the physical reservoir/fluid properties have been concerned primarily with the exponential decline of single phase oil reservoirs. A number of attempts[10] at establishing the theories of hyperbolic decline of solution-gas drive reservoirs have yielded expressions relating the decline exponent b to reservoir/fluid properties. However, the values computed from such expression, although theoretically sound, are not constant through time. More disturbing is the fact that the values did not exhibit any equivalence with the empirically determined decline exponent. This fact suggests there is a missing link between the theoretical and the empirical domains of the decline curves analysis.

The purpose of this work is therefore to establish the missing link, to derive a functional relationship between the empirical decline exponent, $b_{emp}$and the theoretical decline

exponentb_{th} and to formulate a new improved technique for reservoir permeability estimation. The work defines a new parameter known as the *time-weighted average of the values of the theoretical decline exponent,* denoted as $\overline{b_{th}}$, and uses this new parameter to correlate the empirical and the theoretical domains of decline curve analysis.

In carrying out this work, a fully penetrating vertical well at the centre of a cylindrical reservoir is considered; the flow from the reservoir into the wellbore is assumed to be radial. Both homogeneous and heterogeneous reservoir cases are considered. The water phase is assumed immobile (connate water), hence a two-phase flow of oil and gas. Rock and water compressibility are taken to be negligible. The presence of near-wellbore skin region is considered.

As a result of the investigations in this work, it was found that there exist a correlation and a functional relationship between the empirical and the theoretical domains of decline analysis of solution-gas drive reservoirs. Consequent upon the derivation of the functional relationship, this work presents a new improved reservoir permeability estimation technique. The technique has been applied to a number of simulated cases and was found to yield excellent estimates of reservoir permeability even for heterogeneous reservoirs. Analyses have been performed on the sensitivity of the results to some key parameters.

CHAPTER 2

LITERATURE REVIEW

2.1 FUNDAMENTALS OF EMPIRICAL DECLINE CURVES ANALYSIS

In 1944, Arps[2] published a comprehensive review of methods of graphical analysis of production decline behavior. Employing the concept of loss-ratio,[16] he defined the relative decline rate, D and the general decline equation known as Arps' equation as follows:

$$\frac{1}{q}\frac{dq}{dt} = D = -aq^b \quad (2.1)$$

Decline curve analysis is essentially based on three empirical mathematical models: exponential decline, hyperbolic decline and harmonic decline.[3] A summary of the governing equations for each model is given in the table below.

Table 2.1: Summary of Empirical Decline Models

Model	Relative Decline Rate Equation	Rate-Time Equation	Cumulative Production Equation
Exponential ($b = 0$)	$\frac{1}{q}\frac{dq}{dt} = -D = -a$	$q = q_i e^{-D_i t}$	$N_p = \frac{1}{D}(q_i - q)$
Hyperbolic ($0 < b < 1$)	$\frac{1}{q}\frac{dq}{dt} = -D = -aq^b$	$q = q_i(1 + bD_i t)^{-\frac{1}{b}}$	$N_p = \frac{q_i}{D_i(1-b)}\left(1 - \left(\frac{q}{q_i}\right)^{1-b}\right)$
Harmonic ($b = 1$)	$\frac{1}{q}\frac{dq}{dt} = -D = -aq$	$q = \frac{q_i}{(1 + D_i t)}$	$N_p = \frac{q_i}{D_i} ln\left(\frac{q_i}{q}\right)$

Nind[17] provided plotting functions for the graphical analysis of rate data. Arps[18] presented methods for extrapolation of rate-time data to estimate primary oil reserves.

2.2 MODERN DECLINE CURVES ANALYSIS: TYPE CURVES

Conventional decline curve analysis involves the curve-fitting of past production data using standard models[4]. The modern approach to decline analysis is the use of type curves to analyze production data. A type curve is a plot of theoretical solutions to flow equations[4]. The type curve decline analysis involves finding the type curve (theoretical solution) that matches the actual production from a reservoir. The strengths of type curve decline analysis over the conventional decline analysis are highlighted as follows:

- The type curve provides unique solutions; a task which is rather difficult with conventional methods as results are subject to a wide range alternate interpretaions[12]
- The type curves combine solutions to the flow equations both in the transient and the pseudo-steady state regimes; this improves the uniqueness of the solution[24].
- Reservoir properties such as permeability, skin and drainage radius can be determined from type curve decline analysis[6].

The deployment of type curves in analyzing production data was introduced by Slider[19] and Gentry.[20] Gentry manipulated the Arps' relationships to solve for some group of parameters in terms of other groups. With his solutions, Gentry constructed two graphs; on each graph, a curve corresponds to each value of Arps' exponent , $(0 \leq b \leq 1)$. The graphs can be used to analyze actual production history.

Fetkovich presented arguably the most significant contribution in the type-curve matching of production data. Fetkovich[12] extended Arps' work[2] by incorporating transient flow regime into the rate-time analysis. By defining a set of decline curve dimensionless variables, he developed analytical solutions for the transient stems as well as the boundary-dominated exponential stems for a well producing at constant bottomhole pressure. He plotted the analytical solutions (transient and exponential boundary-dominated) on the same plot with the empirical Arps' hyperbolic boundary-dominated decline stems to produce a unified type curve that permits both transient rate decline and pseudo-steady (boundary-dominated) rate decline data to be analyzed simultaneously. Fetkovich's decline curve dimensionless variables are defined as below[12].

Decline Curve Dimensionless Flowrate:

$$q_{Dd} = \frac{q}{q_i} = q_D \left[ln\left(\frac{r_e}{r_w}\right) - \frac{1}{2} \right] \quad ----------(2.2)$$

Decline Curve Dimensionless Time:

$$t_{Dd} = D_i t = \left[\frac{t_D}{\frac{1}{2}\left[\left(\frac{r_e}{r_w}\right)^2 - 1\right] ln\left[\left(\frac{r_e}{r_w}\right) - \frac{1}{2}\right]} \right] \quad ----------(2.3)$$

Fetkovich et al[13] published a number of field case histories analyzed with type curves and provided discussions concerning interpretation of production data with type curves. The authors observed that analyzing transient rate data using Arps' equation yields invalid interpretation.

The Fetkovich method is only valid for constant-bottomhole pressure production. McCray[21] proposed a new time variable known as equivalent constant pressure time, t_{cp}, that could be used to transform a variable rate/variable pressure drop system to an equivalent constant bottomhole pressure system.

$$\frac{N_p}{\Delta P(t)} = \int_0^{t_{cp}} \frac{q(t)}{\Delta P(t)} dt \quad ---------(2.4)$$

Blasingame et al[22] presented methods for computing t_{cp}. Palacio and Blasingame[23] presented a general solution for the variable rate/variable pressure drop for single phase using the pressure drop normalized flowrate, $\frac{q}{\Delta P}$, and the material balance time, $\frac{N_p}{q}$. They showed that for liquid flow, any production history (constant rate, constant pressure or variable rate/variable pressure drop) will match the harmonic ($b = 1$) stem on Fetkovick[12] type curves if the normalized flowrate and material balance time is used.

2.3 EFFECT OF RESERVOIR/FLUID PROPERTIES AND DRIVE MECHNISMS ON PRODUCTION RATE DECLINE

Reservoir factors are known to govern past production trend of reservoirs[6]; a review of these factors and how they affect the decline parameters is therefore necessary to establish theoretical basis of the decline models.

Gentry and McCray[6] classified such factors as physical characteristics of the reservoir, characteristics of the reservoir fluids and primary recovery drive mechanisms. In a study to

investigate the effect of reservoir fluid and rock characteristics on production histories of solution-gas drive reservoirs, Muskat and Taylor[7] made the following conclusions:

1. The ultimate recovery of a solution-gas drive reservoir is very sensitive to oil viscosity. The stock tank oil recovery decreases with increasing oil viscosity.
2. Increased solution gas oil ratio, R_s would ordinarily favor increased recovery; however, the consequent oil shrinkage results to lower recovery.
3. Additional gas provided by an overlying gas cap is less effective in oil expulsion than the liberated solution gas.
4. Relative permeability characteristics that provide for no critical gas saturation would lead to rapid increase in producing GOR.
5. The ultimate recovery is more sensitive to the relative permeability characteristics at high liquid saturations than at lower liquid saturations
6. The ultimate reservoir volume voidage is less sensitive variations in rock and fluid properties than is the ultimate stock tank recovery.
7. Due to the twin effects of reduced permeability to oil and increased oil viscosity as it loses gas, the productivity indexes of well producing from a solution-gas drive will continuously decrease.

Arps and Roberts[8] found out that ultimate recovery increases with oil gravity except for higher solution-gas oil ratios. They also reported that the rock type as identified by its relative permeability characteristics have significant effect on recovery; with sandstones reservoirs showing higher recovery than carbonate reservoirs.

Attempts have been made by various investigators to associate the decline model parameters with the physical properties of the reservoir as well as the active drive mechanism. Mead[9] noted in his discussion of b factor (decline curve exponent) that: "as b approaches zero, for the same initial maximum (peak) production rate and same ultimate recovery, a greater and greater amount of oil can be produced before decline sets in." This means that as b approaches zero, the peak production phase of the reservoir is extended and hence the decline phase is delayed. On the other hand, as b approaches zero, when the decline finally sets in, it occurs rapidly.

Gentry and McCray[6] conducted simulation studies in order to investigate the effect or reservoir and fluid properties on the decline trend of solution-gas drive reservoirs. They summarized their observations as follows:

1. The fluid properties and the reservoir dimensions had greater influence on the decline parameter D_i than did the relative permeability relationship. Specifically, changing the fluid system resulted to 200% - 400% change in D_i as compared to 15% - 18% change when relative permeability characteristics were altered.
2. Conversely, the relative permeability characteristics had greater influence on the decline model parameter b than did the fluid properties. Changing relative permeability characteristics resulted into b value changing from 0 to 1 on one instance and from 0.3 to values above 1 on the other instance. Changing fluid system however resulted in to b ranging from 0 to 0.3 on one instance and from 1.0 to slightly above 1 on the other hand.

3. The parameter q_i, a measure of the onset of decline phase depends on reservoir properties such as absolute permeability and water saturation as well as the fluid properties.
4. Separate zones producing into the same wellbore could have significant effects on the decline parameters and could in fact produced values of b greater than 1.

In 1956, Mathews & Lefkovits[11], conducted an experimental study with models and theoretical deductions and they published results showing, that for a well with free surface (secondary gas cap) in a homogeneous gravity drainage reservoir (dipping bed), the decline is of the hyperbolic type with the hyperbolic exponent b having a value of 0.5 (b = 0.5). In 1958, Lefkovits and Matthews[25] extended the experimental work to actual field cases with results showing that when the well is producing from the two layers of different thickness and permeability or two layers having different skin effects, the value of b may be greater than 1; however, they predicted that the value of b would approach 0.5 again as the higher permeability zone depletes.

2.4 PERFORMANCE PREDICTION OF TWO-PHASE FLOWS IN SATURATED RESERVOIRS

Prediction of reservoir future performance (production rate as a function of time) typically involves combining the reservoir material balance equations ($N_p vs\ P$) with well inflow equations($q\ vs\ P_{wf}$). The two performance data ($N_p vs\ P$; $q\ vs\ P_{wf}$) are then correlated with time to yield the rate-time performance[4]. Analytical solutions to diffusivity equation also give rate-time performance.

2.4.1 Material Balance for Saturated Reservoirs

First, the material balance equation for a single-phase volumetric reservoir is commonly presented thus[4]:

$$N_p = Nc_e\left(\frac{B_o}{B_{oi}}\right)\Delta P \quad ---------(2.5)$$

The effective compressibility term, c_e is defined by Hawkins[26] as follows:

$$c_e = \frac{S_{oi}c_o + S_{wi}c_w + c_f}{1 - S_{wi}} \quad ------(2.6)$$

The material balance equation for a saturated volumetric reservoir is presented thus[4]:

$$N = \frac{N_pB_o + \left(G_p - N_pR_s\right)B_g}{(B_o - B_{oi}) + (R_{si} - R_s)B_g} \quad --------(2.7)$$

Equation 2.7 above contains two unknowns, N_p *and* G_p. Many techniques employed in performance prediction of saturated reservoirs are based on combining the MBE above with the instantaneous GOR equation and the saturation equation[4]. One of such method is the Muskat method. Muskat[27] expressed the MBE for saturated volumetric reservoir as follows:

$$\frac{d\bar{S}_o}{d\bar{P}} = \frac{\frac{\bar{S}_oB_g}{B_o}\frac{dR_s}{d\bar{P}} + \frac{\bar{S}_o}{B_o}\frac{k_{rg}}{k_{ro}}\frac{\mu_o}{\mu_g}\frac{dB_o}{d\bar{P}} - \frac{(1 - \bar{S}_o - S_{wi})}{B_g}\frac{dB_g}{d\bar{P}}}{1 + \frac{\mu_o}{\mu_g}\frac{k_{rg}}{k_{ro}}} \quad ---------(2.8)$$

In compact notation, equation the Muskat MBE is written thus:

$$\frac{dS_o}{d\bar{P}} = \frac{\bar{S}_o}{B_o}\frac{dB_o}{d\bar{P}} + \bar{c}_t\frac{\bar{\lambda}_o}{\bar{\lambda}_t} \quad ----------(2.9)$$

In the above equation,

$$\bar{c}_t = \frac{\bar{S}_o}{B_o}\frac{dB_o}{d\bar{P}} - \frac{\bar{S}_g}{B_g}\frac{dB_g}{d\bar{P}} + \frac{\bar{S}_o B_g}{B_o}\frac{dR_s}{d\bar{P}} --------(2.10)$$

$$\bar{\lambda}_t = \bar{\lambda}_o + \bar{\lambda}_g = \frac{\bar{k}_{ro}}{\mu_o} + \frac{\bar{k}_{rg}}{\mu_g} --------(2.11)$$

Camacho and Raghavan[10] developed the MBE for saturated reservoir as follows:

$$\frac{dN_p}{d\bar{P}} = -\frac{\bar{c}_t\bar{\alpha}\phi hA}{5.614\bar{\lambda}_t} --------(2.15)$$

Other forms of material balance equation for saturated reservoirs are the Tarner[28] MBE and the Tracy MBE[29]

2.4.2 Inflow Performance Relationships for Solution-gas Drive Reservoirs

The various material balance techniques described above show the relationship that exist between the cumulative production, N_p and the average reservoir pressure, $\bar{P}$; however, they do not relate the production rate to time. The correlation of production to time is typically accomplished by the use of relationships that are designed to predict the flowrate of wells. The functional representation of the relationship that exists between oil flowrate, q and bottomhole flowing pressure, P_{wf} is called the inflow performance relationship, IPR[4].

For a well producing from an undersaturated reservoir, the IPR is expressed thus[4]:

$$q = J\left(\bar{P} - P_{wf}\right) - - - - - - - - - - (2.16)$$

The parameter J in the above equation is known as productivity index and given as follows:

$$J = \frac{0.00708kh}{\mu B\left[ln\left(\frac{r_e}{r_w}\right) - 0.75 + s\right]} - - - - - - - - (2.17)$$

Unlike the undersaturated reservoir, the productivity index of a well producing from a solution-gas drive will continuously decrease due to the twin effects of reduced permeability to oil as gas evolves out of solution and the increased oil viscosity as it loses gas. Evinger and Muskat[30] observed that a straight line IPR (constant productivity index) may not be expected when two-phases are flowing in the reservoir. The relative permeability characteristics, the viscosities and formation volume factors in solution-gas drive reservoirs vary as function of average reservoir pressure and saturation. To account for variation of the productivity index, a number of empirical IPRs have been developed to predict the pressure-production rate behavior during two-phase flow in solution-gas drive reservoirs.

In a simulation study involving twenty-one wide-ranged reservoir/fluid data sets, Vogel[31] developed a quadratic IPR in terms of dimensionless flowrate and dimensionless pressure to describe the pressure-production behavior of saturated reservoirs as follows:

$$\frac{q_o}{q_{o,max}} = 1 - 0.2\left(\frac{P_{wf}}{\bar{P}}\right) - 0.8\left(\frac{P_{wf}}{\bar{P}}\right)^2 - - - - - - - - - - - (2.18)$$

Fetkovich[32] suggested the applicability of isochronal testing to oil wells; the isochronal testing is originally based on the Rawlins and Schellhardt[33] gas well deliverability equation. Using multi-rate test data from forty wells in six different fields, Fetkovich proved the suitability of the approach to oil wells performance prediction. He developed his IPR thus:

$$q_o = C\left(\bar{P}^2 - {P_{wf}}^2\right)^n \text{ – – – – – – – – – – (2.19)}$$

In a form similar to Vogel's IPR, the Fetkovich IPR is represented thus:

$$\frac{q_o}{q_{o,max}} = \left[1 - \left(\frac{P_{wf}}{\bar{P}}\right)^2\right]^n \text{ – – – – – – – – (2.20)}$$

Jones, Blount and Glaze[31] proposed an IPR thus:

$$\frac{\bar{P} - P_{wf}}{q_o} = C + Dq_o \text{ – – – – – – – – – – (2.21)}$$

The above IPR was based on the Forchheimer's[35] non-Darcy flow model that divides flow into laminar (Darcy) and turbulence (non-Darcy) components. In the above equation, C is the laminar flow coefficient while D is the turbulence coefficient. The coefficients $C\ and\ D$ are determined from multipoint tests, thereafter; the performance of the well can be predicted using the equation below:

$$q_o = \frac{-C + \sqrt{C^2 + 4D\left(\bar{P} - P_{wf}\right)}}{2D}$$

Klins and Majcher[36] developed an IPR that incorporates the bubble point pressure using Vogel's data. The IPR is given thus:

$$\frac{q_o}{q_{o,max}} = 1 - 0.295\left(\frac{P_{wf}}{\bar{P}}\right) - 0.705\left(\frac{P_{wf}}{\bar{P}}\right)^d \text{ – – – – – – – – – – –(2.22)}$$

In the equation, the parameter d is determined using the equation above:

$$d = \left(0.28 + 0.72\frac{P_{wf}}{P_b}\right)(1.235 + 0.001P_b) \text{ – – – – – – – – – – – – (2.23)}$$

Sukarno[37] developed an IPR that accounts for the variation of flow efficiency due to the rate dependent skin. The Sukarno IPR is given thus:

$$\frac{q_{o,actual}}{q_{o,max@S=0}} = FE\left[1 - 0.1489\left(\frac{P_{wf}}{\bar{P}}\right) - 0.4418\left(\frac{P_{wf}}{\bar{P}}\right)^2 - 0.4093\left(\frac{P_{wf}}{\bar{P}}\right)^3\right] \text{ – – – –(2.24)}$$

In the equation above, the flow efficiency term, FE is given thus:

$$FE = a_o + a_1\left(\frac{P_{wf}}{\bar{P}}\right) + a_2\left(\frac{P_{wf}}{\bar{P}}\right)^2 + a_3\left(\frac{P_{wf}}{\bar{P}}\right)^3 \text{ – – – – – – – – – – (2.25)}$$

The coefficients $a_o, a_1 \ldots a_n$ are given thus:

$$a_n = \ b_o + \ b_1 s + b_2 s^2 + b_3 s^3 + \cdots \text{ – – – – – – – – – – –(2.26)}$$

The $b_o, b_1 \ldots b_n$ coefficients are given in reference 37; the s refers to the skin factor.

Gallice and Wiggins[38], in a comparative study of two-phase IPR correlations, gave recommendations on the use of the IPR correlations described above, the collection of data and the quality and reliability of the performance estimates made from such IPR correlations. They concluded that the multipoint methods (Fetkovich and Jones, Blount and Glaze gives better estimates than the single point methods (Vogel, Klins and Majacher, and Sukarno).

Ilk et al[39] provided the analytical developments of "Vogel" type IPR using characteristic flow behavior.

2.4.3 Diffusivity Equation for Solution-gas Drive Reservoirs

The inflow performance relationship discussed above are based on statistical regression of field data, hence the outcomes of using such correlations are dependent on the condition at which the data are sampled[40]. Solution to diffusivity equation therefore provides analytical approach to performance prediction is solution-gas drive reservoirs[40].

The radial flow diffusivity equation for flow of any fluid in a porous media is given as[41]:

$$\frac{1}{r}\frac{d}{dr}\left(\frac{k\rho}{\mu}r\frac{dp}{dr}\right) = \phi c\rho\frac{\partial P}{\partial t} \quad ---------(2.27)$$

This general equation above is non-linear as the coefficients of the equation are functions of the dependent variable – pressure. With relevant assumptions pertinent to slightly compressible liquid flow, equation 2.27 has been linearized and presented as follows[41]:

$$\frac{1}{r}\frac{\partial}{\partial r}\left(r\frac{\partial p}{\partial r}\right)=\frac{\phi\mu c}{k}\frac{\partial P}{\partial t}---------(2.28)$$

The solution to the diffusivity equation for single phase slightly compressible liquid flow (equation 2.28) is a well established concept. A number of such equations have been presented for both constant rate and constant pressure production conditions[42,43,44].

A number of integral transforms of time and pressure have been proposed to linearized the diffusivity equation for multiphase flow conditions (as well as the single phase gas flow) and to correlate the multiphase flow (and the gas flow) solutions with the well established single phase liquid solutions. Pressure integral transforms (known as pseudo-pressure functions) are employed in linearizing the LHS of equation 2.27 while time integral transforms (known as pseudo-time functions) are used to linearize the RHS.

The first pseudo-pressure function was proposed by Al-Hussainny et al[45] to linearize the LHS of equation 2.27 for real gas flow. Agarwal[46] provided the pseudo-time function to linearize the RHS of the equation for real gas flow. Jones and Raghavan[47] provided a pseudo-pressure function to linearize the LHS of the equation for gas condensate systems. They arrived at the pseudo-pressure function by integrating the mobility-density product, $\frac{k\rho}{\mu}$ over the pressure profile from the wellbore, P_{wf} to the reservoir boundary, P_e, and at the boundary, they integrated the product from P_e to the initial reservoir pressure, P_i.

For oil wells, Fetkovich[32] provided the basis for pseudo-pressure functions when he used field experiments to validate the applicability of isochronal test for oil wells. He presented the following equation for boundary-dominated flow:

$$q_o = \frac{kh}{141.2(\ln\frac{r_e}{r_w} - 0.75 + s)}\int_{P_w}^{\bar{P}(t)}\left(\frac{K_{ro}}{\mu_o B_0}\right)dP \text{ ------(2.29)}$$

Camacho and Raghavan[48] provided solution-gas pseudo-pressure and pseudo-time functions with which they were able to correlate solution-gas drive systems with single phase slightly compressible liquid systems. Their pseudo-pressure and pseudo-time functions and the consequent correlations of the solution-gas drive systems to single phase systems was found to be valid for both transient and boundary-dominated flow and also valid for constant-oil rate and constant-pressure production conditions. The Camacho and Raghavan[48] pseudo pressure definition is essentially a unification of similar definitions given by references 32 and 49.

Their pseudo-pressure and pseudo-time definitions which were based on the Muskat's material balance equation[27] are given as follows:

$$P_p(r,t) = \int_{P(r,t)}^{\bar{P}(t)}\left(\frac{K_{ro}}{\mu_o B_0}\right)dP + \int_{\bar{P}(t)}^{P_i}\left(\overline{\frac{K_{ro}}{\mu_o B_0}}\right)dP \text{ -------(2.30)}$$

$$\tilde{t}_{AD} = \frac{0.006328k}{\phi A q(t)}\int_0^t \frac{q(t)\bar{\lambda}(t)}{\bar{c}_T(t)}dt \text{ ------(2.31)}$$

$$\bar{\tilde{t}}_{AD} = \frac{0.006328k}{\phi A}\int_0^t \frac{\bar{\lambda}(t)}{\bar{c}_T(t)}dt \text{ ------(2.32)}$$

Equation 2.32 is only valid for constant rate condition.

The Camacho and Raghavan work is valid for solution-gas drive reservoirs where oil is the dominant flowing phase. Fraim and Wattenbarger[50] extended the Camacho and Raghavan work to predict the flow of all mobile phases. They achieved this by defining integral transforms for time, pressure and rate known as equivalent liquid time, equivalent liquid pressure and equivalent liquid rate respectively. The purpose of the Fraim and Wattenbarger work was to develop a method to analyze multiphase flow with the Fetkovich[12] type curve (the exponential stem).

Marhaendrajana and Permadi[40] presented pseudo-pressure and pseudo-time functions for three phase flow that included oil water and gas.

2.5 DECLINE CURVES ANALYSIS FOR MULTIPHASE FLOWS

The Fetkovick[12] unified type curve is made up of analytical stems (transients and exponential boundary dominated) and empirical stems (boundary-dominated hyperbolic). In order to perform a fully analytical decline analysis (for the purpose of parameter estimation), multiphase flow systems are typically correlated with single phase slightly compressible liquid system (exponential decline) to permit the use of Fetkovich's type curves as well as other existing type curves. The correlation is typically accomplished by the use of special variables in place the conventional variables (time, flowrate).

One of such methods for analyzing production data of wells producing from a solution-gas drive reservoir employs the use of special variables known as equivalent liquid time and equivalent liquid rate; the method was proposed by Fraim and Wattenbarger[50] This method generates the equivalent total mass flow of multiple phases for the total history of

the well which can then be analyzed on any of the existing type curves. Frederick and Kelkar[51] modified the dimensionless rate and the dimensionless cumulative production equations (defined by Fetkovich[12] for single phase model) to generate a new set of equations to approximate the ultimate recovery of solution-gas drive reservoirs.

Chen and Poston[55] introduced the normalized pseudo-time to account for the effects of variations in system mobility and compressibility. The rate-time data for the single phase flow condition (exponential decline) characteristically yields a straight line on a semi-log plot while the hyperbolic decline (multiphase) yields a non-linear relationship on the semi-log plot[4]. The Chen and Poston normalized pseudo-time transform linearizes the semi-log rate-time relationship for the multiphase case and thus removes the ambiguities inherent in analyzing the hyperbolic decline trend. In essence, replacing the conventional 'time' variable with the 'normalized pseudo-time' on the semi-log analysis yields a straight line for multiphase data. The pseudo-time and the pseudo-pressure terms in Chen and Poston formulation are normalized by the initial conditions. A step-by-step procedure of this technique is given in reference 55. The pseudo-time is defined thus[55]:

$$t_p = \int_{t_b}^{t} \frac{\lambda/c_t}{\left(\lambda/c_t\right)_i} \quad \text{(2.33)}$$

2.6 THEORETICAL BASIS FOR DECLINE CURVES ANALYSIS IN SOLUTION-GAS DRIVE RESERVOIRS

A number of attempts have been made to analytically establish the theories of empirical decline analysis and to express empirical decline parameters as functions of physical reservoir and fluid properties. A result of such attempts is the establishment of the fact that the exponential decline is a consequence of single phase slightly compressible liquid production[3,12] Guo et al[3] showed that the relative decline rate and production rate decline equations for exponential decline model can be derived rigorously by combining the pseudo-steady state flow equation for a volumetric reservoir model with the single phase material balance equation. They derived an analytical expression for the empirical decline parameter, D_i in terms of physical reservoir/fluid property thus:

$$D_i = \frac{kh}{141.2\mu c_t N_i \left[ln\left(\frac{0.472r_e}{r_w}\right) + s\right]} \quad -------(2.34)$$

2.6.1 Fetkovich Type Curves

Fetkovich,[12] using a combination of simple material balance equation and the oil well rate-pressure relationships previously developed in reference 32 was able to analytically derive a rate-time relationship for single phase flow. The rate-time relationship so derived was a form of the exponential decline equation but in terms of reservoir variables. From the relationship, he developed an analytical expression for the empirical decline parameter, D_i in terms of physical reservoir/fluid property thus:

$$D_i = \left[\frac{0.00634k}{\varphi\mu c_t r_w^2}\right]\left[\frac{1}{\frac{1}{2}\left[\left(\frac{r_e}{r_w}\right)^2 - 1\right]\left[ln\left(\frac{r_e}{r_w}\right) - \frac{1}{2}\right]}\right] \quad ----------(2.35)$$

Additionally, Fetkovich[12] combined analytical solution of the transient (early-time) period with empirical solution of the boundary-dominated (late-time) period on the same log-log dimensionless type curve. Hence, the type curves have two regions: the transient (early-time) and the boundary-dominated (late-time) curves; this effectively encompasses the entire production life. The entire Fetkovich type curve analysis is based on the following dimensionless variables derived from the general Arps' hyperbolic equation.

$$q_{Dd} = \frac{q}{q_i} \quad ----------(2.36)$$

$$t_{Dd} = D_i t \quad ---------- (2.37)$$

The early-time curves of Fetkovich type curves were gotten by transforming the analytical constant well pressure solutions (for single phase slightly compressible liquid) of diffusivity equation. The original solution has been presented in terms of dimensionless flowrate and dimensionless[43]. The dimensionless flowrate and time are defined thus:

$$Dimensionless\ Flowrate\ q_D = \frac{141.3q\mu B}{kh(P_i - P_{wf})} \quad ------- (2.38)$$

$$Dimensinless\ Time\ t_D = \frac{0.00634kt}{\varphi\mu c_t r_w^2} ------- (2.39)$$

Fetkovich transformed the solutions from the original variables q_D and t_D to the decline dimensionless variables q_{Dd} and t_{Dd} using the following relationships which he had derived[12]:

$$q_{Dd} = \frac{q}{q_i} = q_D\left[ln\left(\frac{r_e}{r_w}\right) - \frac{1}{2}\right] = \frac{q}{\frac{kh(P_i - P_{wf})}{141.3q\mu B\left[ln\left(\frac{r_e}{r_w}\right) - \frac{1}{2}\right]}} \quad ----------(2.40)$$

And

$$t_{Dd} = \left[\frac{t_D}{\frac{1}{2}\left[\left(\frac{r_e}{r_w}\right)^2 - 1\right] ln\left[\left(\frac{r_e}{r_w}\right) - \frac{1}{2}\right]}\right]$$

$$= \left[\frac{0.00634kt}{\varphi\mu c_t r_w^2}\right]\left[\frac{1}{\frac{1}{2}\left[\left(\frac{r_e}{r_w}\right)^2 - 1\right] ln\left[\left(\frac{r_e}{r_w}\right) - \frac{1}{2}\right]}\right] --(2.41)$$

The transformed solutions were plotted for various values of$\frac{r_e}{r_w}$. At the onset of boundary-dominated flow, all the curves were found to converge to a single exponential curve at t_D value of about 0.1. This shows that the late-time (boundary-dominated) behavior of the system for all single phase reservoir sizes obeys the exponential decline model.

The late-time portion of the Fetkovich type curves were gotten by plotting the Arp's empirical equation in dimensionless terms given below as:

$$q_{Dd} = \frac{1}{(1 + bt_{Dd})^{\frac{1}{b}}} \quad -------(2.42)$$

Plotting equation 2.42 above, i.e. q_{Dd} versus t_{Dd} for various values of b, it was found that all the curves converged at t_D = 0.3 to a single curve corresponding to b = 0.

2.6.2 Camacho and Raghavan Attempt

The theoretical considerations in the Fetkovich work were based on the assumption of a single phase reservoir. For solution-gas drive reservoirs leading to hyperbolic decline, Camacho and Raghavan[10] provided a theoretically rigorous derivation of the decline exponents(D_i *and* b). Using the pseudo-pressure and pseudo-time functions defined in reference 48, they developed expressions for the dimensionless pseudo-pressure, $\bar{P}_{pD}$ corresponding to the average reservoir pressures, in terms of the two dimensionless pseudo-time definitions (equations 2.31 and 2.32 above). The expressions for the average dimensionless pseudo-pressures are as follows:

$$\bar{P}_{pD} = \frac{kh}{141.2q(t)} \int_{\bar{P}(t)}^{P_i} \left(\overline{\frac{K_{ro}}{\mu_o B_0}}\right) dP \;\; = 2\pi \tilde{t}_{AD} - - - - - (2.43)$$

$$\bar{P}_{pD} = \frac{kh}{141.2q(t)} \int_{\bar{P}(t)}^{P_i} \left(\overline{\frac{K_{ro}}{\mu_o B_0}}\right) dP \;\cong -D\left(1 - \exp\left(\frac{2\pi \bar{\bar{t}}_{AD}}{D}\right)\right) - - - - - (2.44)$$

Where $D = \frac{1}{2}\left[ln\frac{4A}{e^{\gamma}C_A r_w^2} + 2s\right]$

Differentiating equations 2.43 and 2.44 above and making a number of substitutions, the authors obtained the following expression:

$$\frac{1}{q}\frac{dq}{dt} = \frac{dlnq}{dt} = -\frac{2\pi 0.006328k}{\phi AD}\frac{\overline{\lambda_T}}{\bar{c}_T} - - - - - -(2.45)$$

Relating equation 2.45 above to Arps' exponential rate-time equation (see table 2.1), they showed that the empirical decline parameter D_i can be expressed in terms of physical rock and fluid properties thus:

$$D_i = \frac{2\pi 0.006328k\left(\frac{\bar{\lambda}}{\bar{c}_T}\right)}{D\varphi A} - - - - - - - - (2.46)$$

Furthermore, employing the concept of loss ratio defined as follows: $\frac{d}{dt}\left(1/\frac{dlnq}{dt}\right) = -b$, they showed that the empirical decline parameter D_i can be expressed in terms of physical rock and fluid properties thus:

$$b = \frac{D\varphi A}{2\pi 0.006328k}\frac{d}{dt}\left(\frac{\bar{c}_T}{\bar{\lambda}}\right) - - - - - - - - (2.47)$$

The authors also gave a discussion on the conditions under which the Arps' equation might be used to analyze data thus:

1. If the ratio $\frac{\bar{\lambda}}{\bar{c}_T}$ is approximately constant through time, then the rate data would fit to the Arps' exponential decline ($b = 0$)
2. If the ratio $\frac{\bar{\lambda}}{\bar{c}_T}$ is a linear function of time, then the rate data would fit to a unique member of the hyperbolic family (b = constant)

However, the authors observed from their simulation studies that the ratio $\frac{\bar{\lambda}}{\bar{c}_T}$ varies non-linearly with time. They also noted that the exponent b is not constant in most of the theoretical studies.

2.6.3 The Non-Darcy Considerations

In the Camacho and Raghavan approach presented above, the non-Darcy flow caused by near-wellbore turbulence effect was not considered. However, non-Darcy flow may be considered as a normal occurrence in solution gas drive reservoirs[52]. In analyzing their results, the authors[10] noted that a given simulation rate data did not match a unique value of exponent b on the Arps' type curves; they suggested that in reality, the presence of rate-dependent variable skin factor such as near wellbore non-Darcy flow effects could yield a fairly constant value of exponent b. Non-Darcy effects are accounted for using one of the equations below:

1. Forchheimer Equation[53]:

$$\frac{dp}{dr} = \frac{\mu}{k}v + \beta\rho v^2 \quad ---------- (2.48)$$

The parameter β in the expression above is known as the inertial coefficient and is given as follows:

$$\beta = \frac{48511}{\varphi^{5.5}k^{0.5}} \quad ---------- (2.49)$$

2. Rate-dependent variable skin factor[54]:

The total skin factor s_T in the flow equation is seen as the sum of a constant mechanical skin factor and a rate-dependent skin factor due to inertial/non-Darcy flow effects.

$$s_T = s_m + Nq \quad \text{----------} \quad (2.50)$$

Where N is known as the Non-Darcy flow coefficient.

The non-Darcy flow coefficient and the inertial coefficient are also related as follows[54]:

$$N = \frac{1.027336 \times 10^{-15} \beta \rho k}{2\pi\mu h}\left(\frac{1}{r_w} - \frac{1}{r_e}\right) \quad \text{----------} \quad (2.51)$$

CHAPTER 3

THEORETICAL DEVELOPMENTS

3.1 OVERVIEW AND BACKGROUND INFORMATION

This work sets out essentially to investigate the fundamental theories of reservoir and fluid interactions underlying the empirically established trends of rate decline in solution-gas driver reservoirs. The motivation for the investigation was to establish a functional relationship between the theoretical domain and the empirical domain; such a relationship is useful not only in verifying results of empirical analyses but also in formulating procedures for reservoir properties (permeability, drainage radius e.t.c.) estimation using field production data.

The subject dealing with the empirical domain of rate decline trends in reservoir is known as decline curve analysis (DCA) and is largely based on Arps[2] 1945 work. Typically, decline curve analysis involves the determination of empirical parameters a *and* b in the Arps

equation; this is conventionally done by fitting historical rate-time data to the Arps general equation. The parameter b, which assigns a given reservoir rate decline trend to a specific member of the Arps hyperbolic family ($0 \leq b \leq 1.0$) is the focus of this work.

Essentially, the theories developed in this work are herein presented in three sections. The foremost consideration in this work is the establishment of a functional relationship between the empirical domain (b_{emp}) and the theoretical domain(b_{th}). A consideration for non-Darcy flow effects in the near wellbore region was then developed as an attempt to investigate suggestions from various researchers[10,32,52] on the effects of non-Darcy flow on the b parameter. Lastly, a theoretical derivation is made to mathematically justify the existence of the hyperbolic family of curves for solution-gas drive reservoirs. This derivation is based on a novel concept of inner boundary condition of the diffusivity equation in terms of solution-gas pseudo pressure and pseudo time functions.

3.2 RELATIONSHIP BETWEEN EMPIRICAL AND THEORETICAL DECLINE PARAMETER ($b_{emp} vs\ b_{th}$)

The empirical domain of decline curves analysis is based on Arps[2] general equation given as follows:

$$-\frac{1}{q}\frac{dq}{dt} = aq^{b_{emp}} \quad ---------(3.1)$$

The parameter b has also been expressed in terms of physical reservoir and fluid properties as follows[10]

$$b_{th} = \frac{\phi A}{2\pi 0.006328k} D \frac{d}{dt}\left(\frac{\bar{c}_T}{\bar{\lambda}_T}\right) - - - - - - - - (3.2)$$

Note: In this work, the b parameter from the empirical domain has been denoted as b_{emp} while that from the theoretical domain is denoted as b_{th}; this is done to distinguish clearly distinguish the two parameters for clarity sake.

Until now, it has been expected that the two parameters above (b_{th} and b_{emp}) represent the same quantity; this expectation is expressed in suggestions by reference 10 on physical phenomena that could yield a constant value of b_{th} (through time) to match a given value of b_{emp}. However, simulations carried out in this work (and reported in chapter 5) yields values of b_{th} that varied considerably with time (for a given reservoir) and exhibited no tendency for constancy even with considerations for non-Darcy flow near the wellbore as suggested by reference 10.

Considering the above trend, this work then proposed the following hypothesis as being the actual implications of b_{th} values (through time) computed from reservoir and fluid properties as compared to a given b_{emp} (constant value) computed empirically from historical rate-time data.

a. The theoretical b_{th} values could possibly not mean the same thing as the empirical b_{emp} value
b. The theoretical values, b_{th} could be seen as reflecting the actual dynamics of the reservoir and the fluid behavior through time; hence it may be expected to have a transient (varying) behavior against any anticipation for its constancy.

c. The empirical value (b_{emp}) might as well be seen as representing some sort of weighted average of the theoretical values (b_{th}) over time.

d. If a relationship between b_{emp} and some sort of weighted average of b_{th} values (say $\overline{b_{th}}$) could be derived, then such link will offer the opportunity for an **improved formation evaluation methods** using decline curves analysis in solution-gas drive reservoirs.

This work then defined a new parameter known as $\overline{b_{th}}$ (being the time-weighted average of b_{th} values over time) and went further to derive a functional relationship between b_{emp} and $\overline{b_{th}}$ in the fourth point above. The derivation is presented below.

3.2.1 Derivation of Relationship

Since the b_{th} values vary widely through time, it is convenient to say b_{th} is a function of time t and not a constant value through time (even with the so-called non-Darcy effect considered)

$$\therefore b_{th} = f(t)$$

A new parameter known as $\overline{b_{th}}$ (being the time-weighted average of b_{th} values over time) is then defined in this work as follows:

$$\overline{b_{th}} = \frac{\sum_{t_o}^{t}(b_{th} \times incremental\ time\ elapsed)}{Total\ Time\ elapsed\ since\ decline}$$

That is,

$$\overline{b_{th}} = \frac{\sum_{t_o}^{t_i}\left(b_{th} \times \left(t_{(i)} - t_{(i-1)}\right)\right)}{t_{(i)} - t_o} \text{ ----------(3.3)}$$

The time denoted by t_o in the equation above corresponds to the onset of decline.

The summation term above was then represented by an integral of $b_{th} = f(t)$, thus;

$$\overline{b_{th}} = \frac{\sum_{t_o}^{t_i}\left(b_{th} \times t_{(i)} - t_{(i-1)}\right)}{t_{(i)} - t_o} = \frac{\int_{t_o}^{t_i} b_{th}\, dt}{t_{(i)} - t_o} = \frac{\int_{t_o}^{t_i} f(t)\, dt}{t_{(i)} - t_o} \text{ ----(3.4)}$$

Since equation 3.2 above gives values of b_{th} varying with time, the RHS of equation 3.2 can be taken as $b_{th} = f(t)$.

Equation 3.2 was then substituted into equation 3.4 to yield the following:

$$\overline{b_{th}} = \frac{\int_{t_o}^{t_i} \frac{\phi A}{2\pi 0.006328k} D \frac{d}{dt}\left(\frac{\bar{c}_T}{\overline{\lambda_T}}\right) dt}{t_{(i)} - t_o}$$

$$\therefore \overline{b_{th}} = \frac{\frac{\phi AD}{2\pi 0.006328k}\left(\frac{\bar{c}_T}{\overline{\lambda_T}}\right)}{t_{(i)} - t_o} \text{ --------(3.5)}$$

But reference 10 has shown that $-\frac{2\pi 0.006328k}{\phi AD}\frac{\overline{\lambda_T}}{\bar{c}_T} = \frac{dlnq}{dt}$

Then,

$$-\frac{\phi AD}{2\pi 0.006328k}\left(\frac{\bar{c}_T}{\overline{\lambda_T}}\right) = \frac{1}{\frac{dlnq}{dt}} = \frac{1}{\frac{1}{q}\frac{dq}{dt}} \text{ --------(3.6)}$$

Substitution of equation 3.6 into equation 3.5 yielded the following:

$$\overline{b_{th}} = -\frac{qdt}{dq}\left(\frac{1}{t_{(i)} - t_o}\right)$$

Therefore,

$$-\frac{1}{q}\frac{dq}{dt} = \frac{1}{\overline{b_{th}}\left(t_{(i)} - t_o\right)} - - - - - - - - -(3.7)$$

Substitution of equation 3.1 into equation 3.7 above yielded the following functional relationship between $\overline{b_{th}}$ and b_{emp}as proposed in one of the hypothesis above:

$$\frac{1}{\overline{b_{th}}\left(t_{(i)} - t_o\right)} = aq_{(i)}{}^{b_{emp}} - - - - - - - - - - -(3.8)$$

Equation 3.8 then presented the anticipated link between the empirical regime and the theoretical regime. In addition, equation 3.8 above showed that in the actual sense, the exponent b_{emp}, computed empirically from production data, may not be taken to represent the same thing as the b_{th} values computed theoretically, rather, b_{emp} should be seen as related to the time-weighted average of b_{th} (i.e. $\overline{b_{th}}$) as given by equation 3.8.

To the best of my knowledge, this view as well as the derived relationship (equation 3.8) has not been presented previously by any investigator and may be a significant contribution of this work.

3.2.2 Significance of the Derived Relationship: Permeability Estimation

The LHS of equation 3.8 can be represented as follows, from equation 3.5:

$$\frac{1}{\overline{b_{th}}\left(t_{(i)}-t_o\right)}=\frac{2\pi 0.006328k}{\phi AD}\frac{\overline{\lambda_T}}{\bar{c}_T}\text{ }-\text{ }-\text{ }-\text{ }-\text{ }-\text{ }-\text{ }-\text{ }-\text{ }-\text{ }-\text{ }-(3.9)$$

The equality (at least in the approximate sense) of the RHS of both equations 3.8 and 3 .9 was verified using simulation results; this verification is presented in chapter 5. Thus, the two RHS can be set to each other thus:

$$aq_{(i)}{}^{b_{emp}}\cong\frac{2\pi 0.006328k}{\phi AD}\frac{\overline{\lambda_T}}{\bar{c}_T}\text{ }-\text{ }-\text{ }-\text{ }-\text{ }-\text{ }-\text{ }-\text{ }-\text{ }-\text{ }-\text{ }(3.10)$$

Solving for permeability k in equation 10 above then yielded the following:

$$k=\frac{aq_{(i)}{}^{b_{emp}}\phi AD}{2\pi 0.006328}\frac{\bar{c}_T}{\overline{\lambda_T}}-\text{ }-\text{ }-\text{ }-\text{ }-\text{ }-\text{ }-\text{ }-\text{ }-\text{ }-\text{ }-(3.11)$$

Equation 3.11 then formed the basis for a new method for estimating reservoir permeability. The proposed method is presented in chapter 5; and is demonstrated with examples.

3.3 CONSIDERATIONS FOR THE EFFECTS OF NON-DARCY FLOW ON THE DECLINE PARAMETER (b_{th})

Reference 10 had suggested that the presence of rate-dependent variable skin factor such as the near wellbore non-Darcy flow effects could yield a constant value of the theoretically computed parameter b_{th}through time. This work then attempted to investigate the possibility of that suggestion by incorporating the non-Darcy term into the derivation of the b_{th} expression. The derivation for the b_{th} expression (equation 3.2) without consideration for non-Darcy flow has been presented by reference 10. Presented below is the current attempt by this work at the same derivation but with considerations for non-Darcy flow.

The total skin factor s_T in the fluid flow equation is seen as the sum of a constant mechanical skin factor and a rate-dependent skin factor due to inertial/non-Darcy flow effects[54].

$$s_T = s_m + Nq_{fg}$$

This work considered the rate term in the equation above to be the rate of the free gas flow in the reservoir since the free gas is the agent of the turbulence leading to the non-Darcy flow effects. The parameter N is known as the Non-Darcy flow coefficient. Incorporating this yields:

$$q = \frac{kh(\bar{P} - P_{wf})}{141.2\mu B(\ln r_D - \frac{3}{4} + s_m + Nq_{fg})}$$

In reference 10, the group $(\ln r_D - \frac{3}{4} + s_m)$ has been denoted as D

Therefore, with considerations for non-Darcy flow effects, the following equation applies:

$$q = \frac{kh(\bar{P} - P_{wf})}{141.2\mu B(D + Nq_{fg})}$$

Whereas, without considerations for non-Darcy flow effects, the following applies:

$$q = \frac{kh(\bar{P} - P_{wf})}{141.2\mu B(D)}$$

In essence, this work considered that the non-Darcy flow effects could be accounted for by replacing $D$with $D + Nq_{fg}$ in the original derivation presented by Camacho and Raghavan[10]

The following expressions concerning the solution-gas pseudo-pressure function has been validated and reported[10]:

$$\bar{P}_{pD} = \frac{kh}{141.2q(t)} \int_{\bar{P}(t)}^{P_i} \left(\frac{\overline{K_{ro}}}{\mu_o B_0}\right) d\bar{P} - - - - - - - - - - (3.12)$$

$$\bar{P}_{pD} \cong -D\left(1 - \exp\left(\frac{2\pi \bar{\bar{t}}_{AD}}{D}\right)\right) - - - - - - - - - - - - (3.13)$$

$$where\ \bar{\bar{t}}_{AD} = \frac{0.006328k}{\phi A} \int_0^t \frac{\bar{\lambda}(t)}{\bar{c}_T(t)} dt - - - - - (3.14)$$

Replacing D with $D + Nq_{fg}$ in equation 3.13 as explained earlier:

$$\bar{P}_{pD} \cong -(D + Nq_{fg})\left(1 - \exp\left(\frac{2\pi\bar{\bar{t}}_{AD}}{D + Nq_{fg}}\right)\right) - - - - - - - - - - - (3.15)$$

Equating the right-hand sides of equations 3.12 and 3.15;

$$\frac{kh}{141.2q(t)} \int_{\bar{P}(t)}^{P_i} \left(\overline{\frac{K_{ro}}{\mu_o B_0}}\right) d\bar{P} = -\left(D + Nq_{fg}\right)\left(1 - \exp\left(\frac{2\pi\bar{\bar{t}}_{AD}}{D + Nq_{fg}}\right)\right) - - - - - - (3.16)$$

Expanding the RHS of equation 3.16;

$$\frac{kh}{141.2q(t)} \int_{\bar{P}(t)}^{P_i} \left(\overline{\frac{K_{ro}}{\mu_o B_0}}\right) d\bar{P} = -D + \mathrm{D}\exp\left(\frac{2\pi\bar{\bar{t}}_{AD}}{D + Nq_{fg}}\right) - Nq_{fg} + Nq_{fg}\exp\left(\frac{2\pi\bar{\bar{t}}_{AD}}{D + Nq_{fg}}\right) - - - (3.17)$$

Differentiating equation 3.17 with respect to time and considering the fact that this is a variable rate-problem; that is a rate decline problem. (Note that for constant rate considerations, (e.g. in well test applications) the differentiation would be straightforward and would yield a rather simple expression)

$$\frac{kh}{141.2}\left[\frac{1}{q}\left(\overline{\frac{K_{ro}}{\mu_o B_0}}\right)\frac{d\bar{P}}{dt} - \frac{1}{q^2}\frac{dq}{dt}\int_{\bar{P}(t)}^{P_i}\left(\overline{\frac{K_{ro}}{\mu_o B_0}}\right)d\bar{P}\right] =$$

$$\left[\left(\frac{(D+Nq_{fg})0.006328k}{\phi A}\frac{\bar{\lambda}}{\bar{c}_T} - \bar{\bar{t}}_{AD}N\frac{dq_{fg}}{dt}\right)\frac{2\pi D}{(D+Nq_{fg})^2}\exp\left(\frac{2\pi\bar{\bar{t}}_{AD}}{D+Nq_{fg}}\right)\right] - \left[N\frac{dq_{fg}}{dt}\right] +$$

$$\left[N\frac{dq_{fg}}{dt}\exp\left(\frac{2\pi\bar{\bar{t}}_{AD}}{D+Nq_{fg}}\right)\right]+$$

$$\left[\left(\frac{(D+Nq_{fg})0.006328k}{\phi A}\frac{\bar{\lambda}}{\bar{c}_T}-\bar{\bar{t}}_{AD}N\frac{dq_{fg}}{dt}\right)\frac{2\pi Nq_{fg}}{(D+Nq_{fg})^2}\exp\left(\frac{2\pi\bar{\bar{t}}_{AD}}{D+Nq_{fg}}\right)\right]-\cdots-\cdots-(3.18)$$

Treating the LHS of the equation 3.18 above:

$$LHS=\frac{kh}{141.2}\left[\frac{1}{q}\left(\overline{\frac{K_{ro}}{\mu_o B_0}}\right)\frac{d\bar{P}}{dt}-\frac{1}{q^2}\frac{dq}{dt}\int_{\bar{P}(t)}^{P_i}\left(\overline{\frac{K_{ro}}{\mu_o B_0}}\right)d\bar{P}\right]$$

$$=\frac{1}{q}\frac{kh}{141.2}\left(\overline{\frac{K_{ro}}{\mu_o B_0}}\right)\frac{d\bar{P}}{dt}-\frac{1}{q}\frac{dq}{dt}\frac{kh}{141.2q}\int_{\bar{P}(t)}^{P_i}\left(\overline{\frac{K_{ro}}{\mu_o B_0}}\right)d\bar{P}----(3.19)$$

From reference 10, the following relationships have been derived:

$$\frac{kh}{141.2}\left(\overline{\frac{K_{ro}}{\mu_o B_0}}\right)\frac{d\bar{P}}{dt}=\frac{2\pi 0.006328k}{\phi A}q\frac{\bar{\lambda}}{\bar{c}_T}-\cdots-\cdots-(3.20)$$

$$\frac{kh}{141.2q}\int_{\bar{P}(t)}^{P_i}\left(\overline{\frac{K_{ro}}{\mu_o B_0}}\right)d\bar{P}=-D\left(1-\exp\left(\frac{2\pi\bar{\bar{t}}_{AD}}{D}\right)\right)-\cdots-\cdots-(3.21)$$

Here, the non-Darcy flow effects is again accounted for by replacing D with $D+Nq_{fg}$ in equation 3.21 to give

$$\frac{kh}{141.2q}\int_{\bar{P}(t)}^{P_i}\left(\frac{\overline{K_{ro}}}{\mu_o B_0}\right)d\bar{P} = -\left(D+Nq_{fg}\right)\left(1-\exp\left(\frac{2\pi\bar{\bar{t}}_{AD}}{\left(D+Nq_{fg}\right)}\right)\right) - - - - - - - - (3.22)$$

Substituting equations 3.20 and 3.22 into 3.19,

$$LHS = \frac{2\pi 0.006328k}{\phi A}\frac{\bar{\lambda}}{\bar{c}_T} - \frac{1}{q}\frac{dq}{dt}\left(-\left(D+Nq_{fg}\right)\left(1-\exp\left(\frac{2\pi\bar{\bar{t}}_{AD}}{\left(D+Nq_{fg}\right)}\right)\right)\right) - - - - (3.23)$$

Now, treating the RHS of the equation 3.18 above:

$$RHS = -\left[N\frac{dq_{fg}}{dt}\right] + \left[N\frac{dq_{fg}}{dt}\exp\left(\frac{2\pi\bar{\bar{t}}_{AD}}{D+Nq_{fg}}\right)\right] + \left[\frac{2\pi}{\left(D+Nq_{fg}\right)}\left(\frac{(D+Nq)0.006328k}{\phi A}\frac{\bar{\lambda}}{\bar{c}_T} - \bar{\bar{t}}_{AD}N\frac{dq_{fg}}{dt}\right)\exp\left(\frac{2\pi\bar{\bar{t}}_{AD}}{D+Nq_{fg}}\right)\right]$$

$$RHS = \left[-N\frac{dq_{fg}}{dt}\left(1-\exp\left(\frac{2\pi\bar{\bar{t}}_{AD}}{D+Nq_{fg}}\right)\right)\right] + \left[\frac{2\pi 0.006328k}{\phi A}\frac{\bar{\lambda}}{\bar{c}_T}\exp\left(\frac{2\pi\bar{\bar{t}}_{AD}}{D+Nq_{fg}}\right)\right] - \left[\frac{2\pi}{\left(D+Nq_{fg}\right)}\bar{\bar{t}}_{AD}N\frac{dq_{fg}}{dt}\exp\left(\frac{2\pi\bar{\bar{t}}_{AD}}{D+Nq_{fg}}\right)\right] - - - - - (24)$$

Coupling the entire equation back by equating equation 3.23 (LHS) to equation 3.24 (RHS):

$$\frac{2\pi 0.006328k}{\phi A}\frac{\bar{\lambda}}{\bar{c}_T} - \frac{1}{q}\frac{dq}{dt}\left(-\left(D+Nq_{fg}\right)\left(1-\exp\left(\frac{2\pi\bar{\bar{t}}_{AD}}{\left(D+Nq_{fg}\right)}\right)\right)\right)$$

$$= \left[-N\frac{dq_{fg}}{dt}\left(1-\exp\left(\frac{2\pi\bar{\bar{t}}_{AD}}{D+Nq_{fg}}\right)\right)\right] + \left[\frac{2\pi 0.006328k}{\phi A}\frac{\bar{\lambda}}{\bar{c}_T}\exp\left(\frac{2\pi\bar{\bar{t}}_{AD}}{D+Nq_{fg}}\right)\right]$$

$$-\left[\frac{2\pi}{\left(D+Nq_{fg}\right)}\bar{\bar{t}}_{AD}N\frac{dq_{fg}}{dt}\exp\left(\frac{2\pi\bar{\bar{t}}_{AD}}{D+Nq_{fg}}\right)\right]$$

Rearranging the terms of the equation above;

$$\left[N\frac{dq_{fg}}{dt}\left(1-\exp\left(\frac{2\pi\bar{\bar{t}}_{AD}}{D+Nq_{fg}}\right)\right)\right] - \left[\frac{2\pi 0.006328k}{\phi A}\frac{\bar{\lambda}}{\bar{c}_T}\exp\left(\frac{2\pi\bar{\bar{t}}_{AD}}{D+Nq_{fg}}\right)\right] + \left[\frac{2\pi 0.006328k}{\phi A}\frac{\bar{\lambda}}{\bar{c}_T}\right] +$$

$$\left[\frac{2\pi}{\left(D+Nq_{fg}\right)}\bar{\bar{t}}_{AD}N\frac{dq_{fg}}{dt}\exp\left(\frac{2\pi\bar{\bar{t}}_{AD}}{D+Nq_{fg}}\right)\right] = \frac{1}{q}\frac{dq}{dt}\left(-\left(D+Nq_{fg}\right)\left(1-\exp\left(\frac{2\pi\bar{\bar{t}}_{AD}}{\left(D+Nq_{fg}\right)}\right)\right)\right)$$

Hence,

$$\left[N\frac{dq_{fg}}{dt}\left(1-\exp\left(\frac{2\pi\bar{\bar{t}}_{AD}}{D+Nq_{fg}}\right)\right)\right] + \left[\frac{2\pi 0.006328k}{\phi A}\frac{\bar{\lambda}}{\bar{c}_T}\left(1-\exp\left(\frac{2\pi\bar{\bar{t}}_{AD}}{D+Nq_{fg}}\right)\right)\right] +$$

$$\left[\frac{2\pi}{\left(D+Nq_{fg}\right)}\bar{\bar{t}}_{AD}N\frac{dq_{fg}}{dt}\exp\left(\frac{2\pi\bar{\bar{t}}_{AD}}{D+Nq_{fg}}\right)\right] = \frac{1}{q}\frac{dq}{dt}\left(-\left(D+Nq_{fg}\right)\left(1-\exp\left(\frac{2\pi\bar{\bar{t}}_{AD}}{\left(D+Nq_{fg}\right)}\right)\right)\right)$$

Simplifying further;

$$\left[N\frac{dq_{fg}}{dt}+\frac{2\pi 0.006328k}{\phi A}\frac{\bar{\lambda}}{\bar{c}_T}\right]\left(1-\exp\left(\frac{2\pi\bar{\bar{t}}_{AD}}{D+Nq_{fg}}\right)\right)+\left[\frac{2\pi}{(D+Nq_{fg})}\bar{\bar{t}}_{AD}N\frac{dq_{fg}}{dt}\exp\left(\frac{2\pi\bar{\bar{t}}_{AD}}{D+Nq_{fg}}\right)\right]=$$

$$\frac{1}{q}\frac{dq}{dt}\left(-(D+Nq_{fg})\left(1-\exp\left(\frac{2\pi\bar{\bar{t}}_{AD}}{(D+Nq_{fg})}\right)\right)\right)$$

So that;

$$-\frac{1}{q}\frac{dq}{dt}=\frac{1}{D+Nq_{fg}}\left[N\frac{dq_{fg}}{dt}+\frac{2\pi 0.006328k}{\phi A}\frac{\bar{\lambda}}{\bar{c}_T}\right]+\frac{\left[\frac{2\pi\bar{\bar{t}}_{AD}}{D+Nq_{fg}}N\frac{dq_{fg}}{dt}\exp\left(\frac{2\pi\bar{\bar{t}}_{AD}}{D+Nq_{fg}}\right)\right]}{\left(-(D+Nq_{fg})\left(1-\exp\left(\frac{2\pi\bar{\bar{t}}_{AD}}{(D+Nq_{fg})}\right)\right)\right)}$$

Therefore;

$$-\frac{1}{q}\frac{dq}{dt}=\frac{1}{D+Nq_{fg}}\left[\frac{2\pi 0.006328k}{\phi A}\frac{\bar{\lambda}}{\bar{c}_T}\right]+\frac{N\frac{dq_{fg}}{dt}}{D+Nq_{fg}}+\frac{\left[\frac{2\pi\bar{\bar{t}}_{AD}}{D+Nq_{fg}}N\frac{dq_{fg}}{dt}\exp\left(\frac{2\pi\bar{\bar{t}}_{AD}}{D+Nq_{fg}}\right)\right]}{\left((D+Nq_{fg})\left(1-\exp\left(\frac{2\pi\bar{\bar{t}}_{AD}}{(D+Nq_{fg})}\right)\right)\right)}$$

Combining the second and the third terms of the RHS of the equation above;

$$-\frac{1}{q}\frac{dq}{dt}=\frac{1}{D+Nq_{fg}}\left[\frac{2\pi 0.006328k}{\phi A}\frac{\bar{\lambda}}{\bar{c}_T}\right]+\frac{\frac{2\pi\bar{\bar{t}}_{AD}}{D+Nq_{fg}}N\frac{dq_{fg}}{dt}\exp\left(\frac{2\pi\bar{\bar{t}}_{AD}}{D+Nq_{fg}}\right)+N\frac{dq_{fg}}{dt}\left(1-\exp\left(\frac{2\pi\bar{\bar{t}}_{AD}}{(D+Nq_{fg})}\right)\right)}{(D+Nq_{fg})\left(1-\exp\left(\frac{2\pi\bar{\bar{t}}_{AD}}{(D+Nq_{fg})}\right)\right)}$$

$$-\frac{1}{q}\frac{dq}{dt}=\frac{1}{D+Nq_{fg}}\left[\frac{2\pi 0.006328k}{\phi A}\frac{\bar{\lambda}}{\bar{c}_T}\right]$$

$$+\frac{\frac{2\pi\bar{\bar{t}}_{AD}}{D+Nq_{fg}}N\frac{dq_{fg}}{dt}\exp\left(\frac{2\pi\bar{\bar{t}}_{AD}}{D+Nq_{fg}}\right)-N\frac{dq_{fg}}{dt}\exp\left(\frac{2\pi\bar{\bar{t}}_{AD}}{(D+Nq_{fg})}\right)+N\frac{dq_{fg}}{dt}}{(D+Nq_{fg})\left(1-\exp\left(\frac{2\pi\bar{\bar{t}}_{AD}}{(D+Nq_{fg})}\right)\right)}$$

Simplifying the expression above by factorizing the common factors of the numerator of its second term yielded the following expression below:

$$-\frac{1}{q}\frac{dq}{dt}=\frac{1}{D+Nq_{fg}}\left[\frac{2\pi 0.006328k}{\phi A}\frac{\bar{\lambda}}{\bar{c}_T}\right]+\frac{N\frac{dq_{fg}}{dt}\left[\left(\frac{2\pi\bar{\bar{t}}_{AD}}{(D+Nq_{fg})}-1\right)\exp\left(\frac{2\pi\bar{\bar{t}}_{AD}}{(D+Nq_{fg})}\right)+1\right]}{(D+Nq_{fg})\left(1-\exp\left(\frac{2\pi\bar{\bar{t}}_{AD}}{(D+Nq_{fg})}\right)\right)}$$

$$-\ -\ -\ -\ -\ -\ -\ -\ -\ -\ -\ -\ -\ -\ -\ -\ (3.25)$$

Assuming the value of $\frac{2\pi\bar{\bar{t}}_{AD}}{(D+Nq_{fg})}$ is small enough, the entire numerator of the second term of equation 3.25 can be said to be negligible compared to the first term. This is shown thus:

If $\frac{2\pi\bar{\bar{t}}_{AD}}{(D+Nq_{fg})}$ is small enough, the exponential term can be approximated by its series expansion truncated from the second degree term thus:

For small values of x; $e^x = 1 + x + \frac{x^2}{2}$ … Truncated from the second degree, $e^x \cong 1 + x$

Therefore equation 3.25 becomes the following;

$$-\frac{1}{q}\frac{dq}{dt}=\frac{1}{D+Nq_{fg}}\left[\frac{2\pi 0.006328k}{\phi A}\frac{\bar{\lambda}}{\bar{c}_T}\right]+\frac{N\frac{dq_{fg}}{dt}\left[\left(\frac{2\pi\bar{\bar{t}}_{AD}}{(D+Nq_{fg})}-1\right)\left(1+\left(\frac{2\pi\bar{\bar{t}}_{AD}}{(D+Nq_{fg})}\right)\right)+1\right]}{(D+Nq_{fg})\left(1-\exp\left(\frac{2\pi\bar{\bar{t}}_{AD}}{(D+Nq_{fg})}\right)\right)}$$

$$-\frac{1}{q}\frac{dq}{dt}=\frac{1}{D+Nq_{fg}}\left[\frac{2\pi 0.006328k}{\phi A}\frac{\bar{\lambda}}{\bar{c}_T}\right]+\frac{N\frac{dq_{fg}}{dt}\left[\left(\left(\frac{2\pi\bar{\bar{t}}_{AD}}{(D+Nq_{fg})}\right)^2-1\right)+1\right]}{(D+Nq_{fg})\left(1-\exp\left(\frac{2\pi\bar{\bar{t}}_{AD}}{(D+Nq_{fg})}\right)\right)}$$

$$-\frac{1}{q}\frac{dq}{dt}=\frac{1}{D+Nq_{fg}}\left[\frac{2\pi 0.006328k}{\phi A}\frac{\bar{\lambda}}{\bar{c}_T}\right]+\frac{N\frac{dq_{fg}}{dt}\left[\left(\frac{2\pi\bar{\bar{t}}_{AD}}{(D+Nq_{fg})}\right)^2\right]}{(D+Nq_{fg})\left(1-\exp\left(\frac{2\pi\bar{\bar{t}}_{AD}}{(D+Nq_{fg})}\right)\right)}$$

If the assumption above is true, then $\left(\frac{2\pi\bar{\bar{t}}_{AD}}{(D+Nq_{fg})}\right)^2$ would even be smaller so as to be approximated by zero thereby rendering the entire second term in the equation above negligible.

Therefore,

$$-\frac{1}{q}\frac{dq}{dt} = \frac{1}{D + Nq_{fg}}\left[\frac{2\pi 0.006328k}{\phi A}\frac{\bar{\lambda}}{\bar{c}_T}\right] - - - - - - - - - - - - - (3.26)$$

The assumption above may not be unique to this work; it could be shown that the same assumption is implicitly the condition upon which equations 7 and 17 of reference 10 represents the same quantity, $\bar{P}_{pD}$.

Equation 3.26 above can be expressed as follows:

$$-\frac{dlnq}{dt} = \frac{1}{D + Nq_{fg}}\left[\frac{2\pi 0.006328k}{\phi A}\frac{\bar{\lambda}}{\bar{c}_T}\right] - - - - - - - - - - (3.27)$$

'Loss ratio' has been defined[16] as $\frac{1}{\frac{dlnq}{dt}}$;

Therefore,

$$Loss\ ratio = \frac{1}{\frac{dlnq}{dt}} = -\frac{\left(D + Nq_{fg}\right)\phi A}{2\pi 0.006328k}\frac{\bar{c}_T}{\bar{\lambda}}$$

$$Loss\ ratio = \frac{1}{\frac{dlnq}{dt}} = -\frac{\phi A}{2\pi 0.006328k}\left(Nq_{fg}\frac{\bar{c}_T}{\bar{\lambda}} + D\frac{\bar{c}_T}{\bar{\lambda}}\right) - - - - - - - (3.28)$$

Recalling that Arps' exponent b is simply the time derivative of loss ratio[2], therefore;

$$-b_{th-nD} = \frac{d}{dt}\left(\frac{1}{\frac{dlnq}{dt}}\right) = \frac{d}{dt}\left(-\frac{\phi A}{2\pi 0.006328k}\left(Nq_{fg}\frac{\bar{c}_T}{\bar{\lambda}} + D\frac{\bar{c}_T}{\bar{\lambda}}\right)\right)$$

The parameter b_{th-nD} here simply refers to a parameter b computed theoretically from physical properties with considerations for near wellbore non-Darcy flow effects.

Then;

$$b_{th-nD} = \frac{\phi A}{2\pi 0.006328k}\left(N\frac{d}{dt}\left(q_{fg}\frac{\bar{c}_T}{\bar{\lambda}}\right) + D\frac{d}{dt}\left(\frac{\bar{c}_T}{\bar{\lambda}}\right)\right) - - - - - - - - - - -(3.29)$$

Equation 3.29 above therefore presents a new expression for the theoretical computation of Arp's exponent b with considerations for the non-Darcy flow effects in the near wellbore region of the reservoir. To the best of my knowledge, this equation has not been presented previously by any investigator and may be a considerable contribution of this work. Efforts to compute b_{th-nD} values using equation 3.29 and compare such values with b_{th} values computed with equation 3.2 are documented and reported in chapter five of this report. Such comparison is necessary in order to investigate the possibility of a constant b_{th-nD} value through time as suggested by reference 10.

3.4 INNER BOUNDARY CONDITION AND THE EXISTENCE OF HYPERBOLIC FAMILY IN SOLUTION-GAS DRIVE RESERVOIRS

This section presents a theoretical derivation made to mathematically justify the existence of the hyperbolic family of curves for solution-gas drive reservoirs. The derivation reported hereunder is based on the concept of inner boundary condition (i.e. constant wellbore pressure) of the diffusivity equation in terms of solution-gas pseudo pressure and pseudo time functions.

The inner boundary condition for the constant wellbore pressure solution of the diffusivity equation in dimensionless form is commonly represented mathematically as follows[56]:

$$P_{D(r_D=1,t_D)} = 1 \quad ----------(3.30)$$

The equation 3.30 above is considered applicable only for a single phase slightly compressible liquid flow. For the case of solution-gas drive reservoirs (multiphase), this work employed the dimensionless solution-gas pseudo-pressure and pseudo-time functions presented by Camacho and Raghvan[10,48] as follows:

$$P_{pD}(r,t) = \frac{kh}{141.2q(t)}\left[\int_{P(r,t)}^{\bar{P}(t)}\left(\frac{K_{ro}}{\mu_o B_0}\right)dP + \int_{\bar{P}(t)}^{P_i}\left(\overline{\frac{K_{ro}}{\mu_o B_0}}\right)dP\right] \quad ------(3.31)$$

$$\tilde{t}_{AD} = \frac{0.006328k}{\varphi A q(t)}\int_0^t \frac{q(t)\bar{\lambda}(t)}{\bar{c}_T(t)}dt \quad ------(3.32)$$

$$\bar{\bar{t}}_{AD} = \frac{0.006328k}{\varphi A}\int_0^t \frac{\bar{\lambda}(t)}{\bar{c}_T(t)}dt \; ------(3.33)\; (for\; constant - rate\; case)$$

Writing equation 3.31 for the wellbore pressure yields:

$$P_{p_wD}(r_w, t) = \frac{kh}{141.2q(t)}\left[\int_{P_w}^{\bar{P}(t)}\left(\frac{K_{ro}}{\mu_o B_0}\right)dP + \int_{\bar{P}(t)}^{P_i}\left(\overline{\frac{K_{ro}}{\mu_o B_0}}\right)dP\right]$$

Hence, the inner boundary condition for solution-gas drive reservoir can then be expressed as follows:

$$P_{D(r_D=1,t)} = P_{p_wD}(r_w, t) = \frac{kh}{141.2q(t)}\left[\int_{P_w}^{\bar{P}(t)}\left(\frac{K_{ro}}{\mu_o B_0}\right)dP + \int_{\bar{P}(t)}^{P_i}\left(\overline{\frac{K_{ro}}{\mu_o B_0}}\right)dP\right] ----(3.34)$$

It has been shown[48] that the following relationship, first published by Fetkovich[32] is valid for boundary dominated flow in solution-gas drive reservoirs:

$$q_o = \frac{kh}{141.2(\ln\frac{r_e}{r_w} - 0.75 + s)}\int_{P_w}^{\bar{P}(t)}\left(\frac{K_{ro}}{\mu_o B_0}\right)dP$$

Therefore

$$(\ln\frac{r_e}{r_w} - 0.75 + s) = \frac{kh}{141.2q(t)}\int_{P_w}^{\bar{P}(t)}\left(\frac{K_{ro}}{\mu_o B_0}\right)dP --------(3.35)$$

Substituting equation 3.35 into equation 3.34 would then yield the following simplified expression;

$$P_{D(r_D=1,t)} = \left(\ln\frac{r_e}{r_w} - 0.75 + s\right) + \left(\frac{kh}{141.2q(t)}\int_{\bar{P}(t)}^{P_i}\left(\overline{\frac{K_{ro}}{\mu_o B_0}}\right)dP\right)$$

As noted earlier, the group $\left(\ln\frac{r_e}{r_w} - 0.75 + s\right)$ is denoted by D, therefore the equation above becomes:

$$P_{D(r_D=1,t)} = D + \left(\frac{kh}{141.2q(t)}\int_{\bar{P}(t)}^{P_i}\left(\overline{\frac{K_{ro}}{\mu_o B_0}}\right)dP\right) - - - - - - - - (3.36)$$

It has also been shown[10] that the dimensionless pseudo-pressure corresponding to the average reservoir pressure $\bar{P}_{pD}$ for constant wellbore production mode can be expressed as either a function of $\tilde{t}_{AD}$ or $\bar{\bar{t}}_{AD}$ as follows:

$$\bar{P}_{pD} = \frac{kh}{141.2q(t)}\int_{\bar{P}(t)}^{P_i}\left(\overline{\frac{K_{ro}}{\mu_o B_0}}\right)dP = 2\pi\tilde{t}_{AD} - - - - - - - - (3.37), \text{ or}$$

$$\bar{P}_{pD} = \frac{kh}{141.2q(t)}\int_{\bar{P}(t)}^{P_i}\left(\overline{\frac{K_{ro}}{\mu_o B_0}}\right)dP \cong -D\left(1 - \exp\left(\frac{2\pi\bar{\bar{t}}_{AD}}{D}\right)\right) - - - - - - - - - (3.38)$$

Substituting equation 3.38 into equation 3.36 yields the equation below:

$$P_{D(r_D=1,t)} = D + -D\left(1 - \exp\left(\frac{2\pi\bar{\bar{t}}_{AD}}{D}\right)\right)$$

This, upon simplification, becomes:

$$P_{D(r_D=1,t)} = D\exp\left(\frac{2\pi\bar{\bar{t}}_{AD}}{D}\right) - - - - - - - - - - - (3.39)$$

Equation 3.39 above (for solution-gas drive reservoirs) then becomes the equivalent of equation 3.30 for (single phase slightly compressible liquid flow).

A comparison of equations 3.39 and 3.30 provides a justification for the existence of the hyperbolic family of curves in the rate decline trends of solution-gas drive reservoirs. This work therefore presents the following points upon comparison of the two equations:

1. From the RHS of equation 3.30, it is clear that **the inner boundary condition for the single phase slightly compressible case is uniquely defined with a constant value (1.0), hence, the diffusivity equation would yield a unique solution, corresponding to the exponential decline curve ($\boldsymbol{b = 0}$).** It has been shown theoretically[12] that the exponential decline curve is the late-time constant wellbore solution of the diffusivity equation.

2. From the RHS of equation 3.39, it is clear that **the inner boundary condition for the solution-gas drive reservoir is not uniquely defined (even for a given reservoir model); rather the expression is a function of fluid properties,** $\left(\bar{\bar{t}}_{AD} = f\left(\frac{\bar{c}_T(t)}{\bar{\lambda}_T(t)}\right)\right)$ **. Hence, solving the diffusivity equation with equation 3.39 as the inner boundary condition would yield a family of curves (hyperbolic family:** $\mathbf{0 < b \leq 1.0}$**) with each member of the family (a given value of** b**) only uniquely defined for a unique fluid model.** In summary, this work is submitting that the hyperbolic behavior of solution-gas drive reservoirs is a direct consequence of the inner boundary condition (constant wellbore pressure) of the dimensionless diffusivity equation for solution-gas drive reservoirs.

3. From the foregoing, it is clear that the ratio $\frac{\bar{c}_T(t)}{\bar{\lambda}_T(t)}$ would be a significant determinant of the value of b for a given reservoir/fluid model. This observation here is in consonance with results published by Gentry and McCray[6] showing that the relative permeability characteristics have a significant influence on the parameter$b$. This is also in agreement with the expression for b parameter presented by reference 10.

This mathematical justification for the existence of the hyperbolic curves in solution-gas drive reservoirs is a major contribution of this work. The significance of this derivation here (equation 3.39) as well as the observations made lies in its ability to pave way for future efforts towards theoretically generating the complete Arp's type curves.

CHAPTER 4

SIMULATION AND COMPUTATIONAL PROCEDURES

A number of theories as well as deductions have been developed in this work as reported in chapter three. In order to verify these theories and deductions, the need arose for a comprehensive set of synthetic data (reservoir, fluid and historical production data) required for such verification. The decision to employ synthetic data in the verification became necessary due to scarcity of comprehensive real life data that will include all the parameters required; more so, using synthetic data offered the possibility of performing sensitivity analysis on some key parameters.

The first part of this chapter therefore presents the static reservoir/fluid properties which essentially constituted the raw data fed into the simulator. The second part of this chapter presents the simulation workflow with which the synthetic data were generated. Furthermore, it was not possible to obtain direct outputs of some required parameters from simulation runs, such parameters were however computed from simulation results. The last part of this chapter presents details of such computations.

4.1 RESERVOIR AND FLUID DATA SET

The reservoir and fluid data set employed in this work is essentially the same as that published in reference 10; this is done in order to avail the opportunity of comparing results from this work with results from previous investigations. However, since the focus of this work is based on sound theoretical considerations, the conclusions therein do not depend on the specific data used.

Basically, a saturated, homogeneous, bounded, cylindrical reservoir is considered; a single fully penetrating well producing at constant wellbore pressure (critical bottomhole pressure P_{wfc}) is located at the center of the reservoir. The table below shows the details of the reservoir properties.

Table 4.1: Reservoir Properties Data Set

Reservoir Properties	Values
Drainage Radius, r_e (ft)	2624.672
Porosity, ϕ, (fraction)	0.3
Permeability, K, (mD)	10
Well Radius, r_w (ft)	0.32808
Initial Pressure = Bubble Point Pressure, $P_i = P_b$, (psi)	5704.78
Skin Factor, s	10
Initial Water Saturation, S_{wi} (fraction)	0.3
Initial Compressibility, c_{ti}, psi^{-1}	0.00001085
Initial Oil Viscosity, μ_{oi} cp	0.298
Thickness, h, (ft)	15.55
Critical Bottom Hole Pressure Constraint, P_{wf} (psi)	1696

The table below shows the oil PVT properties at various pressure nodes, the same data is shown in the plots that follow:

Table 4.2: Oil PVT Properties Data Set

Pressure, P (psi)	Solution GOR, Rs (MCF/STB)	Bo (RB/STB)	Oil Viscosity (cp)
100	0.0100	1.0622	1.3957
200	0.0263	1.0650	1.3525
300	0.0427	1.0683	1.3104
400	0.0594	1.0721	1.2695
500	0.0763	1.0765	1.2296
600	0.0933	1.0814	1.1909
700	0.1107	1.0868	1.1532
800	0.1282	1.0926	1.1165
900	0.1460	1.0990	1.0809
1000	0.1641	1.1059	1.0463
1500	0.2588	1.1469	0.8882
2000	0.3617	1.1984	0.7534
2500	0.4739	1.2593	0.6400
3000	0.5969	1.3284	0.5462
3500	0.7318	1.4044	0.4702
4000	0.8800	1.4864	0.4101
4500	1.0428	1.5731	0.3640
5000	1.2214	1.6633	0.3300
5500	1.4172	1.7558	0.3063
5704.78	1.5026	1.7941	0.2992

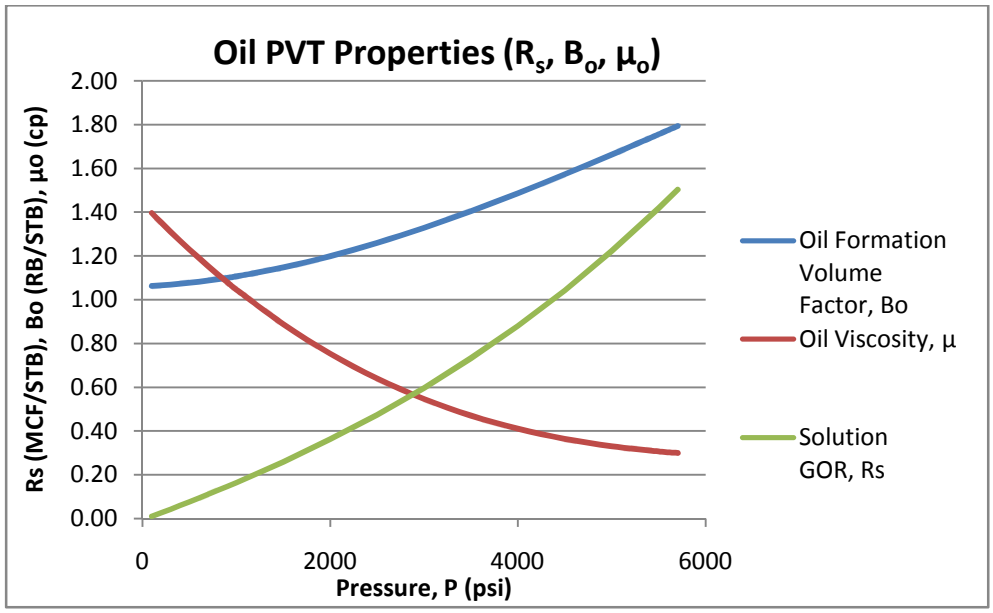

Figure 4.1: Oil PVT Properties (Solution GOR, Oil Formation Volume Factor and Oil Viscosity)

The table and the plots below show the Gas PVT properties at various pressure nodes.

Table 4.3: Gas PVT Properties Data Set

Pressure P (psi)	Gas FVF, B_g (RB/MCF)	Gas Viscosity μ_g (cp)
100	3.86E+001	0.010443
200	1.80E+001	0.010786
300	1.15E+001	0.011129
400	8.39E+000	0.011472
500	6.57E+000	0.011815
600	5.37E+000	0.012158
700	4.54E+000	0.012501
800	3.92E+000	0.012844
900	3.44E+000	0.013187
1000	3.06E+000	0.013530
1500	1.96E+000	0.015245
2000	1.43E+000	0.016960
2500	1.12E+000	0.018675
3000	9.15E-001	0.020390
3500	7.72E-001	0.022105
4000	6.67E-001	0.023820
4500	5.86E-001	0.025535
5000	5.22E-001	0.027250
5500	4.70E-001	0.028965
5704.78	4.51E-001	0.029667

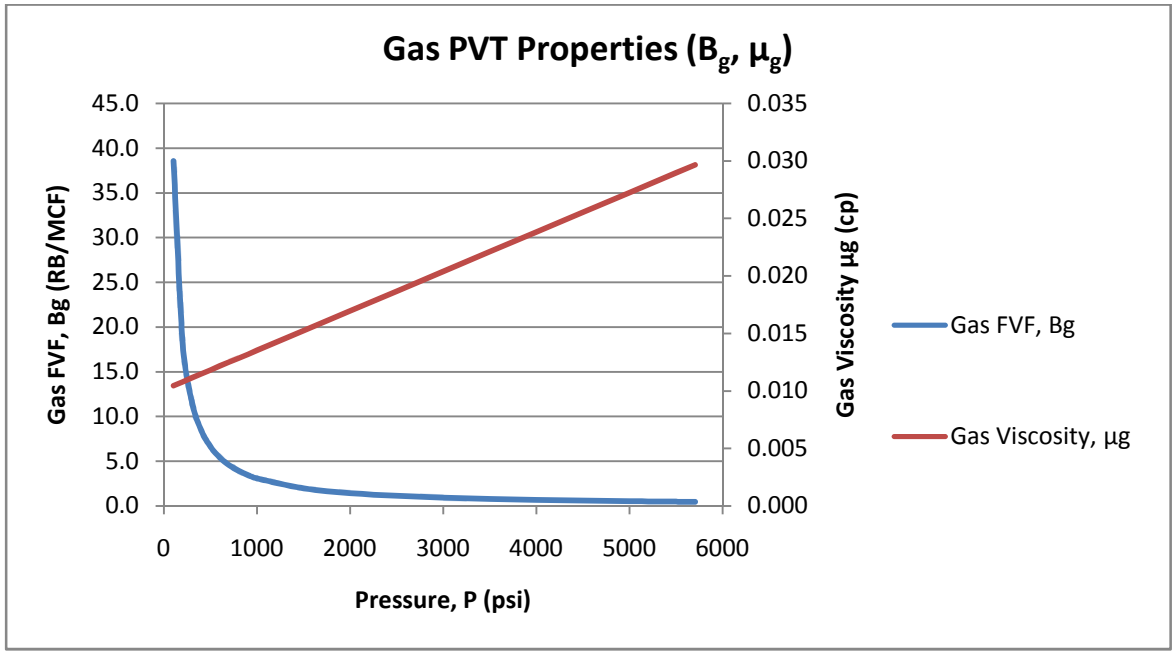

Figure 4.2: Gas PVT Properties (Gas FVF, Gas Viscosity)

Additionally, the simulation required values of undersaturated oil compressibility at the pressure nodes indicated in the PVT tables above. The compressibility values were computed using the Vasquez-Beggs[57] correlation as shown below:

$$c_o = \frac{5R_{sb} + 17.2T_F - 1{,}180\gamma_g + 12.61\gamma_{API} - 1{,}433}{10^5 P}$$

The following values of indicated parameters are employed in computing the compressibility data.

$$Reservoir\ Temperature = T_F = 220F$$

$$Gas\ gravity = \gamma_g = 0.65$$

$$Oil\ gravity = \gamma_{API} = 45.5$$

The table below shows the computed compressibility data.

Table 4.4: Undersaturated Oil Compressibility Data Set

Pressure, P (psi)	Solution GOR, Rs (MCF/STB)	Undersaturated Oil Compressibility (psi^{-1})
100	9.9967	3.64E-004
200	26.2638	1.86E-004
300	42.7214	1.27E-004
400	59.3801	9.72E-005
500	76.2500	7.94E-005
600	93.3415	6.76E-005
700	110.6650	5.92E-005
800	128.2306	5.29E-005
900	146.0489	4.80E-005
1000	164.1300	4.41E-005
1500	258.8400	3.26E-005
2000	361.6700	2.70E-005
2500	473.9100	2.38E-005
3000	596.8500	2.19E-005
3500	731.7800	2.07E-005
4000	879.9900	2.00E-005
4500	1042.7700	1.96E-005
5000	1221.4100	1.94E-005
5500	1417.2000	1.94E-005
5704.78	1502.6372	1.95E-005

The relative permeability characteristics of the reservoir/fluid model considered is displayed in the figure below. These relative permeability curves were however approximated as straight line functions in the simulations and computations in this work.

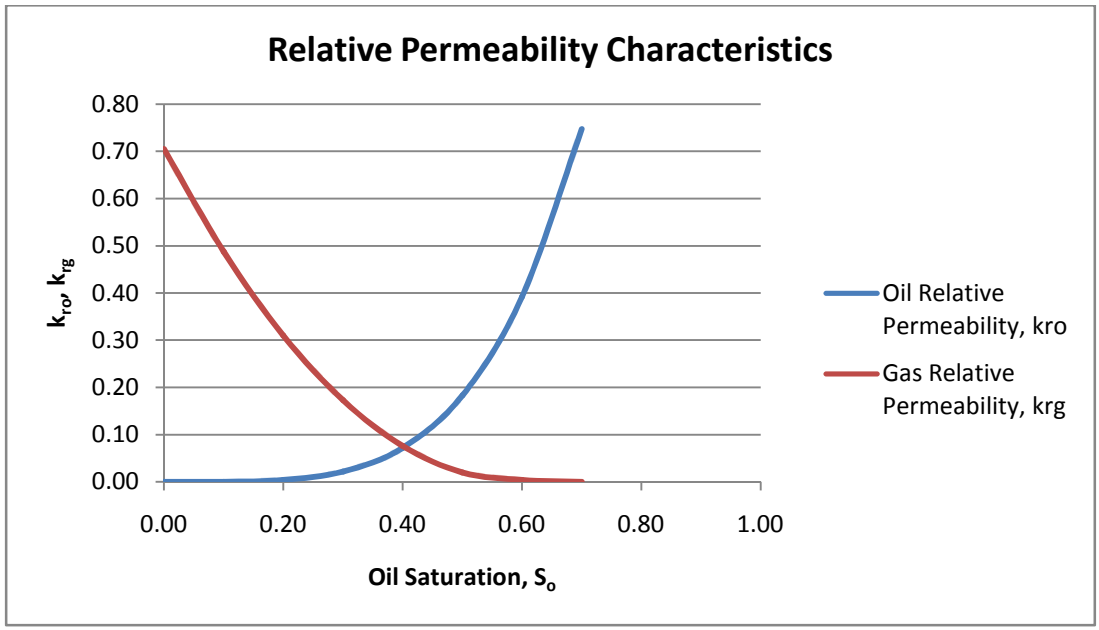

Figure 4.3: Relative Permeability Characteristic Curves

4.2 SIMULATION DATA DECK AND RUN SPECIFICATIONS

The reservoir simulation software ECLIPSE 100 was employed in running the simulations in this work. This section gives details of the ECLIPSE data deck as well as various run specifications implemented in the simulation runs.

4.2.1 Simulator Data Deck

The various raw data shown above were presented in a text file in a format compatible with ECLIPSE input data format. Various run specifications as well as output requests were

also specified in the text file using the relevant ECLIPSE keywords. The content of the input data deck is presented in Appendix of this report.

4.2.2 Simulation Specifications and Controls

The following specifications and control parameters as required by the simulator were specified:

1. **Well Control**: The well was initially placed on a constant oil rate control (peak rate) until the bottomhole pressure dropped to the critical value of P_{wfc} at which point the control was switched to BHP control in order to create the effects of a declining oil well.
2. **Peak Rate**: The peak rate (rate at onset of decline) which is a measure of the reservoir/wellbore capacity was set at 70% of the absolute open flow rate as suggested by Fraim and Wattenbarger[50]
3. **Economic Limit**: An oil rate economic limit of 50STB/D was implemented to terminate the simulation as soon as this limit is violated.
4. **Non-Darcy Coefficient**: The value for the non-Darcy coefficient, N, for the well was calculated using the expression[54] given below and fed into the simulator

$$N = \frac{2.715 \times 10^{-15} \beta M P_{sc} K}{\mu T_{sc} h r_w}$$

Also, the following expression for gas density (g/cm^3) at standard condition is presentted[59]

$$\rho_{sc} = 1.4935 \times 10^{-3} \frac{P_{sc} M}{T_{sc}}$$

Combining the two equations above;

$$N = \frac{2.715 \times 10^{-15} \beta \rho_{sc} K}{1.4935 \times 10^{-3} \mu h r_w}$$

The turbulence factor β was computed using the Geertsma correlation[58] shown below

$$\beta = \frac{48511}{\phi^{5.5} K^{0.5}}$$

4.2.3 Output Requests

The following output parameters were requested to be reported at each time step of the simulation:

1. Field oil production rate (STB/D)
2. Field gas production rate (MCF/D)
3. Field cumulative oil produced (STB)
4. Field cumulative gas produced (MCF)
5. Field free gas production rate (MCF/D)
6. Field solution gas production rate (MCF/D)
7. Field GOR (MCF/STB)
8. Well bottomhole pressure, BHP, (psi)
9. Field average oil saturation
10. Field average gas saturation
11. Field average reservoir pressure (psi)
12. Fraction of oil rate due to solution-gas drive mechanism
13. Fraction of oil rate due to gas-cap influx

The last two parameters were requested in order to ascertain the reservoir is actually producing due to solution-gas drive mechanism. Simulation results showed that the fraction of oil produced due to solution-gas drive was approximately 1.0 throughout the producing time. The output parameters listed above formed the basis for the computations presented in the last section of this chapter. The time step for the simulation run as well as the output reporting was set for an interval of one month; however, in order to accurately capture the exact time of the onset of the decline, the month corresponding to the start of decline was expanded into its constituent days so that the simulator's output for this month was reported in daily interval thereby capturing the exact day corresponding to onset of decline. It was observed that this effort improves the results.

4.2.4 Simulation Initial Solution

In order to verify the correctness of the reservoir/fluid model fed into the simulator, a request for the initial solution of the simulation run was incorporated. This was deemed necessary so as to obtain the simulator's result for initial fluid in place (oil in place, gas in place and water in place). The simulator's output for fluid in place was found to agree with values calculated using simple volumetric formulae for fluid in place calculations.

4.3 COMPUTATIONAL PROCEDURES

It was not possible to obtain direct outputs of some parameters required to verify the various theories developed in this work from simulation runs. Such parameters which are essentially the total compressibility and mobility terms (and the various derivatives needed to compute them) were however computed from simulation results using relevant equations. This part of this chapter presents details of such computations.

To employ either of the equations presented in chapter 3 to compute b_{th} *or* b_{th-nD} values, the total compressibility term $\bar{c}_T$ and the total mobility term $\overline{\lambda_T}$ are defined as follows[10]:

$$\bar{c}_T = -\frac{\overline{S_o}}{B_o(\bar{P})}\left[\frac{dB_o(\bar{P})}{d\bar{P}} - B_g(\bar{P})\frac{dR_s(\bar{P})}{d\bar{P}}\right] - \frac{\overline{S_g}}{B_g(\bar{P})}\left[\frac{dB_g(\bar{P})}{d\bar{P}}\right] - - - -(4.1)$$

$$\overline{\lambda_T} = \frac{k_{ro}(\overline{S_o})}{\mu_o(\bar{P})} + \frac{k_{rg}(\overline{S_g})}{\mu_g(\bar{P})} - - - - - (4.2)$$

The detailed computational procedures required for various terms in equations 4.1 and 4.2 above and the eventual computation of b_{th} *or* b_{th-nD} as a function of time is herein presented.

1. Time (t), average pressure ($\bar{P}$), average saturations($\overline{S_o}$ *and* $\overline{S_g}$) data were obtained from the simulator output file.

2. The PVT data $\left[B_o(\bar{P}), B_g(\bar{P}), R_s(\bar{P})\right]$ as functions of time were evaluated at average reservoir pressure using the curve-fitting functions generated from the raw input data.

3. The derivatives (wrt $\bar{P}$) of the PVT data $\left[\frac{dB_o(\bar{P})}{d\bar{P}} = B_o{}', \frac{dB_g(\bar{P})}{d\bar{P}} = B_g{}', \frac{dR_s(\bar{P})}{d\bar{P}} = R_s{}'\right]$ as functions of time were computed using the following numerical derivative algorithm

$$\frac{dB_o(\bar{P})}{d\bar{P}} = B_o{}' = \frac{\left(\frac{B_{o(i)} - B_{o(i-1)}}{\bar{P}_{(i)} - \bar{P}_{(i-1)}}\right)\left(\bar{P}_{(i+1)} - \bar{P}_{(i)}\right) + \left(\frac{B_{o(i+1)} - B_{o(i)}}{\bar{P}_{(i+1)} - \bar{P}_{(i)}}\right)\left(\bar{P}_{(i)} - \bar{P}_{(i-1)}\right)}{\bar{P}_{(i+1)} - \bar{P}_{(i-1)}} - - - (4.3)$$

$$\frac{dB_g(\bar{P})}{d\bar{P}} = B_g{}' = \frac{\left(\frac{B_{g(i)} - B_{g(i-1)}}{\bar{P}_{(i)} - \bar{P}_{(i-1)}}\right)\left(\bar{P}_{(i+1)} - \bar{P}_{(i)}\right) + \left(\frac{B_{g(i+1)} - B_{g(i)}}{\bar{P}_{(i+1)} - \bar{P}_{(i)}}\right)\left(\bar{P}_{(i)} - \bar{P}_{(i-1)}\right)}{\bar{P}_{(i+1)} - \bar{P}_{(i-1)}} - - - (4.4)$$

$$\frac{dR_s(\bar{P})}{d\bar{P}} = R_s{}' = \frac{\left(\frac{R_{s(i)} - R_{s(i-1)}}{\bar{P}_{(i)} - \bar{P}_{(i-1)}}\right)\left(\bar{P}_{(i+1)} - \bar{P}_{(i)}\right) + \left(\frac{R_{s(i+1)} - R_{s(i)}}{\bar{P}_{(i+1)} - \bar{P}_{(i)}}\right)\left(\bar{P}_{(i)} - \bar{P}_{(i-1)}\right)}{\bar{P}_{(i+1)} - \bar{P}_{(i-1)}} - - - (4.5)$$

In the scheme above, index i referred to current time step while i+1 and i-1 referred to next and previous time step respectively.

4. The total system compressibility term $\bar{c}_T$ was then computed for each time node using equation 4.1 above and the results of previous steps.
5. The viscosity data ($\mu_o(\bar{P})\ and\ \mu_g(\bar{P})$) as functions of time were evaluated at average reservoir pressure using the curve-fitting functions generated from the raw input data.
6. The relative permeability data ($k_{ro}(\overline{S_o})and\ k_{rg}(\overline{S_g})$) as functions of time were evaluated at average reservoir saturations using the curve-fitting functions generated from the raw input data.
7. The total system mobility term $\overline{\lambda_T}$ was then computed for each time node using equation 4.2 above and the results of previous steps.
8. The ratio $\frac{\bar{c}_T}{\overline{\lambda_T}}$ was then computed for each time node using results from steps 4 and 7.
9. The time derivative of $\frac{\bar{c}_T}{\overline{\lambda_T}}$ i.e. $\frac{d}{dt}\left(\frac{\bar{c}_T}{\overline{\lambda_T}}\right)$ for each time node was then computed using the numerical derivative algorithm below:

$$\frac{d}{dt}\left(\frac{\bar{c}_T}{\overline{\lambda_T}}\right) = \frac{\left(\frac{\frac{\bar{c}_T}{\overline{\lambda_T}}_{(i)} - \frac{\bar{c}_T}{\overline{\lambda_T}}_{(i-1)}}{t_{(i)} - t_{(i-1)}}\right)\left(t_{(i+1)} - t_{(i)}\right) + \left(\frac{\frac{\bar{c}_T}{\overline{\lambda_T}}_{(i+1)} - \frac{\bar{c}_T}{\overline{\lambda_T}}_{(i)}}{t_{(i+1)} - t_{(i)}}\right)\left(t_{(i)} - t_{(i-1)}\right)}{t_{(i+1)} - t_{(i-1)}} - - - (4.6)$$

10. Lastly, the theoretical values of b, i.e. b_{th} *or* b_{th-nD}, for each time node were then computed using either equation 3.2 or 3.29 presented in chapter 3.

The results of the simulations and the computations that followed as well as the verifications of the various theories developed in chapter 3 and the relevant discussions is the focus of chapter five of this report.

CHAPTER 5

VERIFICATION OF THEORIES AND RESERVOIR PROPERTY ESTIMATION

The derivation of a functional relationship between the empirical domain and the theoretical domain of the decline parameter ($b_{emp}\ vs\ b_{th}$) which is the foremost contribution of this work has been presented in chapter three alongside other theories and deductions developed. The details of the simulations and computational procedures employed in generating data and parameters needed for the verification of the theories has also been presented in chapter four. This chapter therefore presents the simulation results as well as the results of the verification attempts. Theoretical justifications for observed trends in the results are also presented in this chapter. In addition, a newly proposed reservoir property estimation technique being a major contribution of this work is herein presented with specific examples. Finally, analyses on the sensitivity of the results to some key parameters were performed and reported in this chapter.

5.1 THEORETICAL DECLINE PARAMETER TREND THROUGH TIME

The reservoir and fluid properties for the base case has been presented in chapter three. Also, the various simulation controls and specifications have been presented in chapter 4. Presented in the figure below is the simulation result namely the oil flowrate through time as well as the solution-gas drive index.

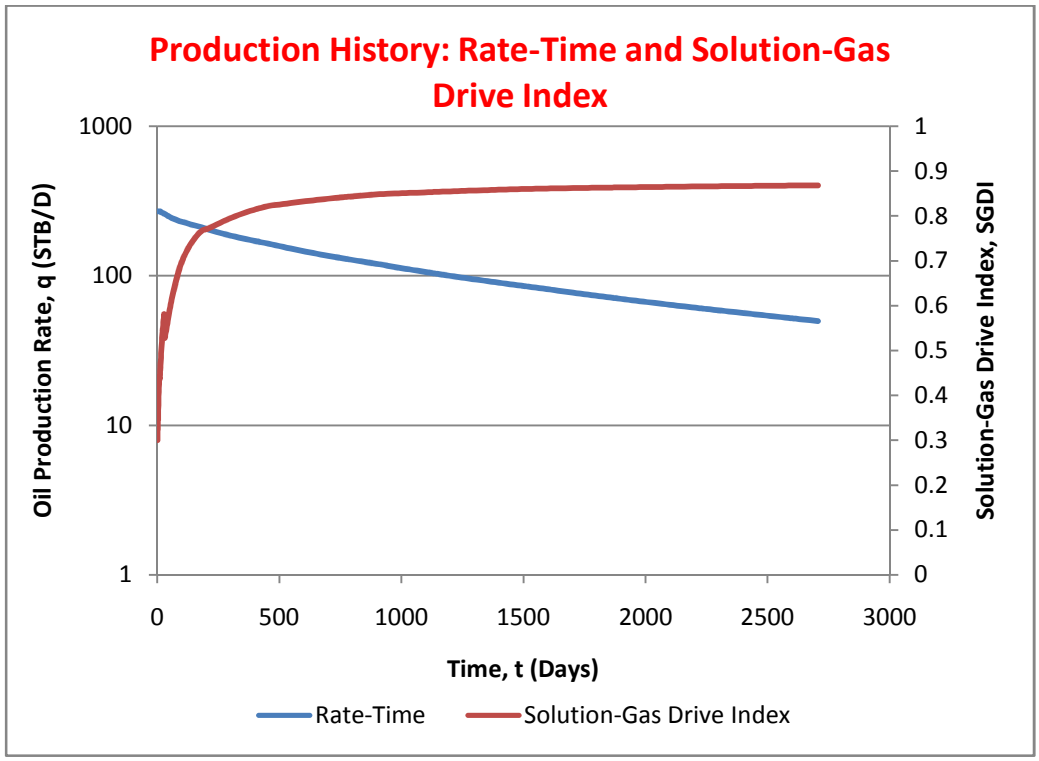

Figure 5.1: Base Case Production History: Rate-Time and Solution Gas Drive Index

The result above shows the dominance of solution-gas drive mechanism in the production. Furthermore, the slight upward curvature of the semilog rate-time plot confirms the

presence of hyperbolic rate decline; as suggested in reference 4. The results also show a short constant (peak) rate production phase before decline sets in at day 12.

Using the simulators outputs (oil flowrate, average reservoir pressure and saturation as functions of time) and employing various computational schemes presented in chapter four, values for the theoretical decline parameter b_{th} were computed as a function of time using equation 3.2. Below is a plot of b_{th} values with time. It should be noted that the time item in the plot below refers to time elapsed since onset of decline, i.e. time $t = 0$ corresponds to start of decline.

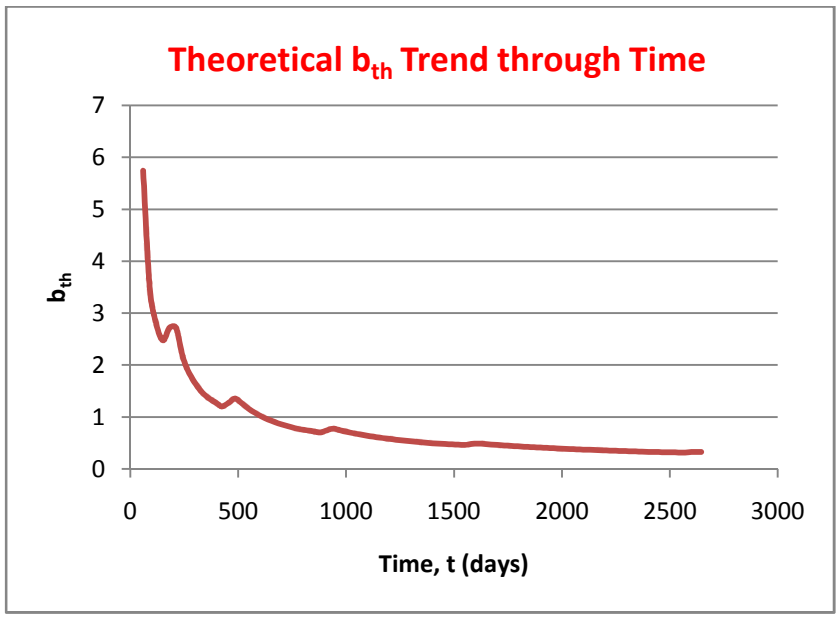

Figure 5.2: Base Case: Theoretical b_{th} Trend through Time

5.2 THEORETICAL JUSTIFICATION FOR THE DECLINE PARAMETER TREND

From figure 5.2 above, it is clear that the b_{th} ranges from values greater than 1.0 to values as low as 0.33. As a precursor to the explanations offered below for the various intervals of values, the theoretical values, $\boldsymbol{b_{th}}$ may be seen as reflecting the actual dynamics of the reservoir and the fluid interaction through time; hence it may be expected to have a dynamic (unstable) behavior through time. Below is the theoretical explanations offered by this work for the various intervals of values of $\boldsymbol{b_{th}}$.

1. **b_{th} > 1.0: Transient Rate Decline Regime**

   This range of values may be attributed to transient rate decline, i.e. a decline period during which the well is yet to feel the external boundary of the drainage area. Various researchers[10,12,13] have suggested that rate data existing in the transient period will yield values of exponent b greater than 1.0. As evidence in support of this proposition, results presented in the sensitivity analysis section of this report showed that this range of values vanished for cases that precluded transient rate decline.

2. **1 >b_{th} >0.67: Transition Decline Regime**

   Empirical surveys [10,12,13] of solution gas drive reservoirs performance has shown that the exponent b should range from 0.33 to 0.67. However, it may be expected there should be a sort of transition regime between the transient decline regime (b_{th} > 1.0) and the boundary-dominated empirically established regime (0.67 >b_{th} > 0.33). In other words, the values between 1.0 and 0.67 in the above plot

may be seen as representing a transition from transient rate decline regime to boundary-dominated rate decline regime. Similar to the transient rate decline regime, results presented in the sensitivity analysis section of this report showed that this range of values vanished for cases where only boundary-dominated rate decline is ensured.

3. **0.67 >b_{th} > 0.33: Boundary-dominated Solution-gas Drive Decline Regime**

   The values in this range should represent the actual boundary-dominated solution-gas drive decline behavior. This fact could be supported by the fact that the reservoir exhibited this range of values for the longest period of the decline time.

4. **b_{th} < 0.33: Approaching Slightly-compressible Liquid Production**

   Some cases considered and reported in later sections of this report exhibited a range of b_{th} values less than 0.33. These values are below the lower limit of the empirically expected range for solution gas drive reservoirs. It may be expected that as the reservoir loses more of the solution gas due to production, its behavior starts to approach that of a slightly compressible liquid single phase flow. Single-phase slightly compressible liquid flows are known theoretically to decline exponentially, i.e. b = 0.[4,3] Hence, as the reservoir approaches the single phase flow behavior, the b_{th} values are seen to be less than 0.33 and are approaching zero.

The propositions above as regards the theories of rate decline in solution-gas drive reservoirs has not been presented previously and is therefore a significant contribution of this work.

5.3 EFFECT OF INCORPORATING NON-DARCY FLOW

Camacho and Raghavan[10] had expressed hopes that the incorporation of near wellbore non-Darcy flow effects into the theoretical developments of rate decline in solution-gas drive reservoirs could yield constant values of b_{th} throughout decline time. In order to verify this anticipation for constant b_{th} values, this work derived a new expression (equation 3.29) for b_{th} as function of physical reservoir and fluid properties using similar formulation as in reference 10 but incorporating the rate-dependent skin factor representing the non-Darcy flow effects. The derivation is presented in chapter three of this report. Values of b_{th-nD} (theoretical decline parameter with consideration for non-Darcy flow) computed using equation 3.29 is presented in the plot below on the same axes with values of b_{th} for comparison.

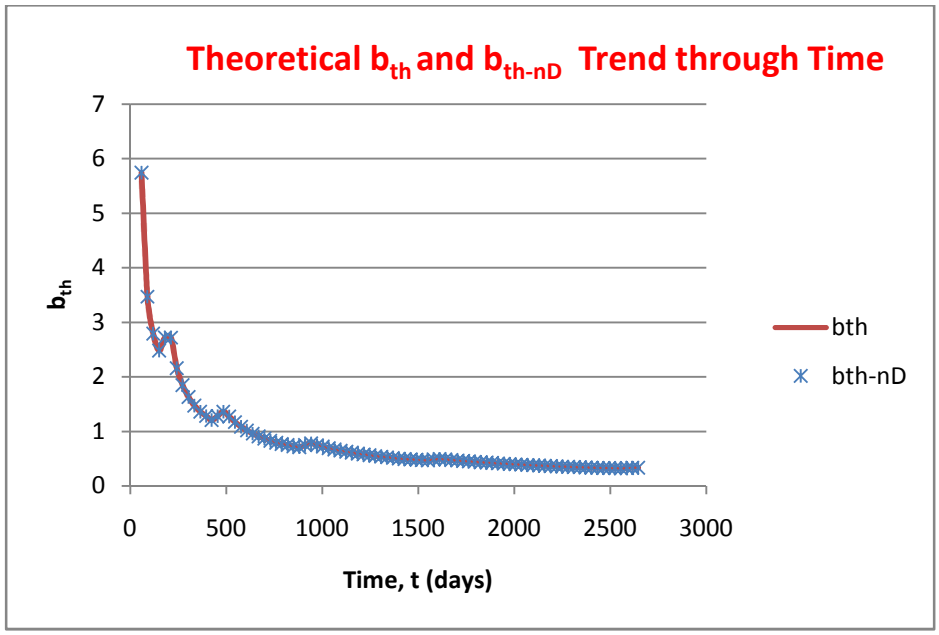

Figure 5.3: Base Case: Theoretical b_{th} and b_{th-nD} through Time

From figure 5.3 above, it is evident that the decline parameter with consideration for non-Darcy effects, b_{th-nD} vary through time much same way as the decline parameter without consideration for non-Darcy effects, precluding any expectation for constant values of b_{th-nD} through time.

If the propositions about the dynamic behavior of the decline parameter as being presented by this work are valid, then the b_{th-nD} values may never exhibit any constancy in spite of considerations for non-Darcy flow effects. The $\boldsymbol{b_{th-nD}}$ values will rather be expected to reflect the dynamics (through time) of the reservoir and fluid interactions (mobility and compressibility characteristics). System mobility (relative permeability and viscosity) as well as compressibility (PVT) in solution gas drive reservoirs are known to be functions of average reservoir pressure and saturation[30] which change with time due to production.

The empirical exponent b has been related to the popular back-pressure curve exponent[4] denoted as n. Fetkovich[32] had attributed exponent **n** values less than unity to non-Darcy flow. Camacho and Raghavan[52] also published results that substantiated Fetkovich's claim. However, Fetkovich[32] submitted that n values can be less than unity strictly as a result of variation in fluid properties. As a matter of fact, Camacho and Raghavan[52] suggest that n values will generally vary with time unless the variation is completely counteracted with the non-Darcy flow effects. However, non-Darcy flow coefficients in solution gas drive reservoirs are rather very small in values (1.7107 X 10^{-6} D/MCF) for the reservoir/fluid model considered here) and may never measure up to values sufficient to counteract the variation due to changes in fluid properties. The results reported in this current work and its emerging propositions confirm the positions already established in literatures.

5.4 VERIFICATION OF DERIVED RELATIONSHIP

A major contribution of this work is the derivation of a functional relationship between the empirical domain and the theoretical domain of the decline parameter($b_{emp}\ vs\ b_{th}$). This relationship is reported in chapter three as equation 3.8 and is presented below for convenience.

$$\frac{1}{\overline{b_{th}}\left(t_{(i)}-t_o\right)} = aq_{(i)}{}^{b_{emp}} \quad ----------(3.8)$$

As a corollary, the LHS of equation 3.8 was also represented as a function of physical reservoir and fluid properties in equation 3.9

$$\frac{1}{\overline{b_{th}}\left(t_{(i)}-t_o\right)}=\frac{2\pi 0.006328k}{\phi AD}\frac{\overline{\lambda_T}}{\bar{c}_T}\ ----------(3.9)$$

Equation 3.8 represents the empirical domain of the decline parameter while equation 3.9 represents the theoretical domain.

From the two equations above, it is expected that the right hand side quantity (RHS) of both equations should be equal since the left hand side (LHS) is essentially equal.

The equality (at least in the approximate sense) of the RHS of both equations 3.8 and 3.9 was verified using simulation results; rate-time data, to compute $a\ and\ b_{emp}$ and employing the various computational schemes presented in chapter four to compute $\overline{\lambda_T}$ and $\bar{c}_T$. The result of the verification attempt is presented below as a plot of the RHS of both equations with time.

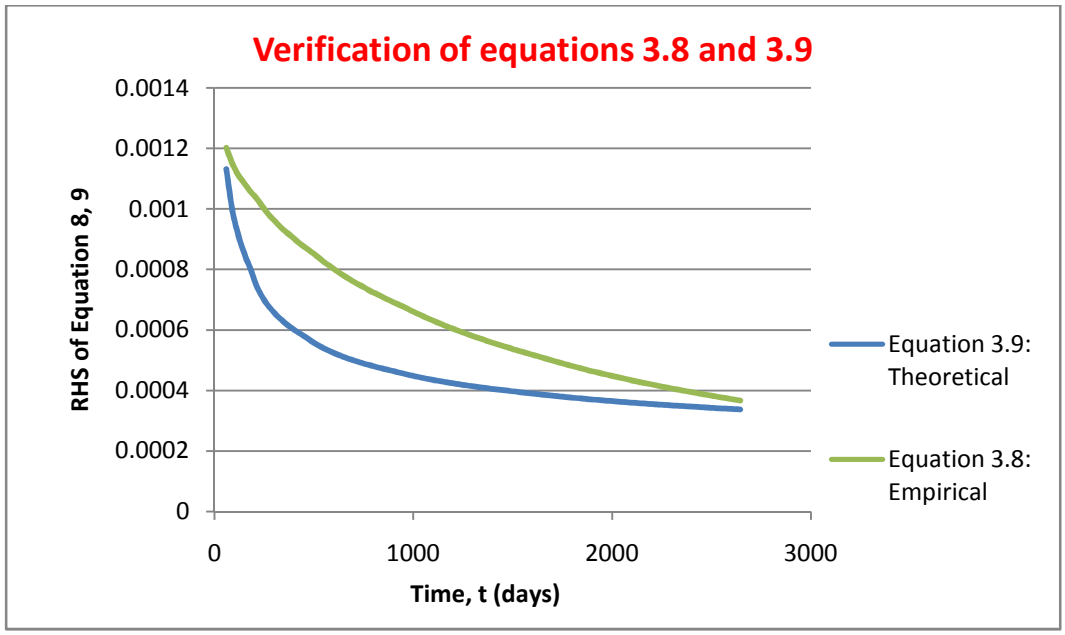

Figure 5.4: Base Case: Verification of Equations 3.8 and 3.9

The following features of the plot are here highlighted.

1. The two curves exhibit similar trends over time.
2. The initial agreement between the two curves may be taken as a pseudo agreement since the empirical domain could not exist until there be sufficient production decline history
3. The discrepancy between the two curves, although initially grew large, narrows down with time. As a matter of fact, the discrepancy is expected to become insignificant if the simulation is extended; here the simulation stops because the economic limit (50 STB/D) constraint imposed has been violated.

4. Point 3 above suggests the equality of the two equations above would be improved as more and more historical production decline data becomes available.
5. At the end of the simulation time, the relative discrepancy has reduced to only 7.7%.

5.5 PROPOSED RESERVOIR PROPERTY ESTIMATION TECHNIQUES

5.5.1 Reservoir Permeability Estimation: Procedure and Application.

Consequent upon the verification of the equality of equation 3.8 and 3.9 (at least in an approximate sense), this current work therefore proposed a new improved technique for estimating reservoir permeability using historical field data. The basis for this proposed technique, derived by equating the RHS of equation 3.8 and 3.9 and solving for reservoir permeability k was presented as equation 3.11 in chapter three and is repeated here for convenience.

$$k \cong \frac{a{q_{(i)}}^{b_{emp}}\phi AD}{2\pi 0.006328}\frac{\bar{c}_T}{\overline{\lambda_T}} \quad ----------(3.11)$$

In the equation 3.11 above, the subscript i represents a given time node, that is reservoir permeability estimates can be made at each time node in the historical data. A detailed step-by-step procedure as well as the data requirement for the proposed technique is hereby presented below.

5.5.1.1 DATA REQUIREMENT:

a. Historical rate-time data of field/well.
b. Average reservoir pressure and saturations as a function of time: these become inevitable since the dynamics of solution-gas drive is driven by the variation of reservoir and fluid properties which are strong functions of pressure and saturation. The average reservoir pressure data could easily be computed from simple material balance equations; for instance, reference 12 has shown that, for solution-gas drive reservoirs, the square of the average reservoir pressure is a linear function of the cumulative production according to the equation below.

$$\bar{P}^2 = -\left(\frac{{P_i}^2}{N_{pi}}\right) N_p + {P_i}^2 \text{ - - - - - - - - - - - -} (5.1)$$

Frederick and Kelkar[51] also suggested a simple iterative scheme to calculate the average reservoir pressure data.

The average saturations data may be computed as a function of average reservoir pressure using some material balance methods, for example, reference 4 presented the following for a two-phase reservoir.

$$S_o = (1 - S_{wi})\left(1 - \frac{N_p}{N}\right)\left(\frac{B_o}{B_{oi}}\right) - - - - - - - - - (5.2)$$

5.5.1.2 PROCEDURES:

1. Acquire the required data as stated above.
2. From the rate-time data, using conventional curve-fitting methods or type-curve matching, determine the values of the empirical decline parameters, $a\ and\ b_{emp}$.
3. Compute values of PVT data $\left[B_o(\bar{P}), B_g(\bar{P}), R_s(\bar{P})\right]$ at average reservoir pressure for each time nodes. Curve-fitted functions of initial PVT data of the reservoir fluid may be used for this computation at later times in the reservoir life.
4. Using the equation below, compute the total compressibility at each of the time nodes. The derivatives in the equation may be computed using numerical differentiation algorithms.

$$\bar{c}_T = -\frac{\overline{S_o}}{B_o(\bar{P})}\left[\frac{dB_o(\bar{P})}{d\bar{P}} - B_g(\bar{P})\frac{dR_s(\bar{P})}{d\bar{P}}\right] - \frac{\overline{S_g}}{B_g(\bar{P})}\left[\frac{dB_g(\bar{P})}{d\bar{P}}\right]$$

5. Compute values of the relative permeability data $\left[k_{ro}(\overline{S_o})and\ k_{rg}(\overline{S_g})\right]$ at average reservoir saturations for each time nodes. Curve-fitted functions of the core-derived relative permeability data of the reservoir may be used for this computation.

6. Compute values of the viscosity data $\left[(\mu_o(\bar{P})\ and\ \mu_g(\bar{P})\right]$ at average reservoir pressure for each time nodes. Curve-fitted functions of initial viscosity data of the reservoir fluid may be used for this computation at later times in the reservoir life.
7. Using the equation below, compute the total mobility at each of the time nodes.

$$\overline{\lambda_T} = \frac{k_{ro}(\overline{S_o})}{\mu_o(\bar{P})} + \frac{k_{rg}(\overline{S_g})}{\mu_g(\bar{P})}$$

8. Substitute the results of the previous steps into equation 3.11 above to solve for permeability estimates, k at each time node.

5.5.1.3 APPLICATION OF TECHNIQUE

The application of this proposed technique to the reservoir model considered in this work yields excellent permeability estimates throughout time. The plot of the permeability estimates through time is hereby presented below.

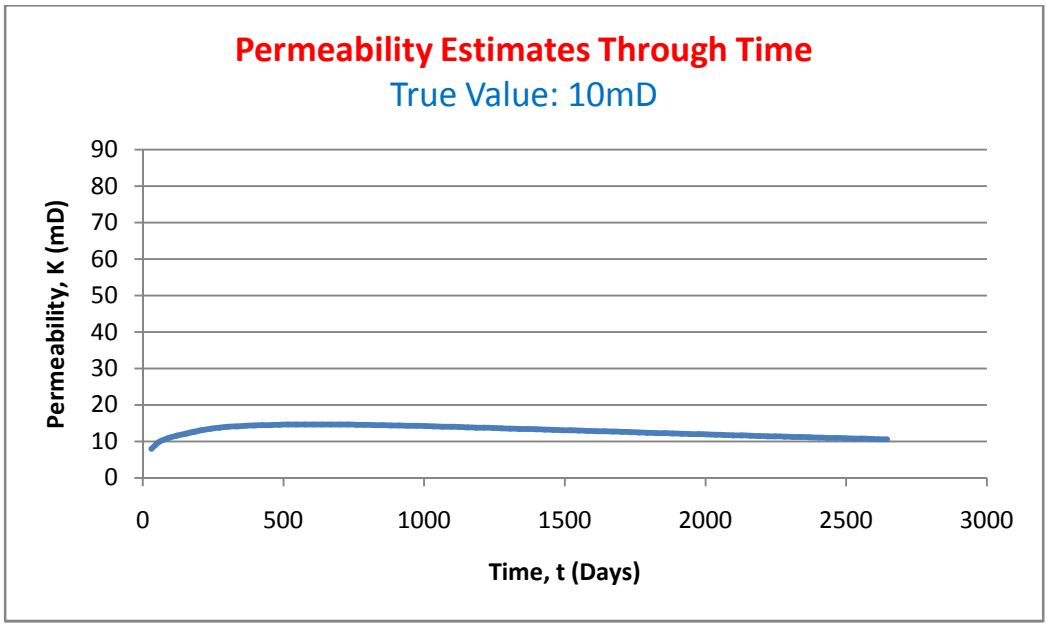

Figure 5.5: Base Case: Permeability Estimates through Time

5.5.1.4 COMPARING PERMEABILITY ESTIMATES USING DIFFERENT TECHNIQUES

Additionally, the possibility of estimating reservoir permeability as direct application of the equation published by Camacho and Raghavan[10] (equation 3. 2 in chapter three) was also explored by solving for k in the Camacho and Raghavan equation to give:

$$k = \frac{\phi A}{2\pi 0.006328 b_{emp}} D \frac{d}{dt}\left(\frac{\bar{c}_T}{\overline{\lambda_T}}\right) - - - - - - - - (5.3)$$

The 'permeability' values through time computed using Camacho and Raghavan[10] equation (equation 5.3) is plotted alongside permeability values computed using the equation proposed by this work (equation 3.11) and is shown below for comparison purposes.

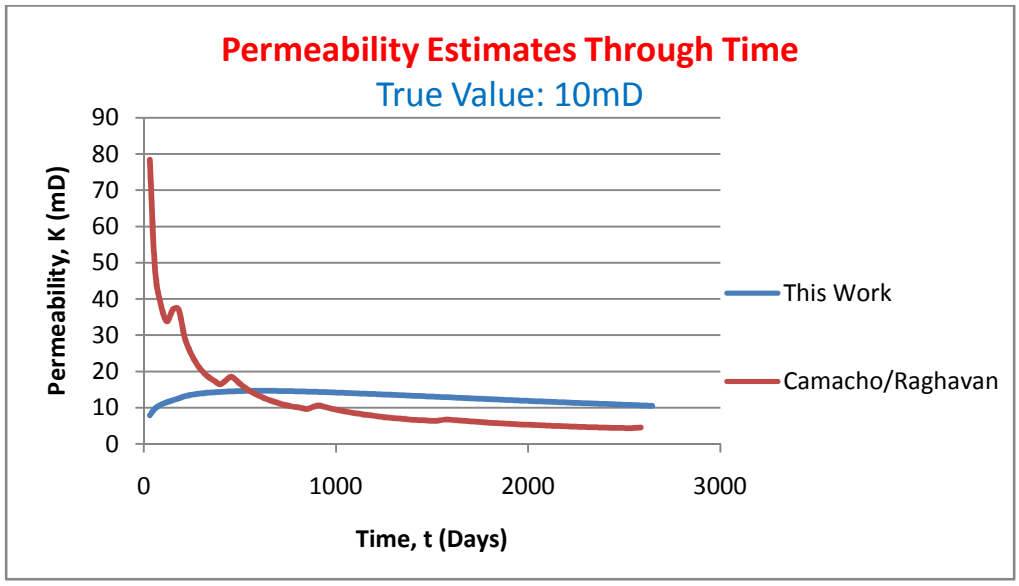

Figure 5.6: Comparing Permeability Estimates using different Techniques

These results showed that the Camacho and Raghavan[10] equation (equation 5.3) cannot be utilized for permeability estimation purposes as it is done with the relationship presented by this current work (equation 3.11). As a matter of fact, the 'permeability' values gotten using Camacho and Raghavan equation varied very widely away from the true value. This is because although the Camacho and Raghavan equation is theoretically correct, it does not have any link with the empirical domain, rather, it based on the expectation that the theoretical decline parameter b_{th} is equivalent to the empirical decline parameterb_{emp}; theories and results reported in this work have shown that expectation does not have a theoretical basis and as a matter of fact, the equivalence of b_{th} and b_{emp}does not exist.

Hence the exponent b_{th} on the LHS (of equation 3.2) cannot be taken as the equivalence of the empirically determined exponentb_{emp}. Instead, as presented by this work, the equivalence between the empirical domain and the theoretical domain of the decline parameter is anchored on a relationship between the empirical parameter b_{emp} and the time-weighted average of the theoretical values$\overline{b_{th}}$. This relationship has been derived in this work and is a major contribution of this work. This relationship forms the basis for the permeability estimation techniques being proposed by this work; hence the accuracy of the technique.

5.5.2 Reservoir Radius (r_e) Estimation

Camacho and Raghavan[10] had presented a form of the material balance equation for solution-gas drive reservoir as given below:

$$\frac{dN_p}{d\bar{P}} = N_p{}' = \frac{\bar{c}_T \bar{\alpha} \phi A h}{5.614\,\overline{\lambda_T}} \quad ---------- (5.4)$$

Where $\bar{\alpha} = \frac{k_{ro}(\overline{S_o})}{\mu_o(\bar{P})B_o(\bar{P})}$ and $A = \pi r_e^2$

Solving for the reservoir/drainage radius r_e in the above equations yields

$$r_e = \sqrt{\frac{5.614 N_p{}' \overline{\lambda_T}}{\bar{c}_T \bar{\alpha} \phi \pi h}} \quad ---------- (5.5)$$

As a direct application of the Camacho and Raghavan[10] work, equation 5.5 was employed in estimating the drainage radius for the reservoir model considered in this work. Excellent estimates of the reservoir drainage radius were obtained as shown in the plot of reservoir radius estimates through time below.

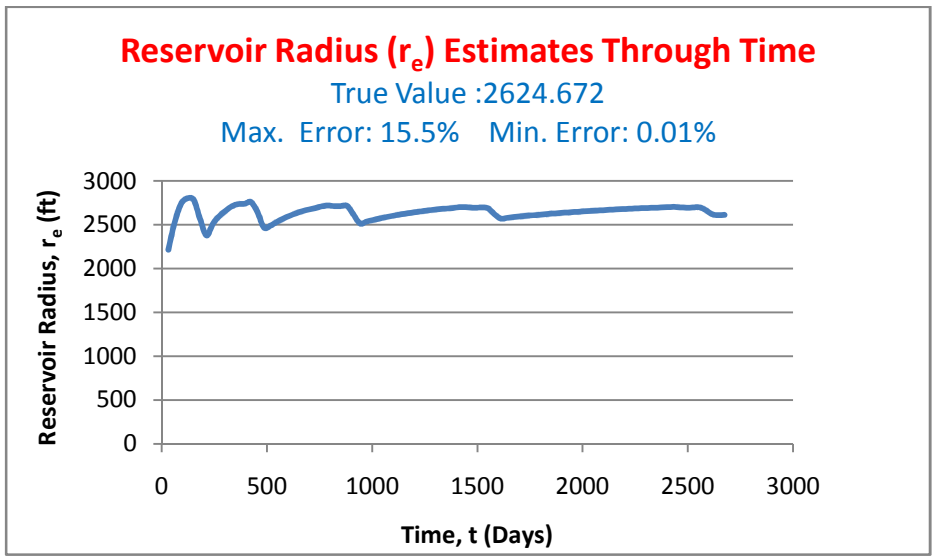

Figure 5.7: Base Case: Reservoir Radius (r_e) Estimates through Time

5.6 SENSITIVITY ANALYSIS

The following analyses were performed with the aim of establishing the effect of changing some key parameters on the results outlined in this work. In each case, the value for a parameter is changed and the result is compared to the base case.

5.6.1 Case 1: Effect of Critical Gas Saturation

In the base case, the critical gas saturation at which gas becomes mobile in the reservoir is set at zero; i.e. $S_{gc} = 0$. In this case however, the critical gas saturation was set at 5% i.e. $S_{gc} = 0.05$. Below is the plot of the simulator output for case 1.

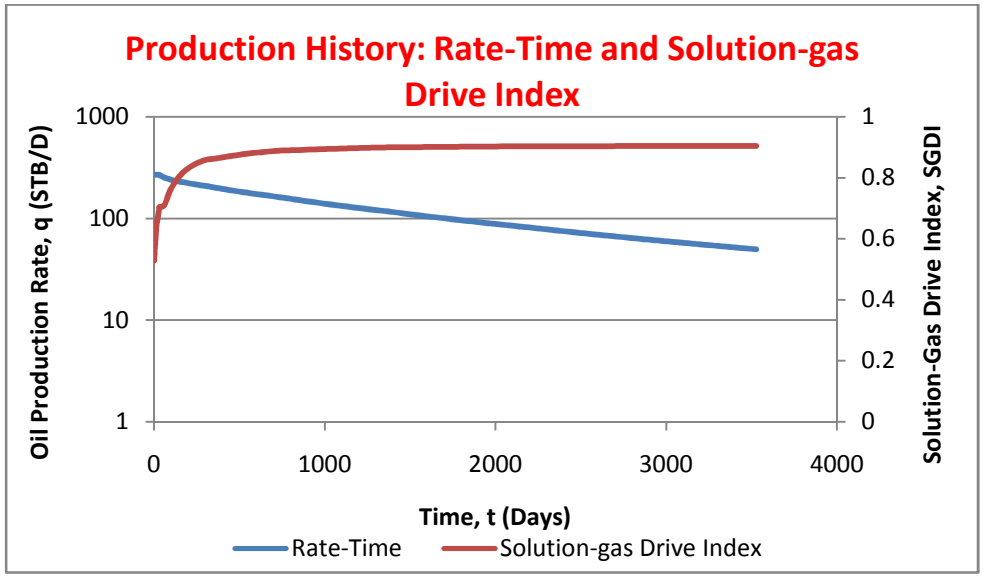

Figure 5.8: Case 1: Production History: Rate-Time and Solution-gas Drive Index

The result presented above exhibits trends similar to the result for the base case. However, in this case, the decline phase started after 29 days as against the base case where the decline phase started just after 12 days. The delay of the onset of decline in this case is explained thus:

1. In case 1, due to the non-zero value assigned to the critical gas saturation, it is expected that free gas flow in the reservoir is delayed until gas saturation attained the critical value. Hence as gas solution-gas evolves out of solution and is retained

due to its immobility, the gas expands and therefore helps to maintain pressure in the reservoir thereby delaying the attainment of the critical bottomhole pressure P_{wfc} due to pressure drop. Decline phase can only start when bottomhole pressure drops to its lowest permissible, P_{wfc}.

2. The trend noticed in the gas-oil ratio (GOR) plots for the two cases (base case and case 1) also lend evidence to the delayed decline phase.

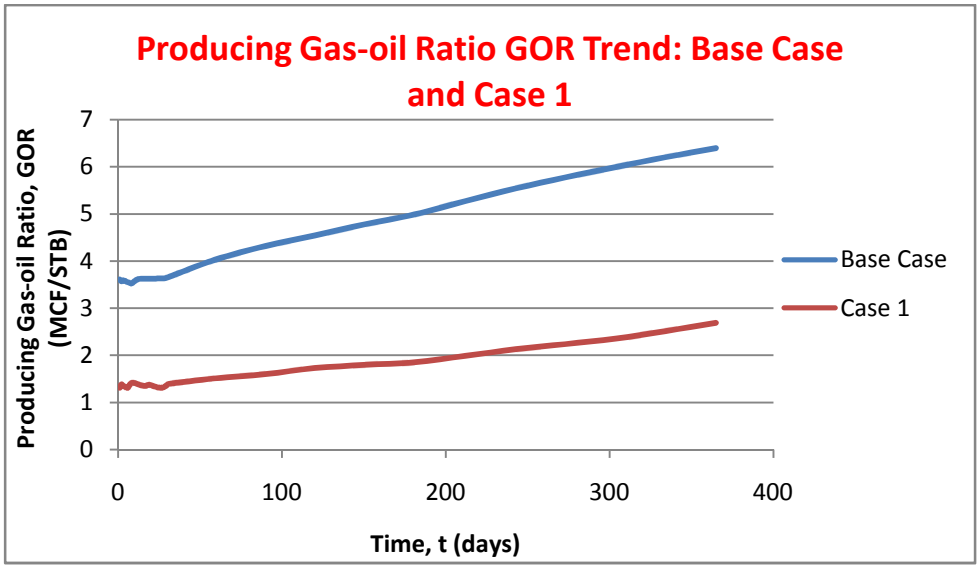

Figure 5.9: Producing Gas-Oil Ratio, GOR Trend: Base Case and Case 1

In the plots above, only the values for the first year of production decline is shown; this is done so as highlight the major difference in the plot which occurs at the beginning of decline phase.

From the plots, it is observed that for case 1, the GOR value reached its lowest and picked up at 27 days while decline started at 29 days. On the other hand, for the base case, the GOR value reached its lowest and picked up at 8 days while decline

started at 12 days. The point at which the GOR values started increasing corresponds to the attainment of the critical gas saturation, S_{gc}. As the critical gas saturation is attained, gas becomes mobile and the reservoir is deprived of pressure maintenance, hence pressure drops quickly to the lowest permissible, P_{wfc}.

Other results obtained for case 1 exhibits similar behavior to those in the base case. The implication of this is that although the value of S_{gc} have the effect of altering the timing of the onset of the decline phase, it has no significant effect on the accuracy of the permeability estimates generated thereby.

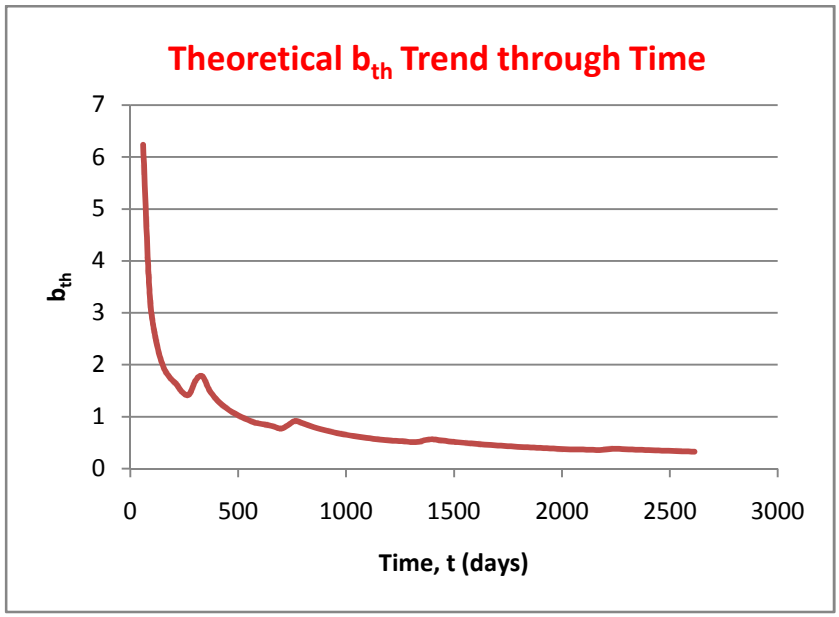

Figure 5.10: Case 1: Theoretical b_{th} Trend through Time

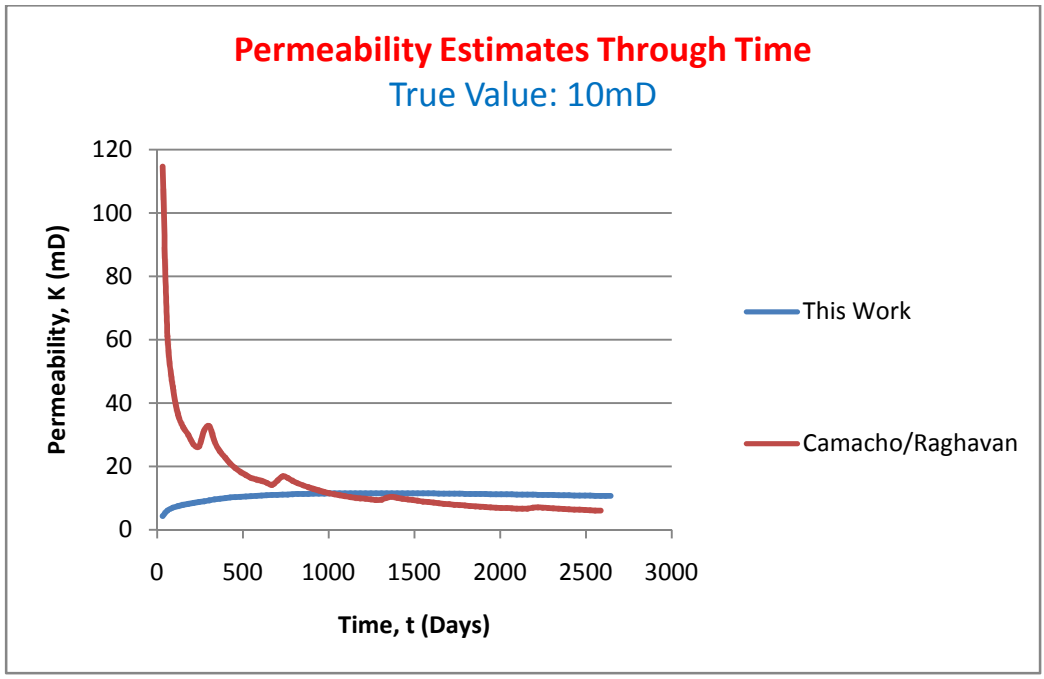

Figure 5.11: Case 1: Permeability Estimates through Time

5.6.2 Case 2: Effect of Permeability Value

The essence of this case study is to create a reservoir model that precludes the occurrence of transient rate decline. It is expected that the higher the absolute permeability of the reservoir rock, the faster the pressure transient travels outwardly from the wellbore through the porous rock to the external boundary of the drainage area; hence the more the likelihood of boundary-dominated flow setting in ahead of the onset of decline phase thereby precluding transient rate decline. For this case, the absolute permeability of the reservoir model was set at 100mD as against 10mD in the base case; also, to accommodate the increased permeability, the peak rate was set at 1000STB/D as against 270STB/D in the base case. Below are the results of this case study and the discussions.

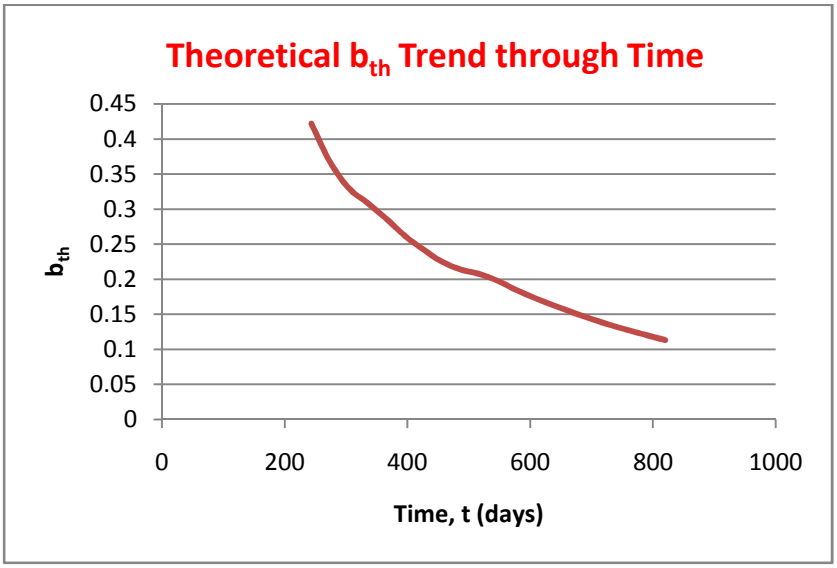

Figure 5.12: Case 2: Theoretical b_{th} Trend through Time

The results in this case run were found to conform to expectations as the b_{th} values reported were less than 1.0 thereby confirming the absence of transient rate decline. If indeed the transient rate decline regime was absent, then it is only proper to expect that the transition regime (between transient and boundary-dominated rate decline regimes) be also absent. The results of this case study also confirmed the absence of the transition decline regime since the transition interval 1 >b_{th} >0.67 was absent. These results therefore lend credence to the correctness of the theoretical justifications, offered by this work, for the various intervals of b_{th} values.

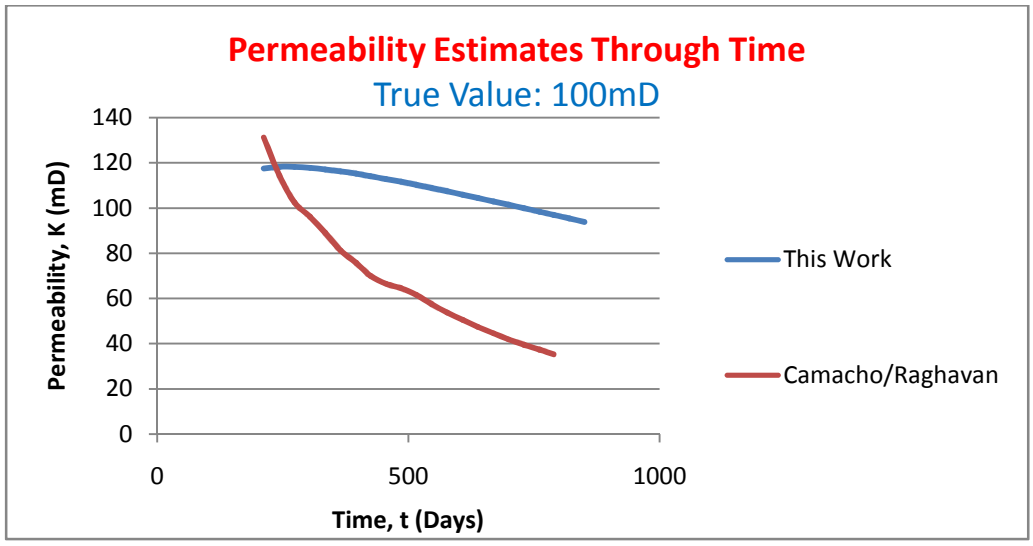

Figure 5.13: Case 2: Permeability Estimates through Time

From, the plots above, it is observed that the accuracy of the permeability estimates is similar to the accuracy observed in the base case; implying that the presence of transient rate decline regime may not have any significant effect on the accuracy of the permeability estimates.

5.6.3 Case 3: Effect of Reservoir Drainage Radius

As in case 2 above, the essence of this case study is to create a reservoir model that precludes the occurrence of transient rate decline. It is expected that the smaller the well's drainage area, the sooner the pressure transient from the well reaches the external boundary of the drainage area; hence the more the likelihood of boundary-dominated flow setting in ahead of the onset of decline phase thereby precluding transient rate decline. For this case, the external radius of the reservoir model was set at 1000ft as against 2624.672ft

in the base case; also, to maintain the intended reservoir pore volume, the reservoir thickness was set at 107ft as against 15.55ft in the base case. Below are the results of this case study and the discussions.

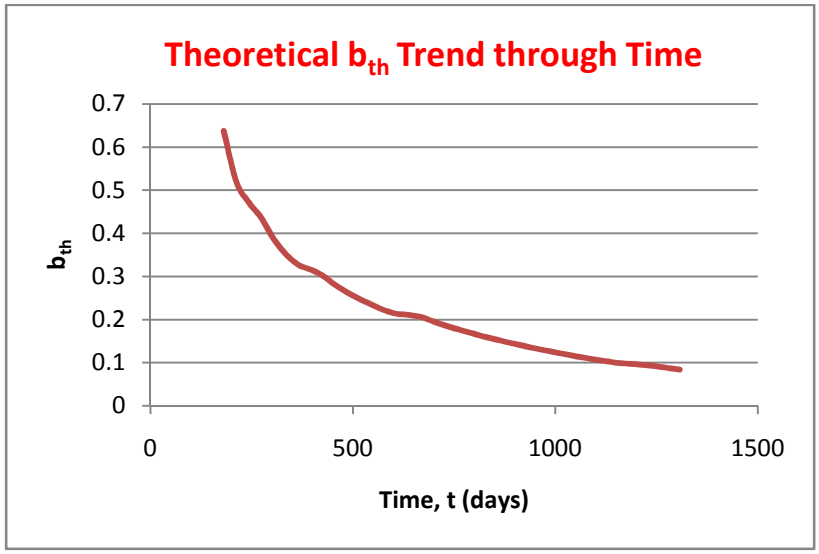

Figure 5.14: Case 3: Theoretical b_{th} Trend through Time

The results in this case run were found to conform to expectations and also to trends already established in case 2. The b_{th} values reported were less than 1.0 thereby confirming the absence of transient rate decline. The results of this case study also confirmed the absence of the transition decline regime since the transition interval $1>b_{th}>0.67$ was absent. These results together with those of case 2 therefore lend credence to the correctness of the theoretical justifications, offered by this work, for the various intervals of b_{th} values. However, as shown in plot below, the accuracy of the reservoir radius estimates is improved compared to the base case. The maximum error in this case is 2.5% while the minimum error is 0.002%; both values represent improvements over the

corresponding values in the base case. This improvement is arguably due to the absence of transient rate decline regime. Fetkovich et al[13] had suggested that reservoir volume-related properties should not be estimated using decline curve analysis (type curve matching) before boundary-dominated flow fully exists. It may then be important to screen a given rate-time data in order to eliminate any transient rate decline data points. Existing method for determining the time for the start of boundary-dominated flow for multiphase conditions[50] involves the computation of various pseudo functions (integrals) that may not be practical for this application. However, an approximation of the time at which the pressure wave propagates to the reservoir boundary can be obtained by employing the equation for radius of investigation for single phase condition.[4]

$$r_{inv} = 0.0325\sqrt{\frac{kt}{\phi\mu c_t}}$$

However, the equation above could only be used if there are estimates of both the permeability and reservoir radius from other formation evaluation sources; in such case, the equation above could be solved for t; being an approximation of the time for the start of boundary-dominated flow.

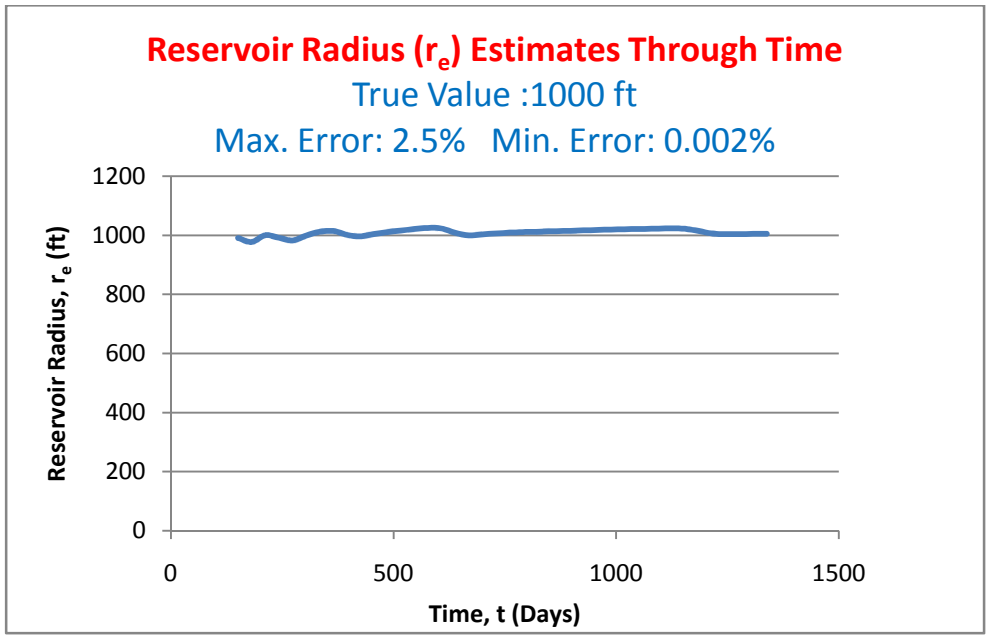

Figure 5.15: Case 3: Reservoir Radius (r_e) Estimates through Time

5.6.4 Case 4: Effect of Critical Bottomhole Pressure

The essence of this case study is to investigate the effect of the critical bottomhole pressure on the theoretical decline parameter, b_{th} as well as on the permeability estimates. The critical bottomhole pressure itself is a function of both the wellbore configuration and the reservoir deliverability. In this case, the critical bottomhole pressure was set at 700psi as against 1696psi in the base case. Results are shown below.

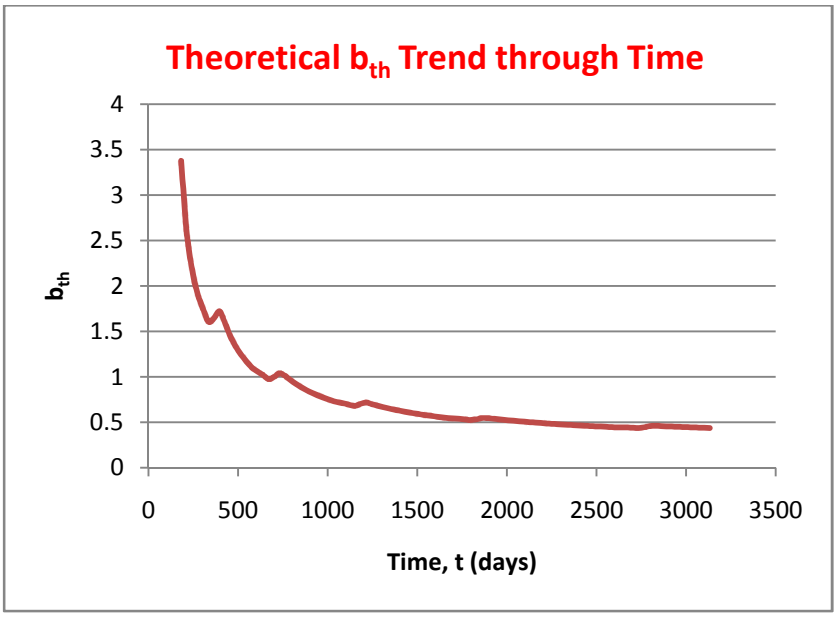

Figure 5.16: Case 4: Theoretical b_{th} Trend through Time

From the b_{th} values in the plot above, it is observed that the transient rate decline regime did not vanish in this case implying that the occurrence or otherwise of the transient rate decline regime is less sensitive to the value of the critical bottomhole pressure of the reservoir/wellbore model.

The accuracy of the permeability estimates is discussed next.

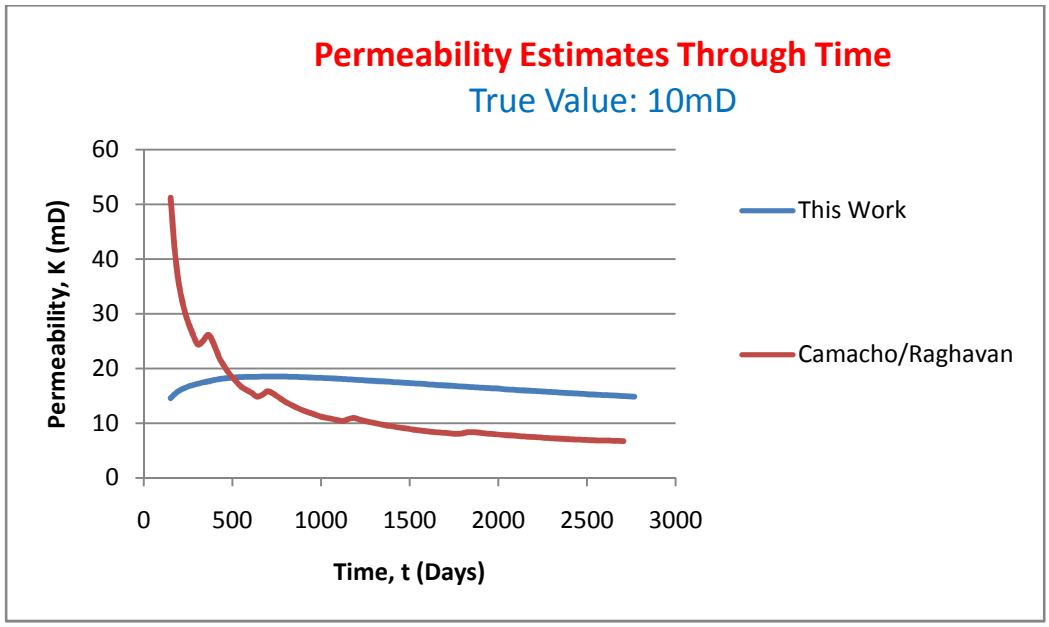

Figure 5.17: Case 4: Permeability Estimates through Time

From the plot above, it is observed that the permeability estimates in this case study are less accurate when compared to the estimates in the base case. The reduced accuracy, when considered side-by-side with the reduced agreement between the empirical domain and the theoretical domain, reveals an interesting trend discussed here. It is noticed that the lowest value of b_{th} recorded is about 0.4; this suggests the condition in the reservoir is still far from being considered to be approaching single phase behavior i.e. the reservoir has not yet exhausted the time span for the solution-gas decline regime. This fact is arguably the reason for the reduced agreement between the empirical and the theoretical curves even at field abandonment production rate as shown in the plots below. The reduced agreement consequently affected the accuracy of the permeability estimates as seen in the plot above. The implication of this is that the accuracy of the permeability estimates depends on the availability of data that spans more and more period of the solution-gas decline regime. The caution here however is that as soon as the entire time

span for the solution-gas decline regime is exhausted and reservoir depletion begins to approach the single phase behavior, the two curves (empirical and theoretical) crosses each other and begin to depart from each other thereby leading to reduced accuracy again. In summary, then, it can be said that the best estimates of the reservoir permeability would be obtained at the time that the reservoir has fully spanned the solution-gas decline regime.

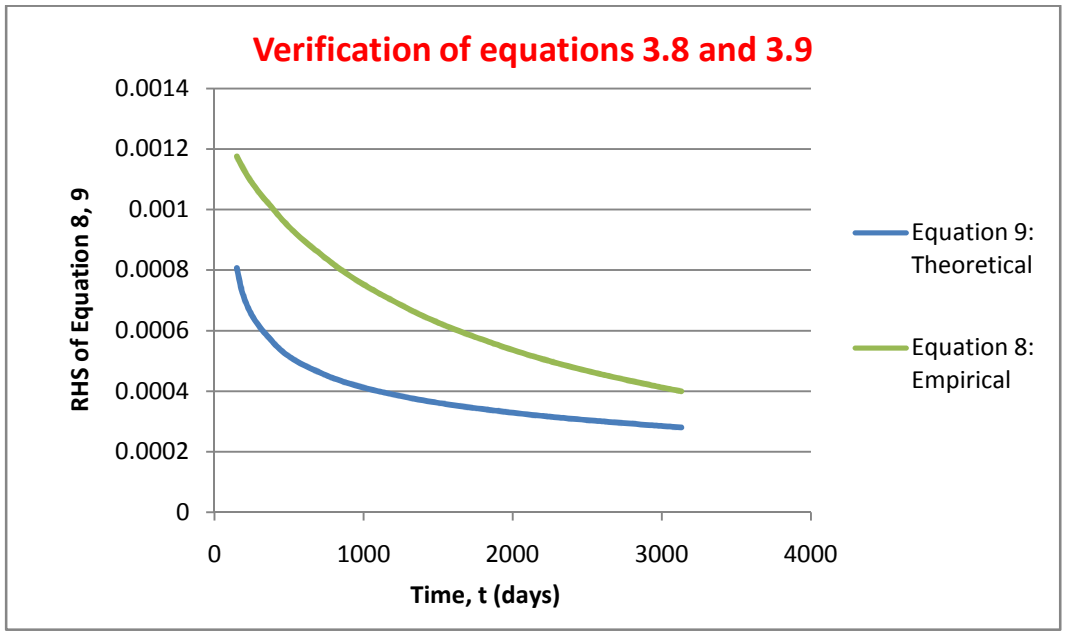

Figure 5.18: Case 4: Verification of Equations 3.8 and 3.9

5.6.5 Case 5: Effect of Peak/Initial Rate

The peak rate (rate at onset of decline) is a measure of the reservoir/wellbore capacity. The essence of this case study is to investigate the effect that factors such as wellbore diameter, wellhead pressure requirement may have on the results of this work. For this case, the

peak rate was set at 200STB/D (about 50% of the Absolute Open Flowrate) as against 270STB/D (about 70% of the Absolute Open Flowrate) in the base case. Lowering the peak rate this way resulted to a delay of the onset of decline for about 246 days (from 12 days in the base case to 258 days in this case). This is expected since producing at a lower rate requires a lower pressure drawdown; hence the attainment of the critical bottomhole pressure is delayed. The simulator output is shown below.

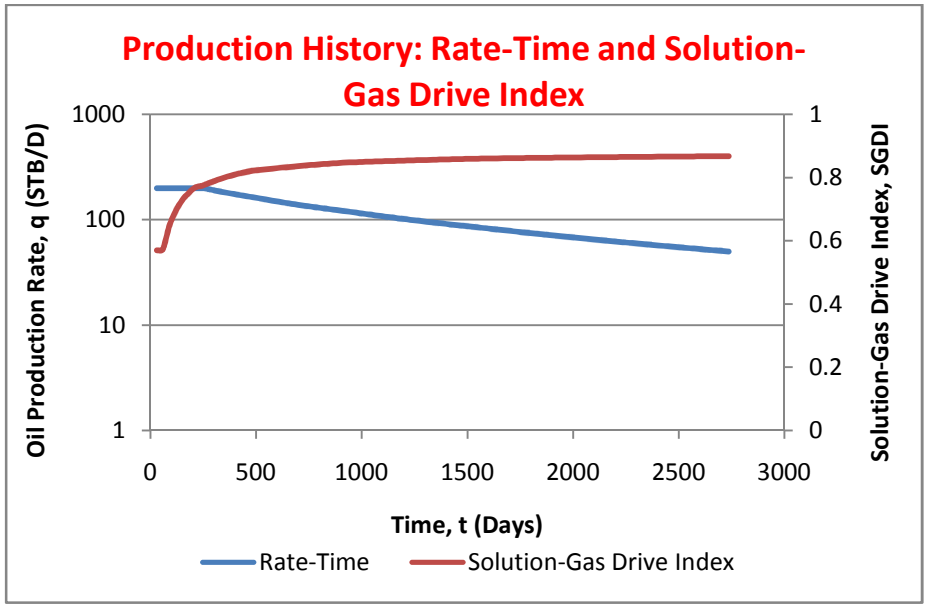

Figure 5.19: Case 5: Production History: Rate-Time and Solution Gas Drive Index

The theoretical b_{th} trend through time is shown below.

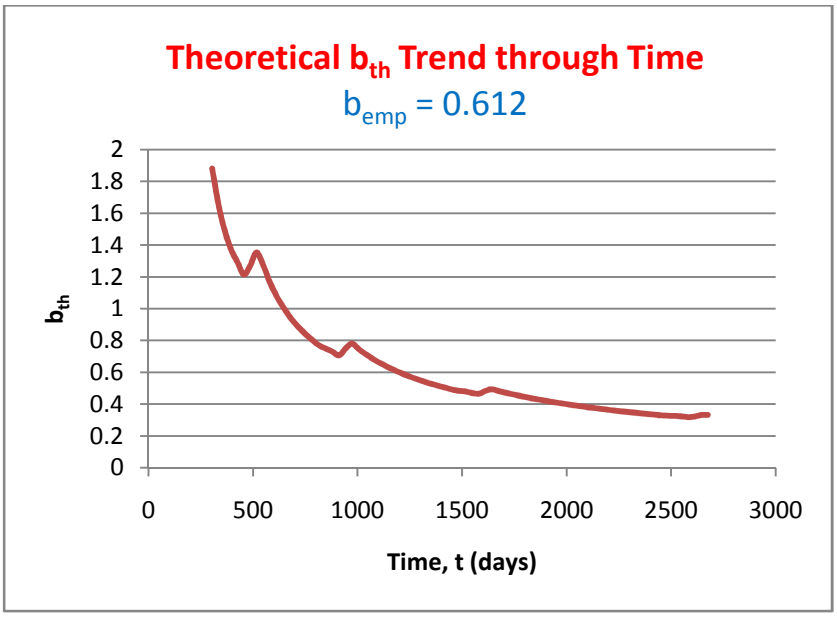

Figure 5.20: Case 5: Theoretical b_{th} Trend through Time

From the plot above it is observed that the maximum (and initial) value of the theoretical b_{th} was 1.88 as against 5.74 for the base case. This is arguably due to the delayed onset of the decline phase. Since decline is delayed, it is expected that there will be less of transient rate decline regime as the onset of decline could have occurred just before the beginning of boundary dominated flow. This result suggest that the more transient rate decline regime experienced by a well, the higher above 1.0 will be its initial b_{th} values. This case also recorded improved accuracy for both the permeability and the drainage radius estimates as shown in the plots below. This improvement is considered to be due to the fact that there is less of transient rate decline regime compared to the base case.

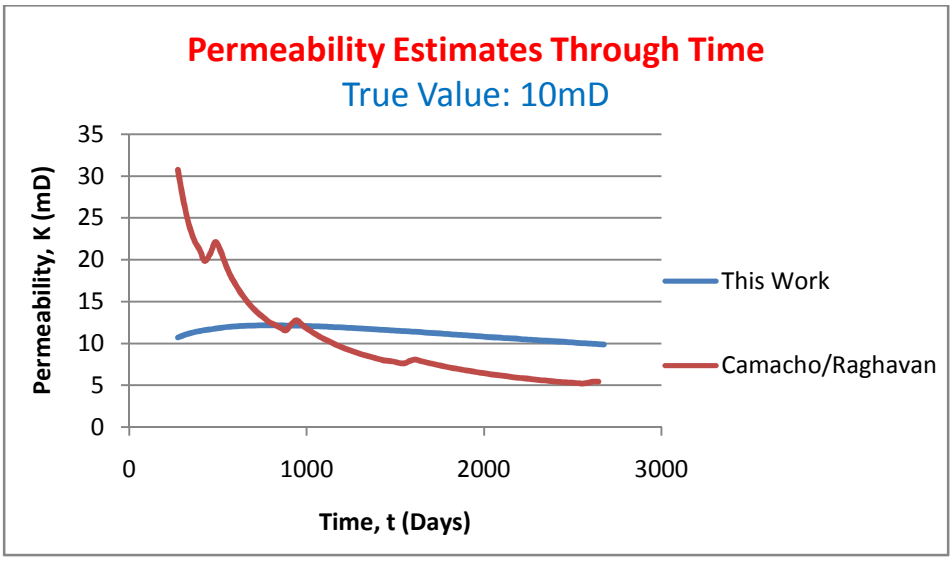

Figure 5.21: Case 5: Permeability Estimates through Time

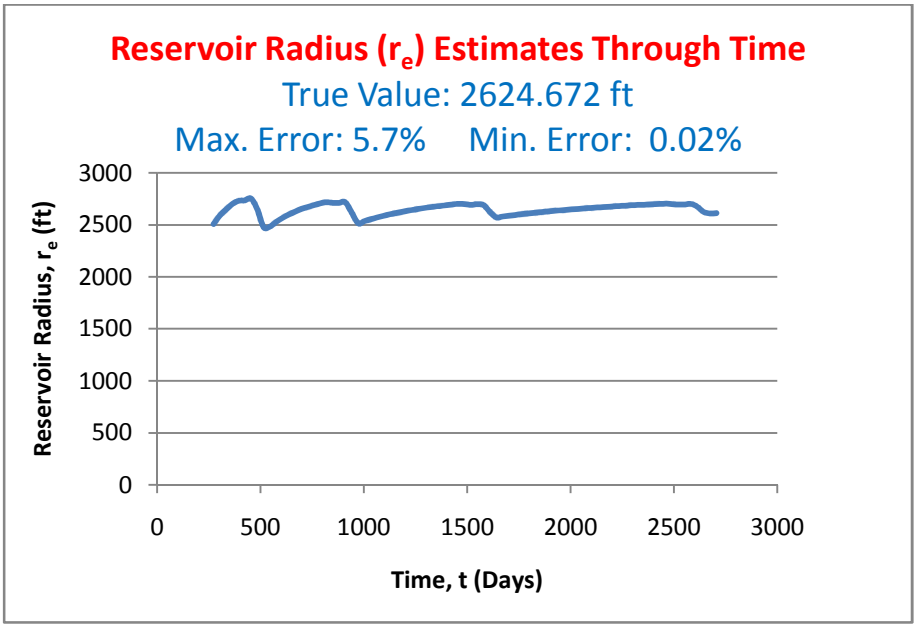

Figure 5.22: Case 5: Reservoir Radius (r_e) Estimates through Time

5.6.6 Case 6: Effect of Reservoir Heterogeneity.

The essence of this case is to investigate the effect of reservoir (permeability and porosity) heterogeneity on the results of the estimates technique presented by this work. Essentially, one would like know to what extent would the permeability estimates be representative of the permeability values of the different layers present in an heterogeneous reservoir. For this case, the reservoir model as described in the base case was divided into two layers. Heterogeneity was introduced into the reservoir by assigning different values of porosity and permeability to different layers according to the grid data shown in the table below. Two heterogeneous cases were considered in order to investigate not just the effect of heterogeneity, but also the effect of the degree of heterogeneity. For the purpose of comparison, the values of properties assigned to each heterogeneous case is such that the thickness-weighted average permeability and the thickness-weighted average porosity is still of the same values as the permeability and porosity values in the base case.

Table 5.1: Grid Data for Heterogeneous Case

Case 6a			
	Layer Thickness	Layer Permeability	Layer Porosity
Layer 1	8	150	0.35
Layer 2	7.55	50	0.25
Thickness-weighted Average		101.4469453	0.301446945
Case 6b			
	Layer Thickness	Layer Permeability	Layer Porosity
Layer 1	8	130	0.35
Layer 2	7.55	70	0.25
Thickness-weighted Average		100.8681672	0.301446945

The results for each of the two heterogeneous cases are presented in the plot below.

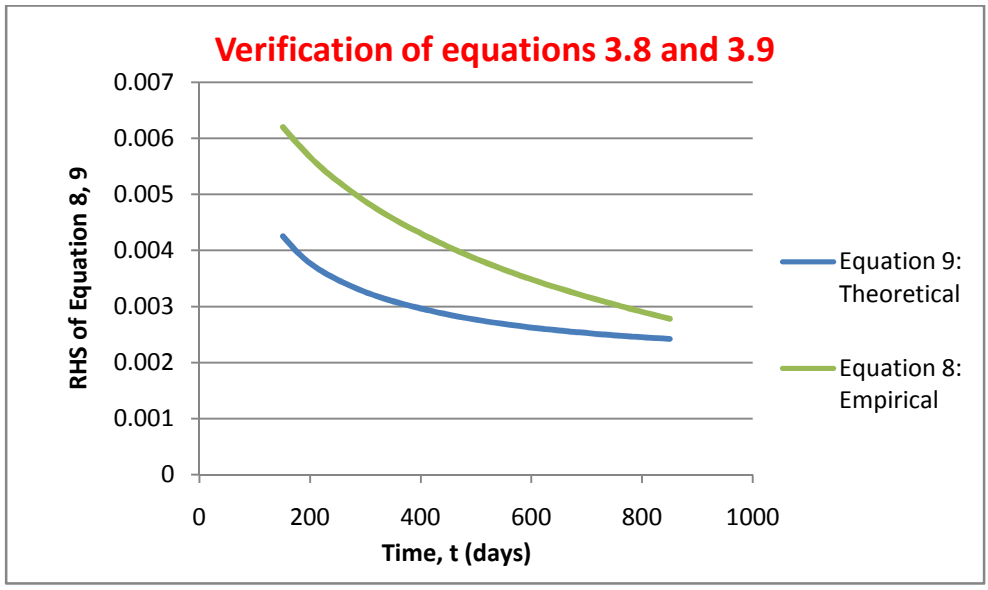

Figure 5.23: Case 6a: Verification of Equations 3.8 and 3.9

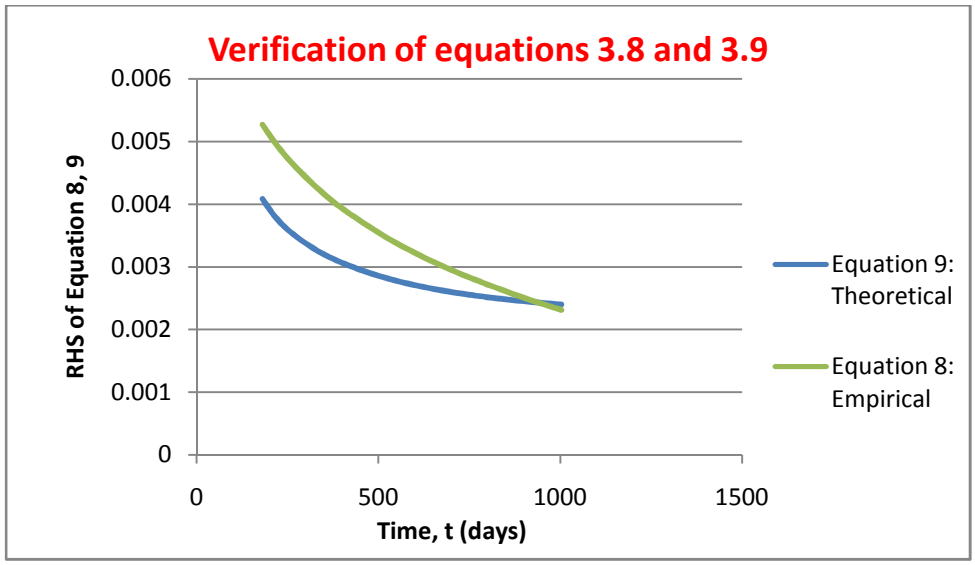

Figure 5.24: Case 6b: Verification of Equations 3.8 and 3.9

The results above showed that generally, there is an agreement between the empirical and the theoretical domains even for heterogeneous reservoirs. Furthermore, the results showed that the degree of agreement reduces with increasing heterogeneity. Note that case 6a has a higher degree of permeability heterogeneity (layer 1: 150mD; layer 2: 50mD) than case 6b (layer 1: 130mD; layer 2: 70mD).

The effect of the heterogeneity on the representativeness of the permeability estimates is discussed with the permeability estimates plots shown below.

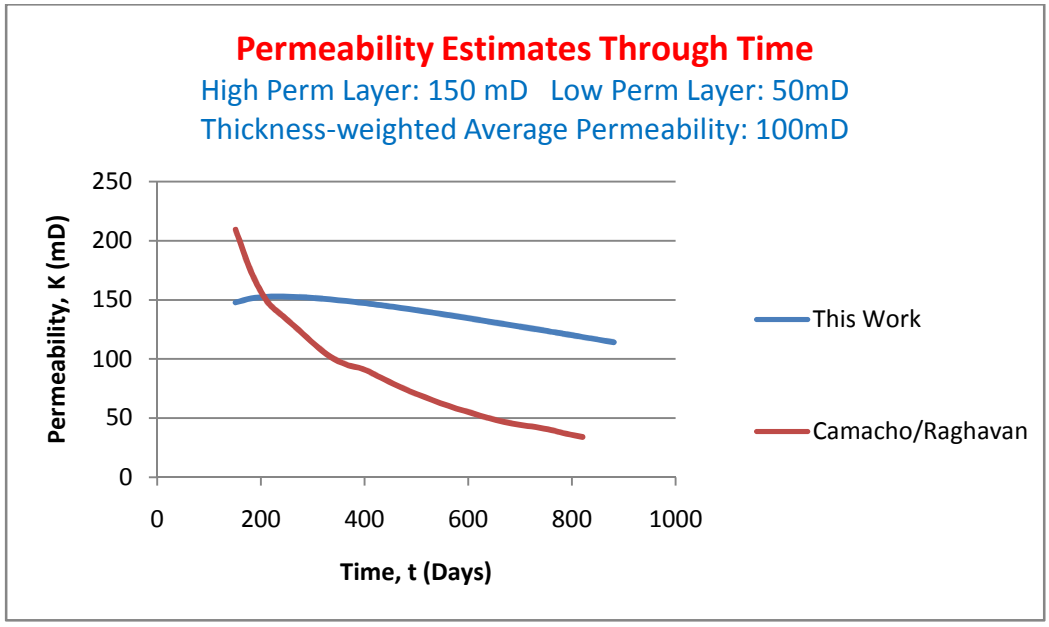

Figure 5.25: Case 6a: Permeability Estimates through Time

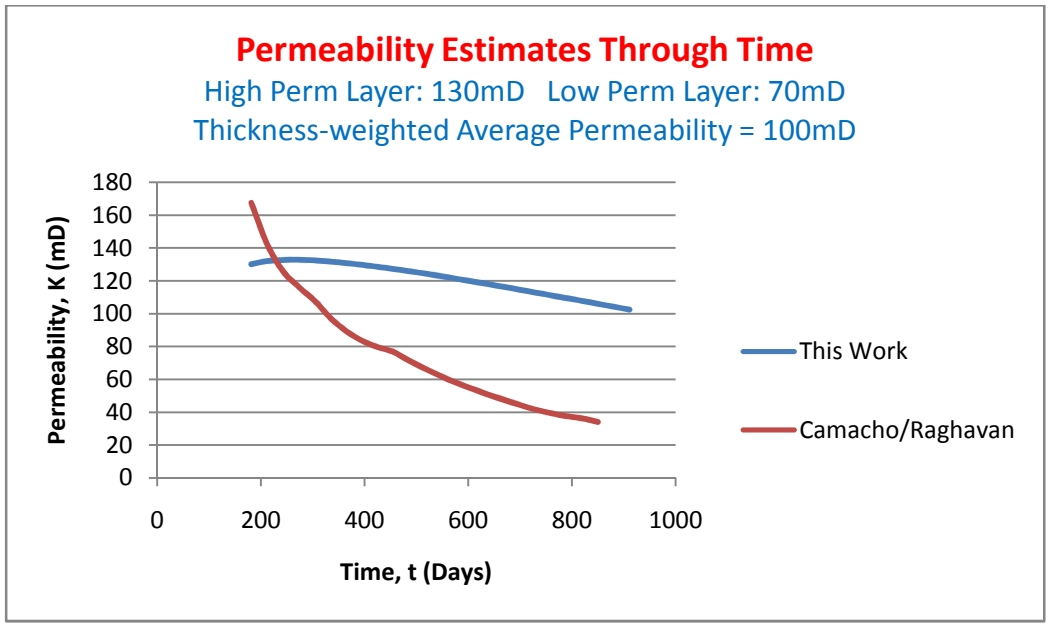

Figure 5.26: Case 6b: Permeability Estimates through Time

From the two heterogeneous cases shown in the plots above, it is observed that at early times, the permeability estimates reflects the permeability value for the higher permeability layer (150mD for case 6a and 130mD for case 6b); however, with time, the permeability estimates reflects values approaching the thickness-weighted average of the permeability values for all layers present (100mD for both cases).

CHAPTER 6

CONCLUSIONS AND RECOMMENDATIONS

6.1 CONCLUSIONS

Previous attempts[10] at establishing the theories of rate decline in solution-gas drive reservoirs have yielded expressions relating the theoretical decline exponent b_{th} to reservoir/fluid properties. However, the values computed from such expression, although theoretically sound, are not constant through time. More disturbing is the fact that the values did not exhibit any equivalence with the empirically determined decline exponent, b_{emp}. This fact suggests there is a missing link between the theoretical and the empirical domains of the decline curves analysis. This work has successfully provided the missing link; expressed as a functional relationship between the empirical decline exponent, $b_{emp}$and the time-weighted average of the values of the theoretical decline exponent known as $\overline{b_{th}}$. In addition, this work has developed a new improved reservoir permeability estimation technique. The technique has been applied to a number of cases and found to yield excellent estimates of reservoir permeability even for heterogeneous reservoirs. Analyses have been performed on the sensitivity of the results to some key parameters.

Based on the results presented in this work, the following conclusions are warranted.

1. The theoretical decline exponent b_{th} for a given reservoir/wellbore model varies considerably through time, and may have values above 1.0
2. The theoretical decline exponent b_{th} may be seen as reflecting the actual dynamics of the reservoir and fluid interaction through production time; hence it may be expected to have a dynamic (unstable) behavior through time.
3. Considering the various intervals of values present in a typical b_{th} trend through time, the following four distinct regimes of rate decline in solution-gas drive reservoirs has been identified.
    a. Transient rate decline regime: $b_{th} > 1.0$
    b. Transition rate decline regime: $1 > b_{th} > 0.67$
    c. Boundary-dominated Solution-gas drive decline regime: $0.67 > b_{th} > 0.33$
    d. Approaching slightly compressible liquid single phase decline: $b_{th} < 0.33$

Results presented in this work confirmed the presence of one more of these regimes in a solution-gas drive reservoir depending on the reservoir/wellbore configuration.

4. The theoretical decline exponent, b_{th} may never exhibit any constancy even with considerations for non-Darcy flow effects as the non-Darcy flow coefficients in solution-gas drive reservoirs are very small in values and may never measure up to values sufficient to counteract the variation in b_{th} due to changes in fluid properties.
5. The time-weighted average of b_{th} values for a given reservoir/wellbore model is related to the empirical decline exponent. The equation showing this relationship has been derived and presented in this work.

6. Consequent upon the derivation of the relationship stated above, a new improved technique for estimating reservoir permeability has been developed. The technique yielded excellent estimates for reservoir permeability even for heterogeneous reservoirs.
7. A technique for estimating a well's drainage area was also presented. This technique is based on the form of material balance equation for solution-gas drive presented by Camacho and Raghavan[10].
8. Although, the value of critical gas saturation S_{gc} has the effect of altering the timing of the onset of decline, it has no significant effect on the accuracy of the permeability estimates.
9. Reservoir with high permeability values may not exhibit the transient rate decline regime as well as the transition rate decline regime; hence the b_{th}intervals for these regimes may be absent in such reservoirs.
10. The presence of transient rate decline regime has insignificant effect on the accuracy of the permeability estimates.
11. The transient rate decline regime as well as the transition rate decline regime may be absent for wells with small drainage area; this is due to the likelihood of boundary-dominated flow setting in ahead of the onset of decline phase.
12. The accuracy of reservoir radius estimates is sensitive to the presence, or otherwise, of transient rate decline regime. The estimates become more accurate where transient rate decline regime is absent.
13. The occurrence, or otherwise, of the transient rate decline regime is less sensitive to the value of the critical bottomhole pressure of the reservoir and wellbore model.

14. The best estimates of the reservoir permeability would be made at the time that the reservoir has fully spanned the solution-gas drive decline regime.
15. The more transient rate decline regime experienced by a well, the higher above 1.0 will be its initial b_{th} values.
16. The relationship between the empirical and the theoretical domains of rate decline analysis derived in this work is also applicable to heterogeneous reservoir.
17. For the heterogeneous cases, at early times, the permeability estimates reflects the permeability value for the higher permeability layer however, with time, the permeability estimates reflects values approaching the thickness-weighted average of the permeability values for all layers present.

6.2 RECOMMENDATIONS FOR FURTHER STUDY

The following improvement on this work is been recommended as the focus for future investigations.

1. **Consideration for partially completed well**:

   Essentially, the various formulations developed in this work have been based on the assumption of a fully-penetrating well leading to a fully-radial flow of reservoir fluid into the wellbore. Partially penetrating wells are known to generate flow patterns that may not be considered fully-radial. As a matter of fact, attempt has been made by this investigator to apply the various techniques developed in this work to such reservoirs; the attempts have not been successful though.

2. **Other Drive Mechanisms:**

It is recommended that similar formulations for rate decline trends in other drive mechanism such as water drive, gravity drainage and combination drive mechanisms be considered.

3. **Multi-well Reservoir:**

This work has considered only reservoirs been drained by only one well. Future efforts should be directed at reservoirs being drained by many wells.

NOMENCLATURE

A	Reservoir drainage area, ft^2
a	Empirical decline parameter
B	formation volume factor RB/STB for liquid and RB/SCF for gas
b	Decline exponent
b_{emp}	Empirical decline parameter
b_{th}	Theoretical decline parameter
b_{th-nD}	Decline parameter with non-Darcy considerations
$\overline{b_{th}}$	Time-weighted average of b_{th}
c_t	Total compressibility, psi^{-1}
D	The group $\ln\frac{r_e}{r_w} - 0.75 + s)$
D_i	Decline parameter, day^{-1}
h	Reservoir thickness, ft
i	Data point position index
k	Permeability, mD
N	Non-Darcy flow coefficient, D/STB
P_i	initial reservoir pressure, psi
$\overline{P}$	Average reservoir pressure, psi
P_D	Dimensionless pressure
Pp_D	Dimensionless pseudo-pressure
q	Oil flowrate, STB/D
q_{fg}	Free-gas flowrate, STB/D
R_s	solution gas oil ratio, SCF/STB
r	Radius, ft
S_o, S_g	Saturations, fraction
s	Skin factor
s_m	Mechanical Skin factor
t	Time, days
$\bar{\bar{t}}_{AD}, \tilde{t}_{AD}$	Dimensionless pseudo-time functions
μ	viscosity, cp
ϕ	porosity, fraction

REFERENCES

1. Hubbert, M.K.: "Nuclear Energy and Fossil Fuels," paper presented at the 1956 Spring Meeting of the Southern District, American Petroleum Institute, Plaza Hotel, San Antonio, Texas, March 7-9.
2. Arps, J.J.: "Analysis of Decline Curves," Trans., AIME (1945) 160, 228-247.
3. Guo, B., Lyons, W.C. and Ghalambor, A.: *Petroleum Production Engineering, a Computer-Assisted Approach,* Elsevier Science and Technology Books, (2007), pages 98-105.
4. Ahmed, T. and McKinney, P.D.: *Advanced Reservoir Engineering,* Gulf Professional Publishing, (2005), pages 237-264
5. Mian, M.A.: *Project Economics and Decision Analysis, Volume 1: Deterministic Models,* Pennwell Corporation, (2002), pages 2-5.
6. Gentry, R.W. and McCray, A.W.: "The Effect of Reservoir and Fluid Properties on Production Decline Curves," JPT (September, 1978) 1327-1341.
7. Muskat, M. and Taylor, M.O.: "Effects of Reservoir Fluid and Rock characteristics on Production Histories of Gas-Drive Reservoirs," Trans., AIME (1946) 165, 78.
8. Arps, J.J. and Roberts, T.G.: "The Effects of the Relative Permeability Ratio, the Oil Gravity, and the Solution Gas-Oil Ratio on the Primary Recovery from a Depletion Type Reservoir," Trans., (AIME) 204, 120-127.
9. Mead, H.N.: "Modifications to Decline Curves Analysis," Trans., AIME (1956) 207, 11-16.
10. Camacho, V. R and Raghavan, R.: "Boundary Dominated Flow in Solution Gas-Drive Reservoirs," SPERE (November 1987)
11. Mathews, C.S. and Lefkovits, H.C.: "Gravity Drainage Performance of Depletion Type Reservoir in the Stripper Stage," Trans., AIME (1956), 207, 265-274.
12. Fetkovich, M.J.: "Decline Curves Analysis using Type Curves," JPT (June, 1980) 1065-1077
13. Fetkovich, M.J., Vienot, M.E., Bradley, M.D. and Kiesow, V.G.: "Decline Curves Analysis using Type Curves: Case Histories," SPEFE (December, 1987) 637-656.
14. Cox, D.O.: "Reservoir Limit Testing using Production Data," The Log Analyst (March-April, 1978) 13-17.

15. Ehlig-Economides, C.A. and Ramey Jr., H.J.: "Transient Rate Decline Analysis for Wells Produced at Constant Pressure," SPEJ (February, 1981) 98-104.
16. Johnson, R.H. and Bollen, A.L.: "The Loss-Ratio Method of Extrapolating Oil Well Decline Curves," Trans., AIME (1927) 77, 771
17. Nind, T.E. W.: *Principles of Oil Well Production,* McGraw-Hill (1981) 43-44.
18. Arps, J.J.: "Estimation of Primary Oil Reserves," Trans., AIME (1956) 207, 182-191.
19. Slider, H.C.: "A Simplified Method of Hyperbolic Decline Analysis," JPT (March, 1968) 235-236.
20. Gentry, R.W.: "Decline-Curves Analysis," JPT (January, 1972) 38-41
21. McCray, T.L.: "Reservoir Analysis using Production Data and Adjusted Time, M.S. Thesis, Texas A & M University, College Station, TX (1990).
22. Blasingame, T.A., McCray, T.C and Lee, W.J.: "Decline Curve Analysis for Variable Pressure Drop/Variable Flowrate Systems," Paper SPE 2153 presented at the 1991 SPE Gas Technology Symposium, Houston, TX, January 23-24.
23. Palacio, J.C. and Blasingame, T.A.: "Decline Curve Analysis Using Type Curves: Analysis of Gas Well Production Data," paper SPE 25909 presented at the 1993 SPE Rocky Mountain Regional/Low Permeability Reservoir Symposium, Denver, CO, April 12-14.
24. Fekkane, A. and Tiab, D.: "Application of Decline-Curve Analysis Technique in Oil Reservoir using Universal Fitting Equation," paper 70036 presented at the 2001 SPE Permian Basin Oil and Gas Recovery Conference, Midland, Texas, May 15-18.
25. Lefkovits, H.C. and Matthews, C.S.: "Application of Decline Curves to Gravity Drainage Reservoirs in the Stripper Stage," Trans., AIME (1958) 213, 275-280.
26. Hawkins, M.: "Material Balances in Expansion Type Reservoirs Above Bubble Point," SPE Transactions Reprint Series (1955) 3, 36-40
27. Muskat, M.: "The Production Histories of Oil Producing gas-Drive Reservoirs," Journal of Physics, (1945) 16, 167.
28. Tarner, J.: "How Different Size Gas Cap and Pressure Maintenance Affect Ultimate Recovery," Oil Weekly, (June, 12, 1944) 32-36
29. Tracy, G.: "Simplified Form of the Material Balance Equation," Trans., AIME (1955) 201 243-246
30. Evinger, H.H. and Muskat, M.: "Calculation of Theoretical Productivity Factors," Trans., AIME (1942) 146, 126-139
31. Vogel, J.V.: "Inflow Performance Relationship for Solution-Gas Drive Wells," JPT (January, 1968) 83-92
32. Fetkovich, M.J.: "The Isochronal Testing of Oil Wells," paper SPE 4529 presented at the 1973 SPE Annual Meeting, Las Vegas, NV, September 30 – October 3.
33. Rawlins, E.L. and Schellhardt, M.A.: "Back-Pressure Data on Natural Gas Wells and their Application to Production Practices," USBM (1935) 7.

34. Jones, L.G., Blount, E.M. and Glaze, O.H.: "Use of Short-Time Multiple Rate Flow Tests to Predict Performance of Wells having Turbulence," paper SPE 6133 presented at the 1976 SPE Annual Technical Meeting and Exhibition, New Orleans, October 3-6.
35. Forchheimer, Ph.D.: Ziets V.deutsch Ing., (1901) 45, 1782.
36. Klins, M.A. and Majcher, M.W.: "Inflow Performance Relationships for Damaged or Improved Wells Producing Under Solution-Gas Drive," JPT (December, 1992) 1357-1363
37. Sukarno, P. and Wisnogroho, A.: Generalized Two-Phase IPR Curve Equation Under Influence of Non-linear Flow Efficiency," Proceedings of the Society of Indonesian Petroleum Engineers Optimization International Symposium, Bandung, Indonesia, July 24-26, 1995, 31-43.
38. Gallice, F. and Wiggins, M.L.: "A Comparison of Two-Phase Inflow Performance Relationships," paper SPE 52171 presented at the 1999 SPE Mid-Continent Operations Symposium, Oklahoma City, Oklahoma, March 28-31.
39. Ilk, D., Camacho-V, R. and Blasingame, T.A.: "Inflow Performance Relationship for Solution gas Drive Reservoirs – Analytical Considerations," paper SPE 110821 presented at the 2007 SPE Annual Technical Conference and Exhibition, Anaheim, California, November 11-14.
40. Marhaendrajana, T.A. and Permadi, A.K.: "Performance Prediction of a Well Under Multiphase Flow Conditions," paper SPE 80534 presented at the 2003 SPE Asia Pacific Oil and Gas Conference and Exhibition, Jakarta, Indonesia, April 15-17.
41. Dake, L. P.: The Practice of Reservoir Engineering, Elsevier Development in Petroleum Science.
42. Van Everdingen, A.F. and Hurst, W.: "The Application of Laplace Transformations to Flow Problems in Reservoir," Trans., AIME (1949) 186, 305-324.
43. Moore, T.V., Schilthuis, R.J. and Hurst, W.: "The Determination of Permeability from Field Data," Bull., API (May 1933) 211, 4.
44. Hurst, R.: "Unsteady Flow of Fluids in Oil Reservoirs," Physics (January 1934) 5, 20.
45. Al-Hussainy, R., Ramey Jr., H.J. Crawford, P.B.: "The Flow of Real Gases Through Porous Media," JPT (May 1966) 624-636.
46. Agarwa, R.G.: "Real Gas Pseudo Time – A new Function for Pressure Build-up Analysis of MHF Gas Wells," paper SPE 8279 presented at the 1979 SPE Annual Technical Conference and Exhibition, Las Vegas, September 23-26.
47. Jones, J.R. and Raghavan, R.: "Interpretation of Flowing Well Responses in Gas-Condensate Wells," SPEFE (September, 1988) 578-594; Trans., AIME, 285.
48. Camacho, V. R and Raghavan, R.: "Some Theoretical Results Useful in Analyzing Well Performance Under Solution Gas Drive," SPERE (June 1991), 190
49. Raghavan, R.: "Well Test Analysis: Wells Producing by Solution-Gas Drive," SPEJ (August, 1976) 196-208; Trans., AIME, 261.

50. Fraim, M.L. and Wattenbarger, R.A.: "Decline Curve Analysis for Multiphase Flow," paper SPE 18274 presented at the 1988 SPE Annual Technical Conference and Exhibition, Houston, Texas, October 2-5
51. Frederick, J.L. and Kelkar, M.: "Decline-Curve Analysis for Solution-Gas-Drive Reservoirs," paper SPE 94859 presented at the 2005 SPE Annual Technical Conference and Exhibition, Dallas, Texas, October 9-12.
52. Camacho-V., R.G., and Raghavan, R.: "Inflow Performance Relationship for Solution Gas Drive Reservoirs," Paper SPE 16204 Presented at the 1987 SPE Production Operations Symposium (March 9-11, 1987), Oklahoma City, Oklahoma.
53. Camacho-V, R., Vasquez-C, M. and Padilla-S, R.: "New Results on Decline Curves Considering Non-Darcy Flow Effects," SPEREE (October, 1998)
54. Zeng, F and Zhao, G.: "Semi-Analytical Model for Reservoirs with Forchheimer's flow," Paper SPE 100540 presented at the 2006 SPE Gas Technology Symposium held in Calgary, Alberta, Canada, 15-17 May 2006
55. Chen, H.Y. and Poston, S.W.: "Application of a Pseudotime Funtion to Permit Better Decline Curve Analysis," SPEFE (September, 1989) 421-428.
56. Lee, J., Rollins, J. and Spivey, J.: *Pressure Transient Testing,* SPE Book Series Volume 9 (2003), pages 5-10.
57. Vasquez, M. and Beggs, H.D.: "Correlations for Fluid Physical Property Prediction," JPT (June 1988) 968-970.
58. Geertsma, J.: "Estimating the Coefficients of Inertial Resistance in Fluid Flow through Porous Media," SPEJ (October, 1974) 445-450.
59. Lee, J. and Wattenbarger, R.A.: *Gas Reservoir Engineering,* SPE Textbook Series Volume 5 (1996) page 18.

APPENDIX

SIMULATOR INPUT DATA DECK

```
RUNSPEC
TITLE
 DECLINE TRENDS IN SOLUTION GAS DRIVE RESERVOIR WITH CONSIDERATIONS FOR
NON-DARCY FLOW EFFECTS

DIMENS
 10 1 2/ SINCE IT IS AN HOMOGENEOUS RESERVOIR, TWO LAYERS SHOULD BE
SUFFICIENT

WATER

OIL

GAS

DISGAS

FIELD

START
 11 JLY 2011/

WELLDIMS
 5 5 2 2/

EQLDIMS
 1/

SMRYDIMS
```

```
 5000 /

FMTOUT

UNIFOUTS

RADIAL

TABDIMS
 1 1 30 50 1* 50/

TRACERS
 2* 1 4* /

--ENDSCALE
-- 4* /

GRID
-- HERE I CAN ONLY TRUST THE ONLY WISE GOD TO HELP ME OUT.

INRAD
 0.32808/ THIS BEING THE WELLBORE RADIUS; I HOPE AM RIGHT

OUTRAD
 2624.672/ THIS BEING THE RESERVOIR EXTENT

DTHETAV
 360/

DZ
 10*8 10*7.55/ SUMMING UP TO H = 15.55.

TOPS
 10*10000 10*10008/ ASSUMING THE RESERVOIR IS ENCOUNTERED AT DEPTH 10000.

PORO
 20*0.3/

PERMR
 20*10/

COPY
PERMR PERMTHT/
PERMR PERMZ/
/
```

```
COORDSYS
 1 2 COMP JOIN/


PROPS

SGFN
-- SG     KRG      PCOG
  0.0000  0.0000    0.0000
  0.7000          0.7050    0.0000 /


SWFN
-- SW     KRW      PCOW
0.30     0       0.0000
0.40     0.0006   0.0000
0.50     0.0062   0.0000
0.60     0.0258   0.0000
0.70     0.0705   0.0000
0.80     0.1540   0.0000
0.90     0.2915   0.0000
1.00     0.5000   0.0000 /



SOF3
  0.0000  0.0000  0.0000
  0.70    0.7470  0.7470      /



ROCK
 5704.78 1.0E-6 /

DENSITY
 49.90491  62.366  0.062428/ THE OIL DENSITY IS BASED ON 45.5 API


PMAX
 5704.78 5704.78/

PVTW
 5704.78 1.0 1.0E-6 2* /
```

```
PVCO
-- P      Rs     Bo      VISCOIL  COMPRESSI VISCOSIBILITY
 100      0.0100       1.0622  1.3957   3.64E-4   1*
 200      0.0263       1.0650  1.3525   1*       1*
 300      0.0427       1.0683  1.3104   1*       1*
 400      0.0594       1.0721  1.2695   1*       1*
 500      0.0763       1.0765  1.2296   1*       1*
 600      0.0933       1.0814  1.1909   1*       1*
 700      0.1107       1.0868  1.1532   1*       1*
 800      0.1282       1.0926  1.1165   1*       1*
 900      0.1460       1.0990  1.0809   1*       1*
 1000   0.1641         1.1059  1.0463   1*       1*
 1500   0.2588         1.1469  0.8882   1*       1*
 2000   0.3617         1.1984  0.7534   1*       1*
 2500   0.4739         1.2593  0.6400   1*       1*
 3000   0.5969         1.3284  0.5462   1*       1*
 3500   0.7318         1.4044  0.4702   1*       1*
 4000   0.8800         1.4864  0.4101   1*       1*
 4500   1.0428         1.5731  0.3640   1*       1*
 5000   1.2214         1.6633  0.3300   1*       1*
 5500   1.4172         1.7558  0.3063   1*       1*
 5704.78       1.5026 1.7941  0.2992   1.95E-5   1* /

PVDG
-- P     Bg        VISCGAS
100     3.86E+001  0.010443
200     1.80E+001  0.010786
300     1.15E+001  0.011129
400     8.39E+000  0.011472
500     6.57E+000  0.011815
600     5.37E+000  0.012158
700     4.54E+000  0.012501
800     3.92E+000  0.012844
900     3.44E+000  0.013187
1000    3.06E+000  0.013530
1500    1.96E+000  0.015245
2000    1.43E+000  0.016960
2500    1.12E+000  0.018675
3000    9.15E-001  0.020390
3500    7.72E-001  0.022105
4000    6.67E-001  0.023820
4500    5.86E-001  0.025535
5000    5.22E-001  0.027250
5500    4.70E-001  0.028965
5704.78  4.61E-001  0.029667 /
```

```
--ENPTVD
-- 10000    0.3 0.3 0.3 0 0 0.7 0 1*
-- 10015.5  0.3 0.3 0.3 0 0 0.7 0 1* /

--ENKRVD
-- 10000    0 0.7050 0.7470 0    0.7050 0.7470 0.7470
-- 10015.5    0 0.7050 0.7470 0    0.7050 0.7470 0.7470 /

TRACER
 'DGS' 'GAS' /
/

RPTPROPS
 DENSITY  KRG  KRGR  PVDG  PVTO  SGFN  SOF2 /

SOLUTION

--EQUIL
-- 9999 5704.78 11000 0 9999 0 0 0 0 /

PRESSURE
 20*5704.78 /

PBUB
 20*5704.78 /

SWAT
 20*0.3 /


SGAS
 20*0.0 /

TBLKFDGS
 20*0 /

TBLKSDGS
 20*1 /

RPTSOL
 DENG DENO DENW EQUIL FIP KRG KRO PGAS POIL RS SGAS SOIL SWAT VGAS VOIL /

SUMMARY

FOPR
FOPT
```

```
FGPT
FGPR
FGPRF
FGPRS
FVPR
FGOR
WBHP
 'SOLOWELL'
/
WSTAT -- 1 FOR PRODUCER
 'SOLOWELL'
/
WMCTL -- 7 FOR BHP
 'SOLOWELL'
/
CDFAC
 'SOLOWELL' /
/
CTFAC
 'SOLOWELL' /
/
FOSAT
FOIPL
FPPO
FOVIS
FGSAT
FPPG
FGVIS
FGDEN
FPR
FOE  -- FIELD OIL EFFICIENCY
FORFS
FORFF
FORFG
EXCEL
RPTONLY
RUNSUM

SCHEDULE

WELSPECS
 SOLOWELL SOLOGROUP 1 1 1* OIL -1 6* /
/

COMPDAT
 SOLOWELL 1 1 1 2 OPEN 2* 0.65616 1* 10 1* Z 1* /
```

```
/

WDFAC
 SOLOWELL 1.7107E-6 /
/

WCONPROD
 SOLOWELL OPEN ORAT 270 4* 1696 3* /
/

WECON
 SOLOWELL 50 5* YES 1* POTN 4* /
/

RPTSCHED
 FIP=2 PBUB=2 RS SUMMARY=1 WELLS=1 /

TSTEP
1       1       1       1       1       1       1       1       1       1       1       1
1       1       1       1       1       1       1       1       1       1       1       1
1       1       1       1       1       1       1
28 31 30 31 30 31 31 30 31 30 31
31 28 31 30 31 30 31 31 30 31 30 31
31 28 31 30 31 30 31 31 30 31 30 31
31 28 31 30 31 30 31 31 30 31 30 31
31 28 31 30 31 30 31 31 30 31 30 31
31 28 31 30 31 30 31 31 30 31 30 31
31 28 31 30 31 30 31 31 30 31 30 31
31 28 31 30 31 30 31 31 30 31 30 31
31 28 31 30 31 30 31 31 30 31 30 31
31 28 31 30 31 30 31 31 30 31 30 31
31 28 31 30 31 30 31 31 30 31 30 31
31 28 31 30 31 30 31 31 30 31 30 31
31 28 31 30 31 30 31 31 30 31 30 31
31 28 31 30 31 30 31 31 30 31 30 31
31 28 31 30 31 30 31 31 30 31 30 31
31 28 31 30 31 30 31 31 30 31 30 31
31 28 31 30 31 30 31 31 30 31 30 31
31 28 31 30 31 30 31 31 30 31 30 31
31 28 31 30 31 30 31 31 30 31 30 31 /
```